AFRL-ML-WP-TR-2006-4200

LOW TEMPERATURE, LOW PRESSURE FABRICATION OF ULTRA HIGH TEMPERATURE CERAMICS (UHTCs)

Yigal Blum
Jochen Marschall

SRI International
333 Ravenswood Avenue
Menlo Park, CA 94025

Hans Joachim Kleebe

Colorado School of Mines

AUGUST 2006

Final Report for 01 August 2004 – 31 March 2006

Approved for public release; distribution is unlimited.

STINFO COPY

MATERIALS AND MANUFACTURING DIRECTORATE
AIR FORCE RESEARCH LABORATORY
AIR FORCE MATERIEL COMMAND
WRIGHT-PATTERSON AIR FORCE BASE, OH 45433-7750

NOTICE AND SIGNATURE PAGE

Using Government drawings, specifications, or other data included in this document for any purpose other than Government procurement does not in any way obligate the U.S. Government. The fact that the Government formulated or supplied the drawings, specifications, or other data does not license the holder or any other person or corporation; or convey any rights or permission to manufacture, use, or sell any patented invention that may relate to them.

This report was cleared for public release by the Air Force Research Laboratory Wright Site (AFRL/WS) Public Affairs Office and is available to the general public, including foreign nationals. Copies may be obtained from the Defense Technical Information Center (DTIC) (http://www.dtic.mil).

AFRL-ML-WP-TR-2006-4200 HAS BEEN REVIEWED AND IS APPROVED FOR PUBLICATION IN ACCORDANCE WITH ASSIGNED DISTRIBUTION STATEMENT.

//Signature//

*MICHAEL K. CINIBULK, Project Engineer
Ceramics Branch
Metals, Ceramics, & NDE Division

//Signature//

PAUL D. JERO, Acting Branch Chief
Ceramics Branch
Metals, Ceramics, & NDE Division

//Signature//

GERALD J. PETRAK, Asst Chief
Metals, Ceramics, & NDE Division
Materials & Manufacturing Directorate

This report is published in the interest of scientific and technical information exchange, and its publication does not constitute the Government's approval or disapproval of its ideas or findings.

*Disseminated copies will show "//signature//" stamped or typed above the signature blocks.

REPORT DOCUMENTATION PAGE

Form Approved
OMB No. 0704-0188

1. REPORT DATE *(DD-MM-YY)*	2. REPORT TYPE	3. DATES COVERED *(From - To)*
August 2006	Final	08/01/2004 – 03/31/2006

4. TITLE AND SUBTITLE
LOW TEMPERATURE, LOW PRESSURE FABRICATION OF ULTRA HIGH TEMPERATURE CERAMICS (UHTCs)

5a. CONTRACT NUMBER
FA8650-04-C-5224

5b. GRANT NUMBER

5c. PROGRAM ELEMENT NUMBER
63500F

6. AUTHOR(S)
Yigal Blum and Jochen Marschall (SRI International)
Hans Joachim Kleebe (Colorado School of Mines)

5d. PROJECT NUMBER
5221

5e. TASK NUMBER
00

5f. WORK UNIT NUMBER
00

7. PERFORMING ORGANIZATION NAME(S) AND ADDRESS(ES)
SRI International
333 Ravenswood Avenue
Menlo Park, CA 94025

Colorado School of Mines

8. PERFORMING ORGANIZATION REPORT NUMBER
SRI P16128

9. SPONSORING/MONITORING AGENCY NAME(S) AND ADDRESS(ES)
Materials and Manufacturing Directorate
Air Force Research Laboratory
Air Force Materiel Command
Wright-Patterson AFB, OH 45433-7750

10. SPONSORING/MONITORING AGENCY ACRONYM(S)
AFRL-ML-WP

11. SPONSORING/MONITORING AGENCY REPORT NUMBER(S)
AFRL-ML-WP-TR-2006-4200

12. DISTRIBUTION/AVAILABILITY STATEMENT
Approved for public release; distribution is unlimited.

13. SUPPLEMENTARY NOTES
Report contains color. PAO Case Number: AFRL/WS 06-2312, 28 Sep 2006.

14. ABSTRACT (*Maximum 200 words*)
The US Air Force is interested in developing fiber-reinforced ceramic composites that perform at ultra-high temperatures (≥1500°C) under oxidative conditions, especially for hypersonic vehicles. Two potential approaches are:
(a) Utilizing existing carbon-fiber-reinforced carbon-matrix composites (C/C) or carbon-fiber-reinforced silicon carbide-matrix composites (C/SiC) coated by thick (>100 μm) ultra-high temperature ceramic (UHTC) coatings, or
(b) Replacing the C and SiC matrices of such composites with an ultra-high temperature matrix, processed by conventional composite techniques.
The most investigated UHTCs are ZrB_2/SiC and HfB_2/SiC particulate composites (70:30 to 80:20 volume ratio). Wet processing via slurries is potentially a practical method for making such thick coatings and matrices. The project focused on developing slurry processing for thick ZrB_2/SiC coatings on SiC and, to a limited extent, C/SiC composite substrates using preceramic and precarbon polymers combined with inert fillers and/or reactive metals. The evolved coatings were tested for their oxidation resistance under various conditions.
A limited effort to assess the capability of bulk compositions made of slurries suitable for processing matrices for fiber-reinforced composites was also performed. Out of two distinctly different approaches and various compositions and preceramic polymers, the most promising stepwise approach was determined to be (a) forming ZrB2/C porous coatings ("preforms") processed from phenolic-based slurries, then (b) reacting the preform coatings with molten Si to form SiC and (c) converting residual Si to SiC. This technique resulted in highly dense, well adhering composite coatings that were 100 μm thick and over. Thick coatings made by this approach provided much better characteristics and performance than other formulations and processes.

15. SUBJECT TERMS
Ultra High Temperature Ceramics (UHTC); Oxidation resistance coatings for fiber reinforced ceramics, Slurry coating processing, ZrB_2/ZrC/SiC particulate composites; Polymer Derived Ceramics (PDC); Polymer derived carbon; Reaction Bonded Silicon Carbide (RBSC)

16. SECURITY CLASSIFICATION OF:			17. LIMITATION OF ABSTRACT:	18. NUMBER OF PAGES	19a. NAME OF RESPONSIBLE PERSON (Monitor)
a. REPORT	b. ABSTRACT	c. THIS PAGE			Michael K. Cinibulk
Unclassified	Unclassified	Unclassified	SAR	120	19b. TELEPHONE NUMBER *(Include Area Code)* N/A

Standard Form 298 (Rev. 8-98)
Prescribed by ANSI Std. Z39-18

CONTENTS

LIST OF FIGURES

LIST OF TABLES

ACKNOWLEDGMENTS

We thank AFRL/MLLN for its active support of this effort throughout the project and in particular we thank Dr. Michael Cinibulk for his technical guidance and support as well as his administrative assistance whenever needed.

We thank Ceradyne Corporation for donating hot pressed SiC substrates that served as the prime material for coating in the project.

1 INTRODUCTION

1.1 Air Force Program Objectives

The Air Force motivation for developing Ultra High-Temperature Ceramics (UHTC) for hypersonic applications in the next generation of aerospace planes lies in the need to minimize or eliminate fuel films and for regenerative cooling of combustion chambers. Cooling systems are currently required because the materials presently in use have an operational limit of 1450°C, which is just 50% of the propellant combustion temperature. Another critical application is related to the severity of aerothermodynamic heating of hypersonic vehicles, which are of growing interest by the Air Force. The hypersonic velocity causes sharp leading edges of currently used aerospace materials such as Inconel X, titanium, or carbon-carbon composites to fail by melting, vaporization, or ablation.

More specifically, the Air Force Research Laboratory (AFRL/MLLN) program supporting this effort called for developing materials and processing methods of UHTCs for potential applications in hypersonic vehicles as either leading edges or scramjet flow path components and for evaluating their oxidation behavior in representative environments. After many years of minimal effort in this area (except perhaps in the Soviet Union), military and civilian government agencies and laboratories such as NASA, the Navy, the Air Force and, to a lesser extent, DOE, are currently expressing a renewed interest in UHTCs for new high-temperature engine designs and as thermal protection materials for sharp leading edges of vehicles flying at hypersonic velocity.

1.2 Project Overall Plan

The research effort focused on exploring and evaluating new slurry formulation processes for composite performance at ultra-high temperatures, with an initial emphasis on developing protective coatings over C/SiC and SiC/SiC fiber-reinforced composite materials. The slurry formulations for obtaining thick coatings are anticipated to be also suitable for producing structural composites. Current processes are not very suitable for the production of fiber-reinforced UHTC matrix composites because of their extreme temperature and pressure conditions, which will destroy or significantly damage the fibers. In addition, the current processing is very costly. Also, a CVI approach for generating such matrices is not feasible, since it is not suitable for fabricating homogeneously mixed phase compositions at the microscale level (e.g., ZrB_2/SiC). Additionally, CVI is an expensive and size-limited process like the hot press approach mentioned above.

The processes that were investigated were based on *in-situ* synthesis (reactions) and formation of the desired compositions at elevated (but not extreme) temperatures (below or around 1500°C). The proposed processing concept encompassed the use of (a) ceramic and carbon precursors (including polymeric precursors and reactive metal powders), (b) intermediate reactive liquid formers, and (c) *in-situ* exothermic reactions.

The research addressed the following critical needs:

- Develop more enabling approaches to the synthesis and processing of UHTCs for use as composite matrices or coatings for conventional CMCs.
- Develop scalable methods for large and complex shaped components under mild or pressureless processing conditions.
- Improve understanding of UHTC composite oxidation in high-speed, dissociated flow environments (via microwave discharge and arc-jet testing).
- Assess UHTC composites containing more than two phases, such as ZrB_2/ZrC/SiC.
- Improve understanding of the role and benefit of a silica former phase and boron content in UHTC composites.

1.3 Proposed Concept

The long-term goal of the project is to explore a new process for developing UHTC particulate composites containing metal borides and silica formers, primarily ZrB_2/SiC and ZrB_2/ZrC/SiC. The investigated approach uses "precursors" to the desired composite components that result in relatively low-temperature development of the final phases and allow for the use of mild conditions for the UHTC composite densification. The precursors were planned to convert to the final phases during the processing and lead to a preferred microstructure via *in-situ* chemistry. The processing temperature target is at or below 1500°C under pressureless conditions.

The ZrB_2/ZrC-based UHTC was selected over the HfB_2/HfC couple for several reasons. First, its density is much lower, while the performance of the two systems was reported to be fairly similar. The density manifested in the form of component weight is a significant issue of concern to aerospace applications. The lower density of Zr and its compounds is also critical for practical processing of slurries. Their particles tend to stay suspended in slurries much longer than Hf-containing particles that are quickly precipitated by gravity. Additional practical reasons for selecting the Zr system are the lower cost of its compounds, broad availability of its ceramic compounds and chemicals, and their much greater studied chemistry, characteristics, and performance.

The intention to use precursor technology for triggering relatively low-temperature chemistry under pressureless conditions is clearly apparent. The formulation of ZrB_2 with polymeric precursors to SiC is an obvious example for powder mixed with a preceramic polymer binder to achieve the desired low-temperature processing. The polymeric precursor serves initially as a binder during the coating or matrix infiltration and then as inter-particle filler that forms homogeneous precipitation of amorphous and, at higher temperature, crystalline silicon carbide around the boride particles.

In addition, polymeric precursors can serve as efficient impregnation materials that will be incorporated as a second step after obtaining an initial porous structure (preform). This infiltration approach may be most useful in the formation of coatings and fiber-reinforced composite schemes. Post-shaping liquid infiltration is also a means to alter the phases of structures generated by relatively low temperature and low pressure processing conditions. For example, the infiltration of polymeric precursor to carbon into porous material containing metal particulates will lead to the formation of carbide phases.

The precursors may also aid the sinterability of the desired composite. A precursor that is processed in a liquid form, or forms a liquid phase at an intermediate temperature, can be dispersed by wetting around the particulates, thereby forming a large area of contact with the particles and subsequently enhancing the rates of inter-diffusivity.

Other approaches to activate the densification of the ZrB_2 or ZrC at relatively mild conditions can be based on the chemistry of the Zr and its compounds that lead to the *in situ* formation of such boride and carbide phases. Such reactions can contribute to the overall phase and microstructure development by leading to thermodynamically favorable phases, being exothermic, or forming a liquid phase to aid sintering and phase transformations.

The concepts for using precursors to ZrB_2/SiC composites can be divided into two major categories: (a) preceramic polymers to either SiC, metal diboride or C intermediate (see discussion below) and (b) powder precursors ("reactive fillers") with favorable reactivity from a thermodynamic standpoint. Additionally, a precursor that leads to a liquid phase intermediate during the thermal cycle would be advantageous, provided that the liquid phase is only a small fraction of the entire formulation, no major volume of gas is evolved, and the liquid phase is transient and consumed during the processing.

Therefore, the concept of using "ceramic precursors" is viewed in this study in broader terms that include:

- Polymeric precursors to the desired composite.
- Precursors to intermediate materials that would further interact to form the final product.
- Reactive liquid formers as a part of the process.
- Reactive powders that would thermodynamically (and preferably exothermically) lead to the desired phases during the thermal processing.
- Reinfiltration reagents that either seal or react and seal pores developed in earlier processing steps.

1.4 Background

1.4.1 Current Processing and Sinterability of Zirconium and Hafnium Based UHTC Composites

The cornerstone of ultra-high-temperature ceramic (UHTC) composites is a small group of metal diborides (MB_2, where M = Hf, Zr, Ti) developed over 30 years ago by the U.S. Air Force [1-7]. In those studies, particulate composites containing silicon carbide (ZrB_2/SiC, HfB_2/SiC and ZrB_2/SiC/C) were identified as the baseline UHTCs because of their enhanced oxidation resistance at high temperature [8, 9].

These composites essentially possess a unique set of material properties including (a) unusually high thermal conductivity, (b) good thermal shock resistance, and (c) modest thermal expansion coefficients that make them particularly well suited for sharp body and leading edge applications on hypersonic vehicles. The composites of ZrB_2/SiC and HfB_2/SiC with volume ratios between 80:20 to 70:30 were found to be particularly efficient UHTCs because the SiC phase enhances the oxidation resistance [10-12].

The main deficiencies of these composites are their high weight and difficult processing. Also, to date, their strength and toughness are not as high as desired. Currently, particulate composites are fabricated in either billet or plate stock using uniaxial hot-press processing, which requires sintering temperatures of 1850°C to 2250°C under a pressure of 7 to 20 MPa (some of the references report the use of higher pressures). Typical components processed by hot pressing are axisymmetric, thus requiring significant amounts of machining and cost to fabricate the parts designed for a leading edge application. A pressureless process plus the capability to obtain near-net-shape configurations would decrease the component fabrication costs making these materials more attractive for aerospace applications.

The high density of HfB_2 (10.5 g/cm^3) and ZrB_2 (6.1 g/cm^3) makes them disadvantageous for lightweight aerospace vehicles. The capability to use these composite materials in the form of thick protective coatings (at least 100 μm thick) over lighter materials such as SiC monolith, SiC/SiC, or C/C composites is in high demand. Such protected structures will also have higher strength and/or toughness and can be processed under more favorable conditions. However, such desirable coatings cannot be processed by the hot-press approach.

Importantly, the sintering mechanisms of hafnium and zirconium borides and carbides are not well studied, and most of the current experimental data has been obtained using an empirical approach. Only within the past year have a few new studies reported sintering of such materials under pressureless conditions or improved densification under hot press conditions in the presence of additives. For example, Loehman reported that the presence of 2% SiC in the hot pressing of HfB_2, and Fahrenholz et. al. revealed that 1 or 2% of WC in hot pressing of ZrB_2/SiC, significantly improved the sinterability of the materials[13]. More recently, the team from U. Missouri has presented a new study demonstrating pressureless sintering of ZrB_2 in the presence of a few percent of boron as an oxide-layer remover additive [14]. Bellosi et al. reported recently that the addition of HfN and Si_3N_4 at the level of a few weight percent improve the sinterability and properties of UHTC [15,16]. This new evidence indicates that the etching of an oxide layer around the boride particles enhances the sinterability. Also, it is possible that the additive aids the formation of an intergranular liquid phase at the processing conditions.

Yet, there is no clear generalization of such sintering mechanisms, and other pathways can be postulated. Compositions of about $MB_{1.9}$ were found to be easier to sinter as well as more resistant to oxidation [17] with respect to the stoichiometric materials. Phase diagrams of such metal boride compositions demonstrate a sharp reduction in what is defined as “incipient melting” when the composition of the metal boride is off the ideal M:2B ratio [18,19].

1.4.2 "Low" Temperature Chemistry and Microstructure Evolution of UHTC Constituents

The current state of the art in processing UHTCs is very empirical and scattered as indicated above and typically performed at temperatures above 1800°C and high pressure conditions. Little is known about the sintering and grain growth mechanisms of the discussed composites, and even less is known about the chemistry of such borides and similar carbides that may be utilized to aid milder condition processing. Furthermore, as found in this reported effort, there are very intriguing phenomena associated with the formation of the SiC phase via reaction bonded SiC (RBSC), which are far from being understood, although major development activities in the past 30 years and significant commercialization of RBSC derived products have been performed.

Effects of ceramic precursors and metallic elements as well as low-temperature reactivities that lead to HfB_2 and HfC and phenomena related to RBSC are currently studied at SRI in an adjacent AFOSR project. In this study we expand the knowledge base of the MB_2/SiC systems through better understanding of the chemistry that affects low-temperature reactions under non-self-propagating high-temperature synthesis (SHS) conditions, microstructure development, densification, as well as the reactivities of the final desired phases in the system of HfB_2/HfC/SiC.[20-22]

1.4.3 Polymeric Precursors to UHTC Constituents

A very limited level of research has been conducted thus far for developing practical preceramic polymer precursors to borides and carbides of Zr, Hf, and other transitions metals. Much more synthesis, processing, and behavior evaluation has been performed in relation to polymeric precursors to SiC and SiOC in the past 20 years, which we planned to assess as potential formers to the SiC phase. Except for a few stoichiometric precursors to SiC such as Starfire's allylhydridocarbosilane polymer (SMP-10), most precursors contain excess of carbon, which can either be used to remove oxide phases via carbothermal reduction or participate in the formation of a transition metal carbide phase, which is part of our strategy.

Approaches based on using preceramic polymer precursors to SiC, can (a) generate a better homogeneity between the MB_2 phase and polymer-derived SiC moiety; (b) enhance the sinterability of the composite via the chemical activation of the amorphous SiC phase during its crystallization and grain growth activity; and (c) promote chemical interactions between the polymer-derived materials and other particulates in mixtures such as the metallic forms of Hf, Zr, or Si. A partial proof of concept for using preceramic polymers for the formation of the desired composites has been reported in the patents of Zank from the mid-1990s [23]. In these patents, ZrB_2 powder is mixed with various polymeric precursors to SiC and heated to between 1900°C to 2250°C under pressureless sintering conditions to produce structures with densities of up to 5.56 g/cm^3 (92% of the theoretical 6.08 g/cm^3). These values are quite impressive considering the fact that any polymeric precursor to SiC shrinks to less than 1/3 of its original volume (from a density of about 1 g/cm^3 to 3.1 of SiC) during the process. The patent includes information about the change of density from the green body stage to the pressureless sintered body. For example, a cured green specimen with density of 3.86 g/cm^3 was sintered to a density of 5.56 g/cm^3 in spite of about 5% weight loss during the process. This indicates that a significant densification mechanism occurs in this system under pressureless conditions.

Recent studies supported by AFOSR have established routes to boron-containing polymeric precursors to MB_2 and MC [24-29]. Some of the efforts have focused on generating processable polymeric precursors containing boron and then blending them with powders of metals or metal oxide to form *in situ* the MB_2 phase at elevated temperature [27-29]. The presence of metal powders causes exothermic SHS-like reactions to proceed, while in the presence of oxide powders, endothermic carbothermal reductions occur and CO gas is evolved. Therefore, the option of incorporating metal powders is favorable for obtaining higher densities. Carbothermal reduction based on molecular blending of Zr or Hf alkoxides with phenolic resin followed by sol-gel processing results in the formation of nanoparticles of the metal carbides, which can be sintered under pressureless conditions [30,31]. Similar alkoxide approaches have also been used to form metal carbide fibers [32-34].

A few other molecular and preceramic polymer approaches have been explored but not yet fully developed. They include (a) direct precursors to Hf and Zr diborides and carbides [35-40] and (b) precursors to SiC and SiOC, which in the presence of reactive fillers (e.g., metals) result in the *in situ* formation of additional carbide phases [41-44].

1.4.4 Reaction Bonded Silicon Carbide (RBSC) and Carbothermal Reactions for Aiding UHTC Processing

RBSC, which is mainly practiced for C/SiC and SiC/SiC composite production and joining SiC structures [45], should be an obvious candidate for pressureless processing of MB_2/(MC)/SiC composites. The rapid reactive infiltration of molten silicon into porous "preforms" is a rational choice for achieving densification under mild processing conditions, especially for making protective coatings. However, using this technique has several drawbacks. First, it is difficult to process RBSC with no presence of residual Si or C in the final composite and the formation of coarse microstructure. In addition, the optimal volume fraction of SiC in the discussed family of UHTC is only around 20 to 30 vol%. It means that the presence of the ultra high temperature component in the preform should already possess 80 vol% and the entire preform should be about 90 vol% dense including the carbon source prior to the Si infiltration. It may be easier to provide such requisite conditions in the processing of a protective UHTC coating, which is very important by itself to protect lightweight fiber-reinforced composites, rather than the processing of bulk structures. Nevertheless, a challenge exists for developing a better chemistry-dependent process that would mitigate the above drawbacks and allow processing of large objects.

Recently, the concept of using RBSC in pressureless processing of ceramic armor is becoming a new developmental trend in the formation of B_4C/SiC composites by infiltrating a carbon-rich B_4C preform with molten silicon. Several of these activities were recently reported at the annual ACerS meeting in 2005 [46,47]. The current state of the art consists of composite products that contain either elemental silicon phase or significant porosity. These activities are highly relevant to our intention for UHTC development by their attempt to bypass expensive and inconvenient hot-press processing at high temperature.

RBSC was first reported in 1960 by Popper [48], who was also the first person to conceive the idea of preceramic polymers in 1966. In spite of 45 years of significant practical activities and cost-effective commercial processing of RBSC, only limited scientific reports have been published about the reaction mechanisms with various carbon sources, the dissolution of the C and/or Si reactants in each other, and the evolution of the SiC crystallization. Two different reaction mechanisms have been proposed: (a) a diffusion-controlled mechanism, proposed by Fitzer and Gadow [49-51] and (b) a liquid phase reaction mechanism in which the carbon is first dissolved in the molten Si, as initially proposed by Pamuch et al. [52,53]. However, it is not clear whether one or both of these mechanisms occur simultaneously or under different conditions. There is also a lack of data about the very efficient capillary infiltration through various micro- and nanoporous carbon structures. Only recently, a study designed to understand the infiltration phenomenon via mathematical modeling was published [54]. This article supports the carbon dissolution mechanism as the initial step of the RBSC but does not rule out the diffusivity of Si through the growing SiC layer at progressive stages of the reactions. The article also emphasizes the physical capillary infiltration of the molten Si as a critical part of the mechanism. The model deals with pore channels of 1 to 5 μm. For the concept discussed in this

proposal we still need to understand how the RBSC reaction progresses in a dense amorphous glassy carbon derived from polymeric precursors, or in the presence of nanopores. Dissolution of SiC in molten Si is another aspect that was not described in the literature in great detail but it is a well known fact that SiC fibers can disappear in the presence of molten Si, if they are not well protected by a BN interface during the matrix formation of reinforced SiC/SiC via RBSC.

A major advantage of using polymeric precursors to carbon is their low cost and existence as commercial products in large quantities. In addition, their initial processing (until the pyrolysis step) can be performed at ambient conditions. Polynaphthalene is a good precursor to meso structured carbon in C/C composites. It can be processed by melt techniques because of its melting point prior to crosslinking at around 300°C. The advantage of the phenolic resin is its complete solubility in water or ethanol and easy processability in a slurry formulation. In this project the phenolic resins were found to be excellent coating formers of slurry compositions.

Another practical function of polymeric precursors to carbon is to serve as a reactant to form *in-situ* SiC phases by interactions with molten Si (see discussion below) and as an oxygen "remover" by carbothermal reduction, if used in a combination with SiOC or MO_2 precursors (e.g., SRI's hydridomethylpolysiloxane precursor chemistry approach [55], alkoxy metal, or $MOCl_2$). The advantages of using the polymeric precursors versus a particulate source of carbon are the simple wet processing capability and the large surface contact between the polymer-derived C and the oxygen-containing components.

Another approach for consideration is the formation of a triple component composite. Studies at NASA and NSWC have indicated that the presence of a metal carbide (ZrC), in combination with the diboride and SiC, can provide a composite that performs similarly to the bicomponent composite [12]. Also, recent studies have demonstrated that equal volume composites are favorable in cases where microstructure tends to coarsened by uncontrolled grain growth at high temperature. Metal diborides tend to do so. Therefore, if a composite with equal volumes of diboride and carbide phases is generated, improvement of the high-temperature performance due to the inhibition of the metal diboride grain growth would be expected. An alternative triple component composite with potential similar capability will be $HfB_2/ZrB_2/SiC$. In this case, it would be preferable to obtain the ZrB_2 as the *in-situ* developed phase, because of easier and lower cost of precursors for Zr-based ceramics.

1.4.5 Oxidation Testing

Oxidation has a large influence on the performance and reliability of UHTC components. Oxidation changes the bulk and surface properties of UHTC materials. Oxides have lower thermal conductivities and lower emittances than virgin UHTC materials, and consequently are less able to dissipate heat by conduction into the interior or re-radiation back to the environment. For reusable applications, the formation of thin, adherent, and self-limiting oxide layers is a requirement.

Since UHTC materials are under development for service in extreme aerothermal heating environments, their oxidation behavior in high-temperature, low oxygen and low total pressure environments needs to be understood. Additionally, during hypersonic flight atomic oxygen is generated by the dissociation of oxygen molecules in the bow shock that forms ahead of vehicle leading edges. Oxygen atoms can diffuse through the boundary layer to the surface, where they

may recombine into molecular oxygen or react with the surface material(s) to form adherent or volatile oxides.

High-temperatures and low pressures of molecular oxygen favor the formation of volatile oxides over adherent oxides. The formation of volatile oxides is known as "active" oxidation, while the formation of adherent oxides is termed "passive" oxidation. Figure 1 below shows the approximate demarcation between the active and passive regimes for SiC on a P_{O2} vs 1/T plot.

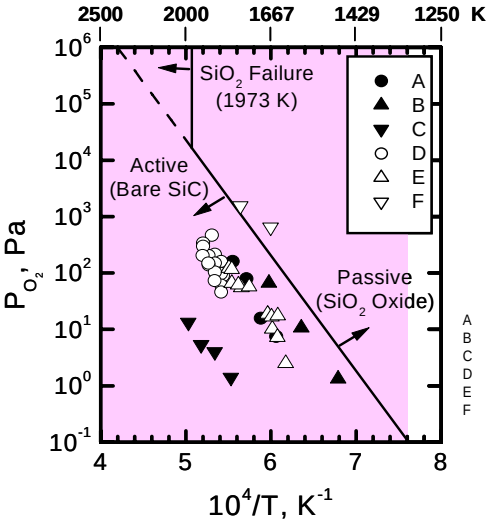

Passive Oxidation:
$SiC(s) + 3/2O_2(g) \rightarrow SiO_2(s) + CO(g)$

Active Oxidation:

$SiC(s) + O_2(g) \rightarrow SiO(g) + CO(g)$

A Hinze, J.W., and Graham, H.C., *Journal of the Electrochemical Society*, Vol. 123, 1976, pp. 1066-1073.
B Gulbranson, E.A., Andrew, K.F., and Brassart, F.A., *Journal of the Electrochemical Society*, Vol. 113, 1966, pp. 1311-1314.
C Rosner, D.E., and Allendorf, H.D., *Journal of Physical Chemistry*, Vol. 74, 1970, pp. 1829-1839.
D Narushima, T., Goto, T., Iguchi, Y., and Hirai, T., *Journal of the American Ceramic Society*, Vol. 74, 1991, pp. 2583-2586.
E Vaughn, W.L., and Maahs, H.G., *Journal of the American Ceramic Society*, Vol. 73, 1990, pp. 1540-1543.
F Balat, M., Flamant, G., Male, G., and Pichelin, G., *Journal of Materials Science*, Vol. 27, 1992, pp. 697-703.

Figure 1. Active and passive oxidation regimes for SiC; experimental data for transition conditions.

Similar behavior is found in diboride materials, which can form either condensed B_2O_3 in the passive regime or volatile boron sub oxides in the active regime. In addition, high-temperature volatilization of the condensed oxides is also possible, but occurs at significant rates at much lower temperatures for B_2O_3 than SiO_2.

Experimental evidence for a variety of other refractory materials suggests that oxidation rates, oxide microstructures, and the boundaries between active and passive oxidation can be significantly different for oxidation by atomic (rather than molecular) oxygen. High-temperature experiments by Rosner and Allendorf [56-58] on the refractory transition metals W, Mo, and Re have demonstrated orders-of-magnitude higher oxidation rates in atomic oxygen versus molecular oxygen. Rosner and Allendorf [56,57] have also shown that atomic oxygen is ~10 times more efficient than molecular oxygen in the high-temperature (1000°K – 2000°K) oxidation of isotropic graphite and ~50 times more efficient in the oxidation of pyrolytic graphite. For SiC, Rosner and Allendorf [58] have shown that the oxidation rates for O and O_2 can cross depending on temperature and pressure. Oxidation by atomic oxygen seems to favor the growth of stable SiO_2 surface oxides under temperature and pressure conditions where oxidation by O_2 leads to the formation of volatile SiO. Likewise, Balat [59] has demonstrated that the boundary between the passive and active oxidation of SiC can be shifted substantially on a temperature-pressure map if atomic oxygen is present. For sintered SiC specimens the temperature-pressure domain, in which a passive surface silica layer formed, was significantly enlarged.

Atom recombination releases chemical energy, some fraction of which may be transferred to the surface as heat. Catalytic recombination can be a substantial contribution to aerothermal heating, as demonstrated in a series of flight experiments on the Space Shuttle [60-62]. Recent laboratory experiments funded by AFOSR show that at moderate temperatures (300 – 1000°K) virgin HfB_2/SiC and ZrB_2/SiC composites have recombination coefficients of ~ 0.01 to 0.005, a value greater than found for silica but lower than oxidized aerospace metals such as Inconel [63]. These experiments also indicate that the surface catalytic efficiency of UHTC materials for recombining oxygen atoms is lowered after surface oxidation. The fractions of the impinging O-atom flux participating in atom recombination or oxidation are coupled and dynamically dependent on the gas environment and the chemical evolution of the surface. Obtaining more experimental data in this area is essential for the further development of materials response models that explicitly include coupling between oxidation, surface catalysis, and aerothermal heating [64].

When UHTC materials are tested in furnace environments, the amounts of atomic oxygen present are insignificant, even at relatively high furnace temperatures. For example, 1 atmosphere of oxygen at a temperature of about 2600°K has an equilibrium dissociation fraction of only ~1% [65]. Thus, conventional furnace oxidation studies do not capture an important oxidant found in flight. On the other hand, testing in large-scale arc-jet facilities (for example the NASA Ames Research Center arc-jets) to simulate atmospheric entry conditions, the oxygen in the gas stream is 100% dissociated [66,67]. This is especially true when testing UHTC materials intended for leading-edge applications, i.e., tests in which the goal is to simulate surface heat flux levels of several hundred W/cm^2. For example, the tests of Bull et al. [68,69] were conducted at enthalpy levels from 18 to 32 MJ/kg and cover a stagnation point heat flux range from about 150 to 600 W/cm^2. Metcalfe et al. [70] reported similar test conditions (enthalpy of 19 MJ/kg and surface heat flux of 400 W/cm^2) for their UHTC arc-jet study, and explicitly stated, "…at this enthalpy, the oxygen is nearly completely mono-atomic." This extreme level of dissociation is unrealistic. Although clear differences in oxide structure and composition between furnace and arc-jet oxidized UHTC materials have been observed, it is not evident how to distinguish between the effects of a supersonic flow environment (e.g., surface shear stresses and transport of reactants and products across shock and boundary layers) and those of oxygen chemistry.

During this research program, we attempted to characterize the oxidation behavior of UHTC coatings in a variety of temperature-pressure-composition gas environments using argon-oxygen mixtures utilizing high-temperature tube furnaces, microwave-discharge flow tubes and a laboratory-scale arc jet.

A 6-kW microwave discharge, formerly used to dissociate semiconductor-processing gases for cleaning and etching operations, was used to generate gas streams with significant concentrations of atomic oxygen. The molecular (discharge off) or partially dissociated (discharge on) gas streams were flown over specimens heated in the tube furnace. The original facility is shown in Figure 2, with a tube furnace limited to ~1000°C. Previous experiments using silicon wafers heated to 900°C for three hours in 4.5 Torr of partially dissociated O_2/Ar or N_2O/Ar streams showed accelerated passive oxidation rates. Silicon oxidation under molecular oxygen is an extremely slow 1 to 10 Å per hour. Oxidized samples were examined using spectral ellipsometry and we found oxide layers 1114 Å and 1381 Å thick for the $0.83O_2/0.17$Ar and the $0.80N_2O/0.20$Ar gas mixtures, respectively, when the discharge is on. In contrast, an

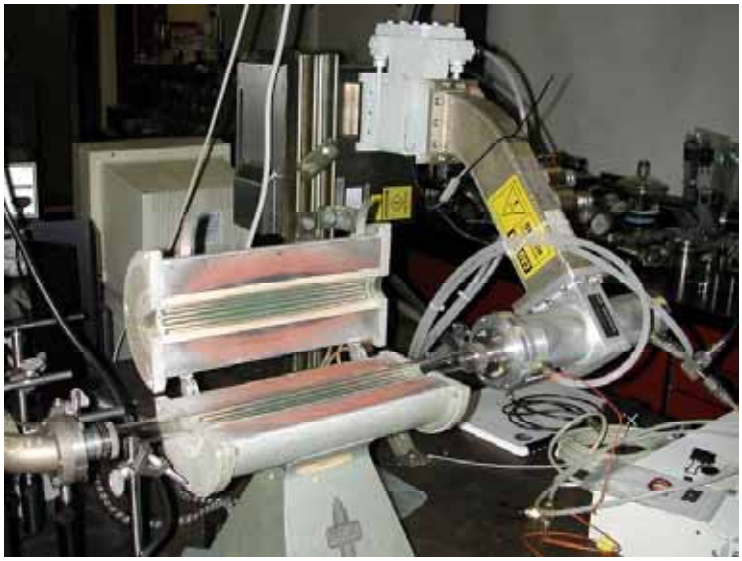

Figure 2: High power microwave discharge facility.

oxide layer of only 65 Å was found for the $0.83O_2/0.17Ar$ mixture when the discharge was off. The growth rate is thus enhanced by factors around 20 by the presence of atomic oxygen in the gas stream. For UHTC studies, this facility was upgraded with two higher-temperature tube furnaces enabling tests up to 1500°C.

Additional experiments were attempted using a laboratory-scale arc-jet constructed at SRI for an AFOSR sponsored research project. The arc-jet has a 13 kW power supply and a roots-blower pumping system capable of maintaining chamber pressures below 1 Torr during operation. However, the design of the arc-jet was susceptible to stream contamination by degrading cathodes in the arc-jet head. Several iterative attempts were made to modify the apparatus to eliminate this contamination problem (these attempts are described below) but unfortunately these proved unsuccessful. Consequently, only very limited testing was conducted in this facility.

2 METHODS, ASSUMPTIONS, AND PROCEDURES

The project focused on evaluating slurry approaches for producing dense UHTC composite coatings to provide protection against oxidation. The emphasis was, therefore, on formulations that can be processed as coatings on C and SiC fiber-reinforced SiC composites. However, selected slurry formulations were also evaluated in a bulk form as potential UHTC matrices for future development of fiber reinforced UHTC composites.

The studied formulations were based on using:

- Polymeric precursors to SiC, SiOC, and C
- Liquid phase formers (Si and $B_2O_{3)}$
- Reactive metal powders (Si, Zr and/or B)
- Inert fillers (ZrB_2, SiC, ZrC, HfC, HfO_2; unexpectedly some were found to be reactive)
- Solvents (type depends on the polymeric precursor).
- Additional additives as necessary.

The exploratory phase involved all aspects of processing: polymer-relevant characteristics, slurry formulations and assessment of the slurry stability, coating deposition parametric evaluation, coating integrity and adhesion prior and post pyrolysis, and phase evolution after further heat treatment or further reaction steps.

2.1 Slurry Formulations

The Zr-containing powders were ball milled prior to their formulation to advance their reactivity or achieve preferred green and final microstructures of coatings. Then, a polymeric precursor was added, already dissolved in an appropriate solvent, and the slurry was ball milled again. For slurries prepared for coatings, it was important to adjust the level of solvent to bring the viscosity to the level required for achieving 30 to 50 µm layers per dip coating operation. The initial criterion for the amount of polymer in each of the formulations was always the calculated level needed to meet the final 80:20 or 70:30 volume ratio between the Zr phases and SiC, based on calculating the post-pyrolysis ceramic yield of the polymer.

However, the precursor rheological characteristics, ceramic yield, and post-pyrolysis microstructures of coatings required frequent deviations from the above criterion. For example, it was necessary to adjust the amount of any chosen polymeric precursor for achieving optimal binding characteristics of the evolved ceramic coatings. If the precursor amount was too low there was inadequate binding between the particles and insufficient adhesion of the coating to the surface. If the amount of the polymer was too high it led to the formation of a microstructure, where the filler particles were separated from each other and "floated" in the polymer. This configuration tends to cause severe mud cracking and delamination from the substrate due to the significant shrinkage that occurs during the conversion of the polymeric precursor to ceramic product. A typical polymeric precursor with a density of about 1 g/cm^3 ends as a pyrolyzed amorphous ceramic product with density varied from 2.2 to 2.9 g/cm^3. This implies a volumetric shrinkage of over 60%.

2.2 Formulation Development Guideline

Past experience in developing slurry-derived ceramic coatings based on preceramic polymers combined with the processing knowledge accumulated in this project led to the establishment of the following practical guideline, which is generic to a broad range of preceramic slurry coating processing.

- The slurry needs to be physically stable for at least 10 minutes without significant segregation of powders by gravity due to incompatibility with the solvent/polymer system.
- The slurry coating needs to wet the surface well during deposition.
- The deposited slurry should be stable enough that no gross separation between powder and polymer will occur before the polymeric precursor is cured or solidified (consolidated).
  - The points above make it difficult to use Hf and its compounds as the primary powder source for formulating UHTC slurry, because they gravitate quickly to the bottom of the slurry.
- The coatings need to adhere to the surface after each of the processing steps: curing, pyrolysis, and heat treatment.
  - If the adhesion is not sufficient after curing, the weak adhesion will be maintained throughout the process.
  - Good post-curing coating adhesion is typically associated with better integrity of the pyrolyzed coating.
- The desired thickness of the coatings was 30 to 50 μm per layer in this project, but at the same time the coatings must remain significantly crack-free and should not delaminate after the pyrolysis step.
- The final coatings should have integrity in the form of (a) relatively high density and (b) adequate inherent strength.
  - This can be accomplished, if the level of polymer just fills the gaps between the self-packed powder particles rather than letting the particles float in the polymer matrix.
    - Polymer levels exceeding the volume necessary to fill the voids between the powder particles lead to severe mud cracking due to polymer shrinkage during pyrolysis.
      - A mild level of coating cracks without affecting the bonding of the coating to the surface is still sufficient. This is especially true in the case of fiber-reinforced composites where the gaps of such cracks can be closed at high temperature, while at low temperature the cracks prevent high interface stresses due to mismatch of coefficient of thermal expansion (CTE).
    - Polymer level below the volume needed to fill the voids between the powder particles results in undesired porosity in the coating.
      - This situation is still acceptable assuming that the coating can be sealed by reinfiltration with additional polymeric precursor. In fact, it is the preferred strategy in some cases.

    - However, polymer reinfiltration followed by its shrinkage during pyrolysis tends to generate significant stresses at the interface with the substrate resulting in severe coating delamination.
- Trade-offs between the coating integrity and the desired compositions are typically required, since it is rare to meet both the coating integrity and the composite volume fractions at the same time.
- The coating formulations need to demonstrate integrity and some mechanical durability in a freestanding cast form.

2.3 Generic Coating Deposition Techniques

The formulated slurries were deposited by a simple dip-coating technique after viscosity adjustment for generating the desired thickness. Multiple layers and graded multiple coatings were also deposited in the same manner and assessed to achieve high-integrity coatings with good bonding to the substrates and minimal defects.

The planned target substrates to be protected by the developed UHTC composite coatings are SiC matrix composites. However, the coating of such composites was perceived to require more processing adjustment for each type of slurry due to the complexity and the roughness of such composite surfaces as well as the surface composition. In addition, for better understanding of the coating behavior by themselves with minimal effects caused by the substrate, it was decided to perform most of the exploratory development on 1”×1/2”×1/16" specimens of monolithic hot-pressed SiC (produced by Ceradyne). This choice allowed us to use hundreds of trial and test specimens during the performance of the project. A few tens of C/SiC composite specimens, produced by GE-CCP’s CVI process (1”x1/2”x1/4") were received from NASA-Glenn Research Center and selectively coated with the most promising coating formulation/process at the end of the project. However, no parametric iterations were performed on such composites.

2.4 Curing, Pyrolysis and Heat Treatment

The deposited slurry coatings were dried overnight and then thermally cured according to the need of each polymeric precursor or binder. Typically, the curing is performed at 100 to 150°C for 1h in air or Ar depending on the precursor sensitivity to oxygen at these temperatures. The coatings were then pyrolyzed by slow heating to 1000°C under flowing atmospheric argon (flow rate of 1 mL/s). It is highly recommended to designate a separate furnace tube and sealing assembly for the pyrolysis step because of the high level of volatilization of organics and organo-silicon compounds and their redeposition in colder parts of the assembly during the pyrolysis process. A standard pyrolysis step consisted of a heating rate of 5°C/min with a dwell period at 1000°C in cases where previous lab experience, literature procedures, or manufacturer given procedures were not available. Nevertheless, it is recommended that during a further developmental stage, the curing and pyrolysis as well as further heating procedures to higher temperatures would be individually studied, to maximize the conversion yields and minimize stresses during temperature stages at which gas is evolved or major restructuring of microstructure occurs.

For most of the multiple layer procedures, each layer was cured and pyrolyzed individually before the deposition of a subsequent layer. However, in the case of depositing

porous ZrB_2/C preform, using phenolic resins as both a binder and a polymeric precursor, a coating technique was used in which up to 3 layers of slurry (30 μm each) were deposited with only a curing step between the deposition of consecutive layers.

Surface processing, such as mechanical roughening or polishing, was considered. Surface polishing decreased in general the adhesion between the coating and the SiC specimens but may prevent undesired voids between the coating and the substrate. In contrast, a slight roughening of the surface with a diamond grinding wheel assisted the bonding to the surface. In that regard, the very rough seal coating covering the CVI processed C/SiC composite specimens was found to be very good for the developed coating process. Chemical treatment of the surface with slight oxidation or coupling agents did not provide any better results.

The coating study involved the assessment of slurry stability and wetting to the surface. It dealt with controlling the thickness of dip coated films to about 30 μm per layer by controlling the viscosity via the type and the level of solvent.

2.5 Potential Concept Adaptation to Structural UHTCs

In parallel to the coating development, selected formulations were also assessed for their ability to make fiber-reinforced UHTC matrix composites. In particular, formulations that form slurries with consistency suitable for fabric infiltration processes were explored. Study of such coating compositions for their own physical and microstructural integrity and oxidation behavior was performed to

- Better verify the intrinsic properties of the coating without incorporating interfacial stresses and physical damage derived from the coating processing.
- Obtain a database for future development, in which the slurry will be used as a matrix precursor in composite formulations.

This effort focused primarily at the combination of ZrB_2 powder mixed with a low viscosity preceramic polymer to stoichiometric SiC (SMP-10, produced by Starfire Systems).

2.6 Coating Characterization

2.6.1 Microstructure Analysis

The homogeneity, integrity, coverage and bonding to substrate, and their behavior as a function of composition, thickness and thermal treatment are critical parts in the evaluation of slurry-based ceramic coatings. Another important issue is to understand the evolution of the different phases and their corresponding microstructures, as well as the characterization of the interface region between coating and substrate (based on the in-situ induced chemistry). These evaluations were extensively performed throughout the progression of the project, using a combination of scanning electron microscopy (SEM), energy-dispersive spectroscopy (EDS) and X-ray powder diffraction (XRD). The SEM analyses followed each of the explored formulations and were performed after each of the processing steps, including topical and cross sectional analyses. The same analyses were also the main analytical tools to evaluate oxidized coatings. Selected coatings were submitted to Colorado School of Mines for further microstructural analysis by high resolution SEM.

2.6.2 Mechanical Properties

Mechanical properties of the coatings were not the main focus of the study. However, during the formulation/process screening, each type of a new coating was evaluated by a razor blade scraping test (laboratory grade blade), in which the coating was scraped at one side of the coated surface along the dipping direction in an attempt to remove the coatings. Poor coatings could be easily removed by this test due to their own low compressive strength (porous coatings) or weak bonding to the substrate. Coatings with medium integrity but strong adhesion to the substrate left a coated layer at the substrate's surface, even if they were partially removed. The best coatings are not scratched by the razor blade. Instead, they wear the blade itself, as manifested by a "smear" of metallic film on top of the coating as analyzed by EDS. A limited number of microhardness analyses were performed at the end of the project on the most promising coating systems.

2.6.3 Oxidation Study

The oxidation characteristics of the UHTC coatings were the second focus of this early development effort. Various coatings and a few promising slurry-derived bulk materials were assessed during the course of this project under the following sets of conditions: (1) high and low partial pressures of oxygen in an overall pressure of 1 atmosphere and argon as the balancing gas; (2) low pressure mixtures of O_2/Ar; (3) low pressure mixtures of dissociated oxygen atoms (O/O_2) generated by a special high-power microwave discharge attached to a tube furnace. It is estimated that approximately 5% of the oxygen is dissociated under the test conditions.

For the discharge experiments, the primary experimental protocol consisted of exposing similar samples at the same temperature, pressure, flow velocity, and inlet gas composition, under equilibrium (discharge off) and activated (discharge on) conditions. The purpose of this part of the study was to (1) compare the oxidation resistance of different UHTC samples and (2) document differences in oxidation observed under equilibrium and activated gas flows.

The oxidation experiments were performed in alumina tubes and the specimen holder was made from hot pressed SiC. Under the high-temperature conditions, especially in the low pressure experiments, aluminum was detected at the surface during the post oxidation analysis by EDS, indicating a low level evaporation of material from the tube furnace itself.

The original plan was to study the performance of the coatings in a laboratory-scale arc-jet apparatus that was built at SRI. The apparatus required several upgrades to reach the high temperature conditions expected for UHTC operations. Several modifications have been incorporated during the performance of this effort but only a few experiments were performed at the desired conditions. For arc-jet experiments, the primary experimental protocol consisted of exposing different UHTC coatings to similar plume conditions. A second experimental protocol involved the exposure of coated samples to multiple rapid heating and cooling cycles by inserting and withdrawing the sample repeatedly from the plume. The goal of both tests was to assess and compare the stability of different coated materials in the same supersonic, reactive flow stream.

The primary comparative evaluation of the oxidized specimens was (1) change of sample mass, (2) overall microstructure analysis to detect deformations, delaminations and phase segregation, (3) depth of oxide layer, and (4) difference in oxide composition and morphology as a function of topological position in the coating and cross-sectional depth. Microstructural

variations of compositions were analyzed by EDS and overall phase change analyses were assessed by XRD analyses of oxidized specimens.

3 RESULTS AND DISCUSSIONS

3.1 Exploratory Process Development

The project began by assessing a processing approach in which Zr-containing powders were mixed with silicon containing preceramic polymers, precursors to SiC and silicon oxycarbide (SiOC). A second processing system based on reaction bonded silicon carbide (RBSC) was introduced after 2 months of research. The variety of the basic formulations evaluated in each system is illustrated in Figure 3. The research of the two basic systems is described separately in this report in a chronological order. It should be noted that the second system was chosen at a later stage as the leading approach for further development. Nevertheless, the information about the first system is considered to be very useful for investigators planning to use ceramic coating approaches based on preceramic polymers in general. Also, some of the preceramic polymer slurries investigated in this study can be easily adapted to CMC processes in which the slurry serves as a precursor to UHTC matrix.

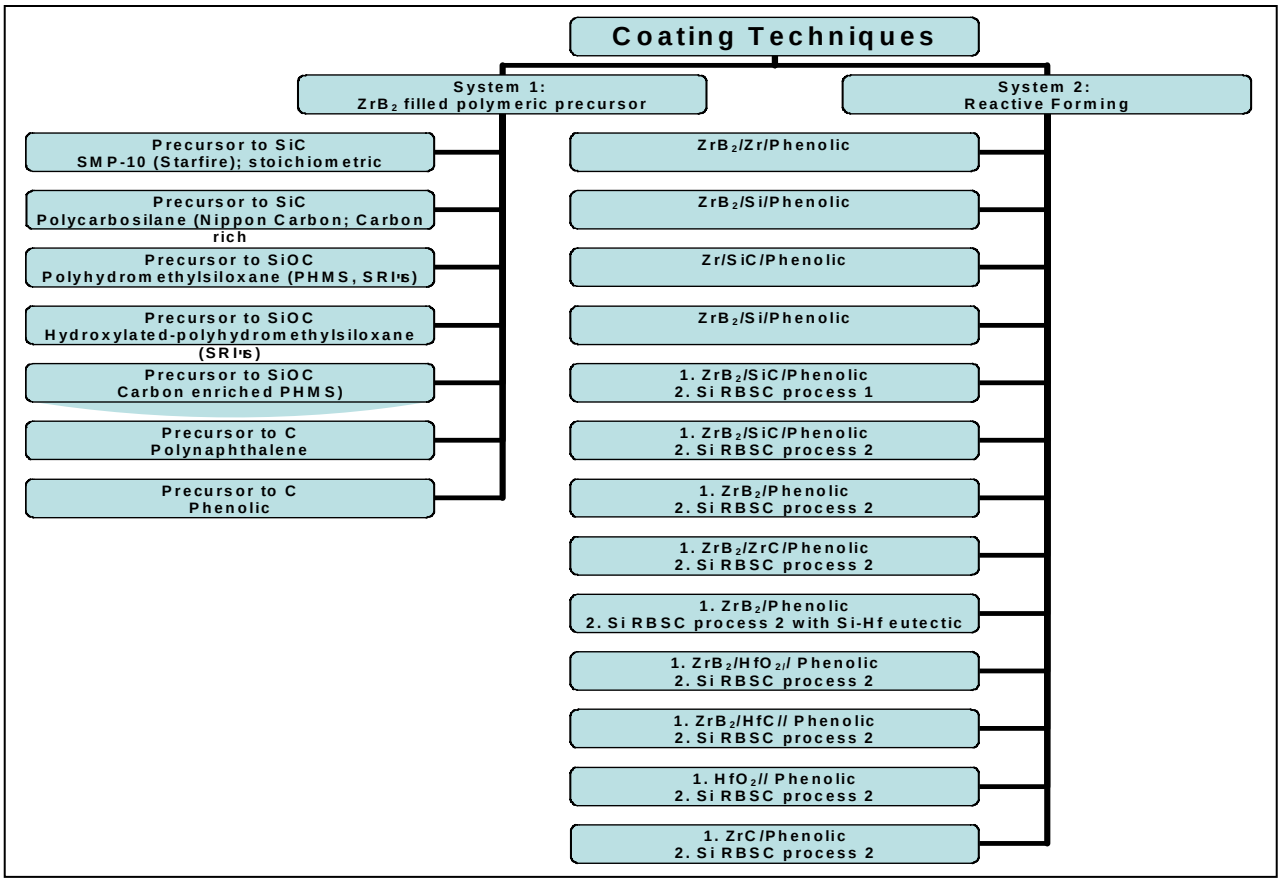

Figure 3. Slurry formulation variations studied under the two approaches during the project.

3.2 Approach 1: Coatings Based on Si-Containing Preceramic Polymers

The preceramic polymer study consisted of assessing the potential of existing preceramic polymers that convert by pyrolysis to SiC, SiOC or C. Potential polymeric precursors to ZrB_2 and ZrC were not selected, because they were not readily available and needed a special exploratory synthesis effort. Furthermore, if such polymers are developed, they will likely be significantly more expensive (even at a commercial level) than any of the commercially available SiC precursors, even if they provide the desired stoichiometry (which is not an easy to achieve). However, polymeric precursors to C were studied because of their capability to form SiC and ZrC in the presence of Si and Zr, respectively.

The base formulations under this approach consist of low viscosity slurries containing (a) polymeric precursors, (b) appropriate powders, and (c) proper solvents. The starting point for each of the formulations was a composition that led to 20 vol% SiC and 80 vol% of ZrB_2 or ZrB_2/ZrC combination. Deviation from the designated composition ratio was done during the process development to improve physical, mechanical and microstructural characteristics according to the assumptions set below.

- If the precursor is liquid prior to curing, the particles can start segregating from the polymer after coating when the volume of the polymer is higher than ~50 vol%.
- If the preceramic polymer phase occupies more than just the free space between the packed particles, then the shrinkage during the pyrolysis causes significant cracking.
- If the amount of the polymer volume is too low, a very porous coating is formed. This part may not be a problem and it may even be advantageous, when a process involving re-infiltration steps of a liquid or solution precursor into the porous coating is considered.

3.2.1 Polymeric Precursor Assessment

The preceramic formulation effort began with reassessing curing, pyrolytic and post pyrolytic characteristics of a series of polymeric precursors that were selected for the process development in their native and formulated version. Some of the polymers required the development of appropriate handling and processing as well as curing procedures since these polymers are not reported for their coating curing procedures, air/moisture sensitivity, or incorporated volatile components (such as crosslinkers). Table 1 summarizes the preceramic polymer evaluation results.

Table 1: Processing Characteristics of Polymeric Precursors

Polymeric Precursor	Handling	Curing Conditions	Pyrolysis Conditions	Conversion Yield	Pyrolyzed Compositions
Precursors to Carbon					
Polynaphthalene	In air	Air at 300°C/ overnight. Curing in a molten phase by partial oxidation according to manufacturer. Not very efficient	Ar, 2°C/min; 1000°C;1h,	Much lower than the 70-80 wt% reported by manufacturer	Assumed to be over 95% carbon
Phenolic Resin (73% in water)	In air	160°C/ 1h	Ar, 5°C/min; 1000°C;1h	62 wt%	Assumed to be over 95% carbon
Precursors to SiC					
Starfire's SMP-10 (polycarbo dihydridosilane)	Mixing formulation in glove box because of moisture sensitivity	1°C/min to 200°C,2h,1°C/min to 400°C, 2h (according to manufacturer)	1°C/min, 600°C, 2h; 2°C/min, 1000°C, 2h, (according to manufacturer)	77 wt%	Assumed to provide stoichiometric SiC
Poly-carbomethylsilane (Nippon Carbon's original product)	In air	150°C/2h (weight increase of 2-3% due to curing by oxygen incorporation)	Ar, 5°C/min; 1000°C;1h	82 wt%	Provides SiC with excess of "free" carbon (and 5% oxygen)
Precursors to SiOC					
SRI's Polyhydridomethyl siloxane (Hydroxylated; PHMS-OH)	In air	110°C, overnight	Ar, 5°C/min; 1000°C;1h	80 wt%	Provides SiOC with some free carbon
SRI's Polyhydridomethyl siloxane (PHMS)/ 5wt% vinyl siloxane crosslinker	In air	Room temperature overnight; 110°C, overnight	Ar, 5°C/min; 1000°C;1h	82 wt%	Provides SiOC with some free carbon Mol ratios: Si 1.0; C 1.28; O 1.08 (less oxygen than PHMS-OH
SRI's Polyhydridomethyl siloxane (PHMS)/ 60 wt% divinylbenzene crosslinker	In air	Room temperature overnight; 110°C, overnight	Ar, 5°C/min; 1000°C;1h	80 wt%	Provides SiOC with some free carbon Mol ratios: Si 1.0; C 2.87; O 1.04 (less oxygen than PHMS-OH; much more "free carbon"

3.2.2 Coating Process and Characterization Study

All the studied formulations were followed through each processing step for assessing the effects on thickness, adhesion, micro integrity, morphology and phase development.

Initially, an extensive number of formulations were studied in parallel. It included the assessment of a variety of polymeric precursors, reactive fillers (Zr, and Si), and a new concept of forming a second phase by re-deposition of a second layer. Initially, the appropriate solvent was adjusted to provide slurries that could be deposited as 10 to 20 μm thick layers. This thickness level is assumed to tolerate mismatch of CTE between the evolved coating and the substrate. Later, the thickness was increased to the range of 30 to 50 μm per layer. The thicker coatings were not necessarily cracked or delaminated in case that some porosity existed in the coating due to polymer filling deficiency. Such porosity could be conceptually re-infiltrated with a second layer coating of polymer solution with no added powder or excessive level of polymer added to the consecutive coating formulation.

Table 2 provides examples of formulations studied at the early stage of the exploratory effort. It details selected formulations and correlates between formulations and the post-processing coating characteristics. Initially, we demonstrated the capability to form coatings based on mixing powders with preceramic polymers. By adjusting the amount of the polymer's volume relative to the powder's we were able to obtain coatings with no or with minimal cracking levels that adhered well to the SiC substrates and did not delaminate.

Table 2. Correlation Between Slurry Formulations and Derived Coatings and Examples of Formulations Practiced at Early Stage of the Effort.

Formulation	Curing	Pyrolysis	Heat Treatment	Characteristics and Comments
Precursors to Carbon				
Polynaphthalene				
Zr (4.56g) polynaphthalene (PN) (5.19g of 16.5wt% in toluene (0.86g PN), toluene (~8g)	300°C/ air/ overnight	→	2°C/min to 1500°C,1h, Ar	Provides a powdery material, does not adhere well to surfaces. Significant weight loss (21wt%). Abandoned at early stage of project.
Zr (4.56g) PN (7.62g of 11.25wt% in toluene (0.86g PN) ZrB_2 (5.64g)	300°C/ air/ overnight	→	2°C/min to 1500°C,1h, Ar	Provides a powdery material, does not adhere well to surfaces. Abandoned at early stage of project.
ZrB_2 (11.28g) Si (1.04g) PN (5.69g of 11.25wt% PN in toluene (0.64g PN)	300°C/ air/ overnight	→	2°C/min to 1500°C,1h, Ar	Provides a powdery material, does not adhere well to surfaces; significant weight loss (6.37wt%). Abandoned at early stage of project.
Phenolics				
4.56 gm zirconium powder 1.51 gm phenolic solution, SP-6877) (Schenectady International) 6.5 gm ethanol	curing at 120°C in air for 2h.	5°C/min to 1000°C, 1h, Ar	5°C/min to 1500°C,1h, Ar	Too thin, may not cover the entire surface with particles. Bulk formulation that fits the stoichiometry of ZrC contains too much polymer for coatings but may be very attractive for lay-up composite, including pressed lamination and curing. **Coatings:** Thin layer, not covering all the substrate surface with particles; powder-polymer separation; bond well to substrate.

Table 2. Correlation Between Slurry Formulations and Derived Coatings and Examples of Formulations Practiced at Early Stage of the Effort. (Continued)

Formulation	Curing	Pyrolysis	Heat Treatment	Characteristics and Comments
Precursors to Carbon				
4.56 g zirconium (2^{nd} pk) powder, 1.51 g phenolic solution (HRJ-14209; Schenectady International) 6.0 g ethanol	Curing at 120°C in air for 2h.	5°C/min to 1000°C, 1h, Ar		**Bulk:** Remains chunky with some strength after curing, pyrolysis and heat treatment. Formulation that fits the stoichiometry of ZrC contains too much polymer for coatings but **may be very attractive for lay-up composite including pressed lamination and curing.** **Coatings:** Some areas are not coated well; no crack; bond well to the surface.
Silicon – Carbon black				
ZrB_2 (11.28g); Si (1.04g); C-black (0.45g) methanol (8g)	NA	NA	2°C/min to 1500°C,1h, Ar	Loose powdery coating on C/SiC comp. after pyrolysis. Provides a powdery material; does not adhere well to surfaces.
Precursors to SiOC				
PHMS-OH				
ZrB_2 (5.64g) ; PHMS-OH (1.63g of 42.86 wt% in EtOH) (0.70g PHMS-OH) EtOH (7g)	100°C/air/ overnight	→	2°C/min to 1500°C,1h, Ar	Coating on C/SiC is bonded after pyrolysis. Also a second layer bonds well to the composite; total weight loss is reasonable (7.95wt%); only ZrB_2 is observed by XRD. No carbide, oxide or silcide phases.
ZrB_2 (5.64g); PHMS-OH (1.63g of 42.86wt% in EtOH) (0.70g PHMS-OH) EtOH (7g)	110°C overnight	5°C/min to 1000°C, 1h, Ar		Uniform coating; bonds well to surface. Only at the bottom where the coating is much thicker, a low level of cracking is developed. The coating is porous; precursor seems to serve as binder, but not as a good filler between the powder particles.
ZrB_2 (22.56g); PHMS-OH -- 6.52g of 42.86wt% in ethanol (0.70g PHMS-OH) ethanol 6g	110°C for 2 hrs, air	5°C/min to 1000°C,1h, Ar	5°C/min to 1500°C,1h, Ar	Good adhering coatings after pyrolysis. Poor bonding of coating after heating to 1500°C. Si content is completely depleted. Both cracking and porosity is observed. The particles are "rounded" suggesting surface reactivity.
ZrB_2 (22.56g) PHMS-OH (6.52g of 42.86wt% in ethanol) (=0.70g PHMS-OH) ethanol (6g)	110°C for 2 hrs, air	5°C/min to 1000°C, 1h, Ar	5°C/min to 1500°C,1h, Ar	Good adhering coatings after pyrolysis; mild cracking but still strong bonding to surface; not scraped by razor blade (the blade smears on the coating) Poor bonding of coating after heating to 1500°C. Si content is completely depleted. Both cracks and porosity are observed. The particles are "rounded," suggesting surface reactivity.

Table 2. Correlation Between Slurry Formulations and Derived Coatings and Examples of Formulations Practiced at Early Stage of the Effort. (Continued)

Formulation	Curing	Pyrolysis	Heat Treatment	Characteristics and Comments
Precursors to SiOC				
PHMS-OH				
ZrB_2 (22.56g) PHMS-OH 6.52g of 42.86wt% in ethanol (=0.70g PHMS-OH) ethanol 6g	110°C for 2 hrs, air	5°C/min/1000° C, 1h, Ar	5°C/min to 1500°C,1h, Ar	Good adhering coatings after pyrolysis; somewhat cracked due to the thickness. Poor bonding of coating after heating to 1500°C. Si content is completely depleted. Both cracking and porosity are observed. The particles are "rounded," suggesting local surface reactivity.
PHMS-vinyl curing				
Zr (7.2g), PHMS (7.5g) tetravinyltetramethylcyclo-tetrasiloxane (0.375g); Pt cat (3 ppm vs PHMS); 45 mg of 5x10-4 Pt/g solution)	120°C/air/ overnight	2°C/min/ 1000°C/ Ar/ 1h	5°C/min/ 1500°C/ Ar/ 1h	Bulk pyrolysis only; lost 11.30wt% during pyrolysis and 15.53wt% during heat treatment
Zr (7.2g), PHMS (7.5g) divinylbenzene (0.75g) Pt cat (3 ppm)	120°C/air/ overnight	2°C/min/ 1000°C/ Ar/ 1h	5°C/min/ 1500°C/ Ar/ 1h	Bulk behavior: 80°C/air: not uniform; formed two layers due to particles sedimentation. No coatings were generated
Zr (7.2g), ZrB_2 (3.0g) PHMS (7.5g) tetravinyl tetramethylcyclo-tetrasiloxane (0.375g), Pt cat (3 ppm/gm PHMS)	110°C; 2h	5°C/min; 1000°C,1hr, Ar;	5°C/min to 1500°C, 1hr, Ar;	Bulk: significant loss when pyrolyzed and when further heated at 1500°C lost 19.2 wt% during pyrolysis and 7.53wt% during heat treatment. Coatings: In spite of the high weight loss there was an excessive amount of polymer, resulting in the formation of a layer of polymer-derived crust. The 20 µm crust is cracked but remains intact and non-delaminated. The bulk is fairly strong. The microstructure of the cross section is dense and showing filling of polymer derived ceramic between the particles. Filling is also shown after heating at 1500°C and integrity is maintained. The microstructure reveals also submicron dots suggesting a reaction with the Zr.
Zr (7.2g), ZrB_2 (3.0g) PHMS (7.5g), divinylbenzene (0.75g) Pt cat (3 ppm/gm PHMS)	110°C; 2h	5°C/min; 1000°C,1h, Ar	5°C/min to **1500**°C, 1h, Ar	Lost 21.86wt% during pyrolysis – too much; 8.80wt% loss during heat treatment – too much; At 1500°C the glassy crust of the polymer-derived material is less observable at a large scale but at higher magnification a thin transparent cracked layer is observed. Zr powder may be too oxidized; polymer amount needs to be reduced
Zr (7.2g), ZrB_2 (3.0g), PHMS (7.5g), tetravinyl tetramethylcyclo-tetrasiloxane (0.375g), Pt cat (9ppm)	110°C overnight	5°C/min; 1000°C, 1h, Ar		Bulk: Pyrolysis caused high weight loss (22.02 wt%). Very rapid curing occurred with heat formation and bubbling due to the high level of catalyst. Coatings: The polymer level seems to be more than needed to fill the voids between the particles. A thin glassy crust is formed with cracks typical to thin amorphous layer of unfilled polymer-derived ceramics; Cross section reveals a "Swiss cheese" macrostructure. Zr powder may be too oxidized.

Table 2. Correlation Between Slurry Formulations and Derived Coatings and Examples of Formulations Practiced at Early Stage of the Effort. (Continued)

Formulation	Curing	Pyrolysis	Heat Treatment	Characteristics and Comments
Precursors to SiOC				
PHMS-vinyl curing				
Zr (7.2g ZrB_2 (3.0g) PHMS (7.5g) tetravinyl tetramethylcyclo-tetrasiloxane 0.375g Pt cat (9ppm)	110°C overnight	5°C/min, 1000°C, 1h, Ar	5°C/min to 1500°C, 1h, Ar	Zr powder may be too oxidized.
Zr (7.2 g) ZrB_2 (3.0g) PHMS (7.5 g) tetravinyl tetramethylcyclo-tetrasiloxane (0.375 g) Pt cat (9ppm)	120° C for 2 hrs	5°C/min to 1000°C, 1hr, Ar		Non-uniform coating; polymer islands are formed with cracks due to local separation between polymer to powder. Approach was abandoned.
Precursors to SiC				
Starfire's polycarbosilane (stoichiometric)				
ZrB_2 3.52g SMP-10 (0.66g) cyclohexane (7.1g)	Weigh SMP-10 and cyclo hexane in dry glove box. 1°C/min to 200°C,2hr,1°C/min to 400°C, 2hr,	1°C/min, 600°C, 2h; 2°C/min, 1000°C, 2h,	5°C/min **1500**°C,1h, Ar	Heat treatment weight loss 3.11wt%; bulk formulation holds together after both pyrolysis and heat treatment. Some dip cracking is observed in the porous structure. It shows porosity, with little evidence of pore filling by the polymer after pyrolysis. After heating at 1500°C, the integrity of the bulk remains good in spite of the porosity. Submicron dots on top of the larger particles and whiskers are observed.
ZrB_2 3.52g SMP-10 (0.825g) cyclohexane (5g)	dry glove box mixing 1°C/min to 200°C,2hr,1°C/min to 400°C, 2h,	5°C/min, 600°C, 2h; 2°C/min, 1000°C, 2h,	5°C/min to 1500°C, 1h, Ar	Lost 3.47wt% during heat treatment. The pyrolyzed bulk has good integrity and relatively low porosity. Almost no cracks. Binder is observed between particles. It seems that a thin polymer layer has been developed at the top surface of the bulk due to precipitation at the pre-curing stage. Higher density is also observed after heating at 1500°C. The large particles are coated with a rough skin that may be the result of the polymer crystallization. The features are submicron and even at the nano scale
ZrB_2 (3.52g) SMP-10 (0.99g) cyclohexane (5g)	dry glove box mixing; 1°C/min to 200°C, 2h, 1°C/min to 400°C, 2h,	5°C/min, 600°C, 2h; 2°C/min, 1000°C, 2h,	5°C/min to 1500°C, 1hr, Ar	Very similar microstructural to observations described above. Lost 2.86wt% during heat treatment; cracks are widening but are not connected like mud cracking. The polymer phase is clearly observed between the particles and densifies the material. Some cracks are observed in the polymer-derived phase. Submicron dots also.

Table 2. Correlation Between Slurry Formulations and Derived Coatings and Examples of Formulations Practiced at Early Stage of the Effort. (Continued)

Formulation	Curing	Pyrolysis	Heat Treatment	Characteristics and Comments
Precursors to SiC				
Starfire's polycarbosilane (stoichiometric) (continued)				
ZrB_2 (14.08g) SMP-10 (3.96g) cyclohexane (5g)	dry glove box mixing; 1°C/min to 200°C, 2h, 1°C/min to 400°C, 2h,	5°C/min, 600°C, 2h; 2°C/min, 1000°C, 2h	5°C/min to 1500°C, 1hr, Ar	Coating 70-80 μm; some dip cracks and a lot of surface shallow cracks; quite dense; a layer of coating remains on SiC surface after coating was scrapped. TOO THICK. The amount of polymer is excessive according to mud cracking pattern and thick glassy layer on top of the coating. Need to reduce level of polymer
ZrB_2 (14.08g) SMP-10 (3.96g) cyclohexane (5g)	1°C/min to 200° C, hold 1 hrs, argon	1°C/min, 200°C, 2h, 1°C/min, 400°C, 2h, 1° C/min, 1000°C,1h 3°C/min 25°C in Ar		Coating cracked significantly; seems to have an excess amount of polymer, resulting in a polymer layer on top of the powder filled region.
ZrB_2 (14.08g) SMP-10 (3.21g) Cyclohexane (5g)	1°C/min to 200° C, hold 1 hr, argon	1°C/min to 200°C, 2h, 1°C/min to 400°C, 2h, 1°C/min to 1000°C, 1h, 3°C/min to 25°C in Ar	5°C/min to **1500**°C, 1hr, Ar	**At 1000°C:** Bonds strongly to surface and not easily removed by a razor blade; slight excess of polymer causing very mild local cracking at the middle of the sample **At 1500:** Porous coating due to binder crystallization; low level of cracking; can be removed quite easily
Polycarbosilane (High carbon content; Nippon Carbon)				
ZrB_2 (6.10gm) polycarbosilane (NIPSU) (1.14g) first dissolved in 2.0g toluene	150°C for 2 hrs, air	5°C/min, 1000°C, 1h, Ar		Significantly cracked; a lot of silicon; too much polymer; 5-20 μm thick.
ZrB_2 (5.00g) Zr (1.07g) polycarbosilane (1.14g) toluene (2.0g)	150°C for 2 hrs, air	5°C/min, 1000°C, 1hr, Ar		Zr powder batch oxidized: to repeat with unoxidized zirconium powder.
ZrB_2 (5.00g) Zr (1.07g) polycarbosilane (1.14g) toluene (2.0g)	150°C for 2 hrs, air	5°C/min to 1000°C, 1hr, Ar	5°C/min to 1500°C, 1h, Ar	At 1000°C: Very cracked due to excess of polymer; easily removed with razor blade. At 1500°C: More cracked and polymer derived material starts to crystallize leaving very faceted pore structure.

3.2.3 Coating Characteristics as a Function of Formulation and Processing

There is a major correlation between the final coating microstructure and integrity and the slurry formulations, the characteristics of the polymeric precursor, the incorporated reactive

powder (if added), and the heating processing parameters. Representative analyses of various slurry-based coatings within Approach One are discussed in the section below.

3.2.3.1 Use of Polymeric Precursors to SiOC

Three approaches for generating SiOC from a low-cost polymeric precursor have been evaluated. The synthesis and processing of these precursors were developed previously at SRI. Two of the polymeric systems were based on using commercially available low-viscosity siloxane oil, polyhydromethylsiloxane (PHMS), that can be easily modified or crosslinked via the catalytic activation of multiple Si-H functional groups. One technique to crosslink the polymer is by reacting it with a multivinyl compound via a hydrosilylation reaction followed by an additional crosslinking through a dehydrocoupling reaction with water (moisture) [71]. The initial crosslinking process can proceed even at room temperature very efficiently in the presence of a few ppm of a Pt-siloxane catalyst [72]. The two chosen crosslinkers were tetravinyltetramethyltetracyclosiloxane, a commonly used hydrosilylation reagent, and divinyl benzene, a low-cost stock monomer widely used in polystyrene and epoxy production. The latter crosslinker introduces an excess of carbon in the final SiOC product, which we originally planned to use in order to form a ZrC phase by incorporating metallic Zr powder into the formulations or additional SiC by adding Si powder. Figure 4 illustrates the chemistry associated with modifications and crosslinking of Si-H-containing molecules and polymers. Figure 5 shows the crosslinking reactions of PHMS with the vinyl-containing reagents.

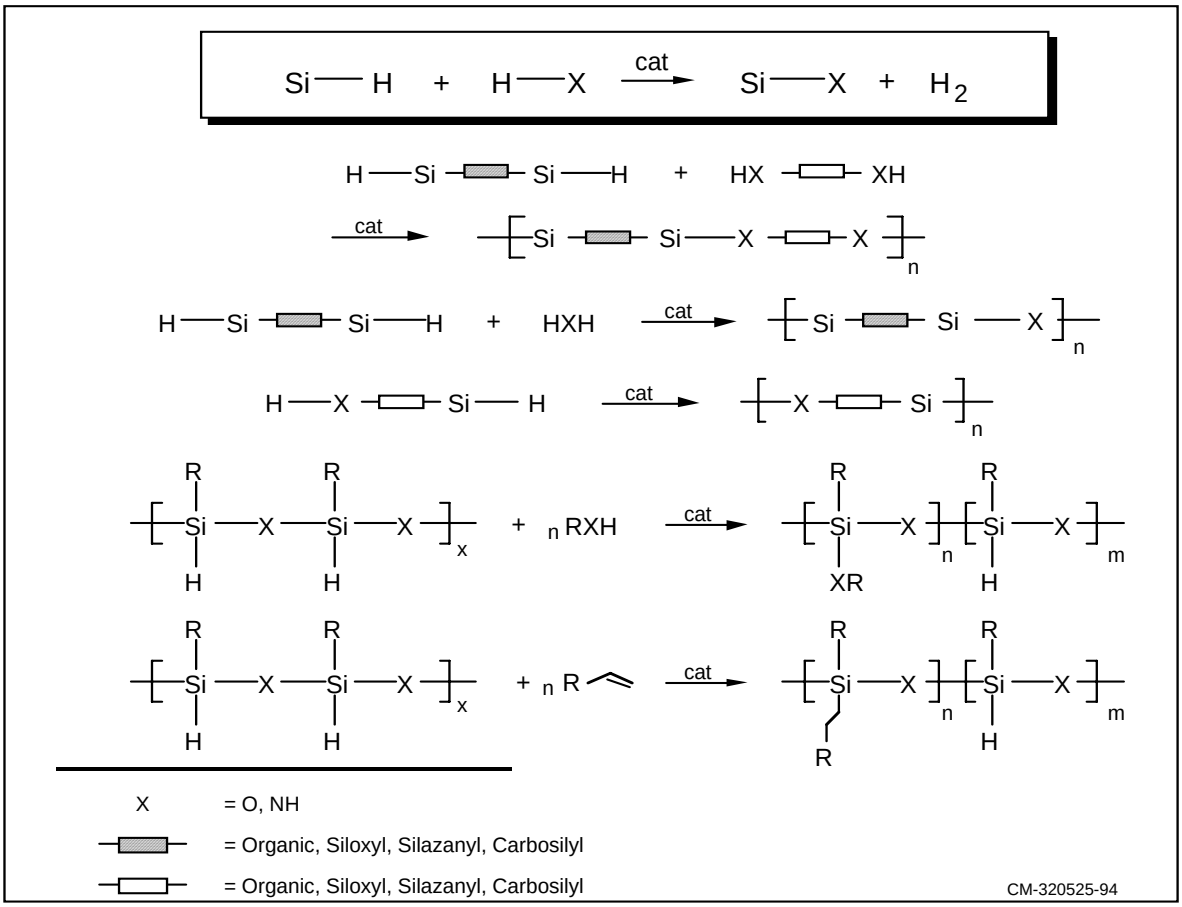

Figure 4. Generic scheme of the dehydrocoupling/hydrosilylation capability of Si-H-containing polymers.

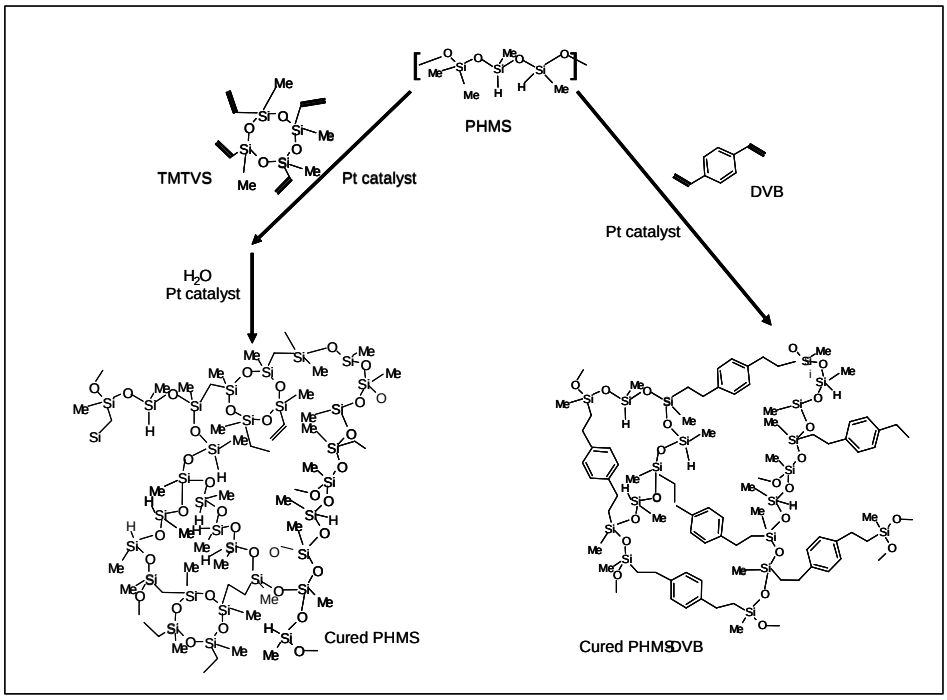

Figure 5. Hydrosilylation reaction scheme of PHMS with vinyl-containing crosslinkers.

The third selected SiOC precursor was hydroxy modified PHMS (PHMS-OH) obtained by reacting the commercial PHMS with water in the presence of a Ru carbonyl catalyst. This reaction was developed previously at SRI and is used for many coating applications and matrix formation for ceramic composites. Although in this case the oxygen content of the derived SiOC is higher, this precursor version is superior in its wetting and adhesion properties to particles and large surfaces, while the PHMS itself does not wet well surfaces due to its very low surface tension characteristics (hydrophobic). Figure 6 summarizes the versatility in the modifications and crosslinking capability of PHMS via dehydrocoupling, hydrosilylation or combinations of the two.

3.2.3.2 PHMS/Crosslinker Formulation with ZrB_2

Formulations based on PHMS plus a vinyl crosslinker that meet the desired 80:20 volume ratio target were not suitable for formulations with ZrB_2. The combination of the relatively high specific density of the particles and the low surface tension of the polymer provided unstable slurries with fast segregation of the particles within the deposited coating before its curing. Figure 7 provides evidence for this phase separation and the formation of a glassy layer on top of a powder containing layer. Aside the inhomogeneity of the coating composition, this phase separation, associated with (a) the shrinkage of the top layer during the pyrolysis and (b) the lack of sufficient binding phase in the bottom layer, led to major mud cracking of the coating.

Further work with similar formulations did not provide any better results and the utilization of ZrB_2/PHMS slurries was abandoned.

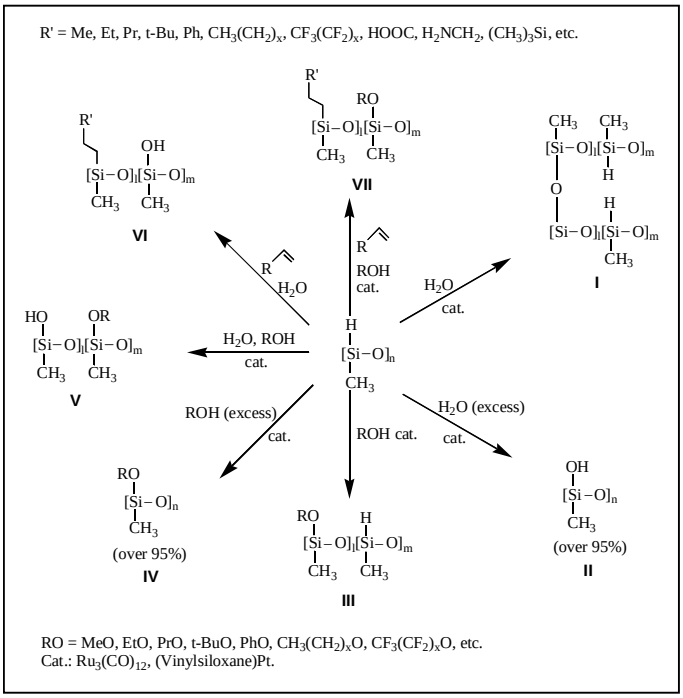

Figure 6. Generic scheme of transition metal catalyzed modifications of PHMS.

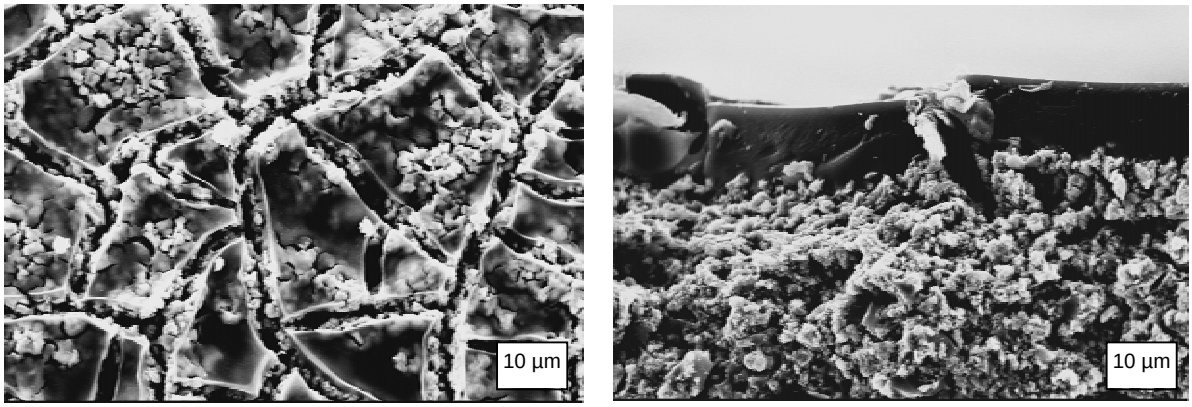

(a) (b)

Figure 7. Inhomogeneous and mud-cracked coatings is obtained with ZrB_2/PHMS slurries.

3.2.3.3 PHMS-OH Formulation with ZrB_2

A ZrB_2/SiOC coating with good integrity was obtained by switching the preceramic polymer from PHMS to PHMS-OH as illustrated in Figure 8. The coating was processed by dip

coating in a slurry composed of ZrB_2 powder and PHMS-OH in a weight ratio of 8.1:1.0 (~78:22 vol ratio after pyrolysis), respectively. This coating was pyrolyzed to 1000°C in a constant heating rate of 5°C/min and dwell period of 1h at the maximum temperature.

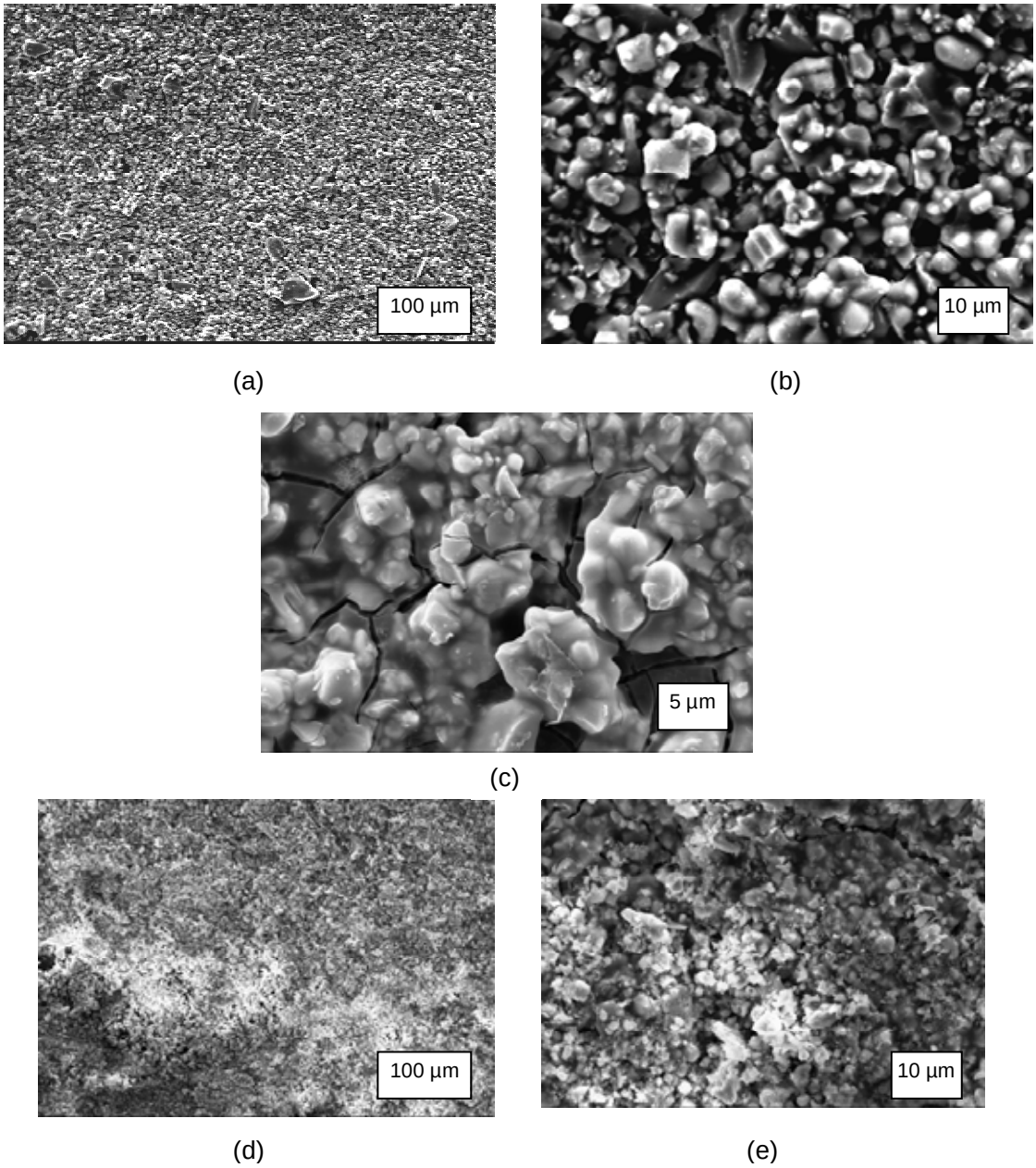

Figure 8. Microstructure observations of a coating with good integrity prepared from ZrB_2/PHMS-OH/ethanol slurry.

The coating is relatively thick at 20 to 30 µm. The cracking level is considered mild and may be a combination of both the thickness and excessive level of the polymer. Clearly, all the voids between the particles are filled with a vitreous polymer-derived material. The coating

bonds very well to the substrate. Attempts to scratch and peel the coating with a laboratory-grade razor blade failed and only a smear of stainless steel was observed (Pictures 1d and 1e).

Coating of ZrB_2 powder with lesser amount of PHMS-OH (ratio of 10:1), indicating less binder between the particles and some open porosity, is shown in Figure 9. No significant cracking is observed for a coating having thickness of around 30 µm.

Once coatings of the formulation presented in Figure 8 (8.1:1) are further heated to 1500°C, the fine cracks observed after the pyrolysis step at 1000°C become larger. The main change in the microstructure is the formation of a very porous structure and disappearance of the polymer-derived phase, as shown in Figure 10. Consequently, the coating can be easily removed from the surface.

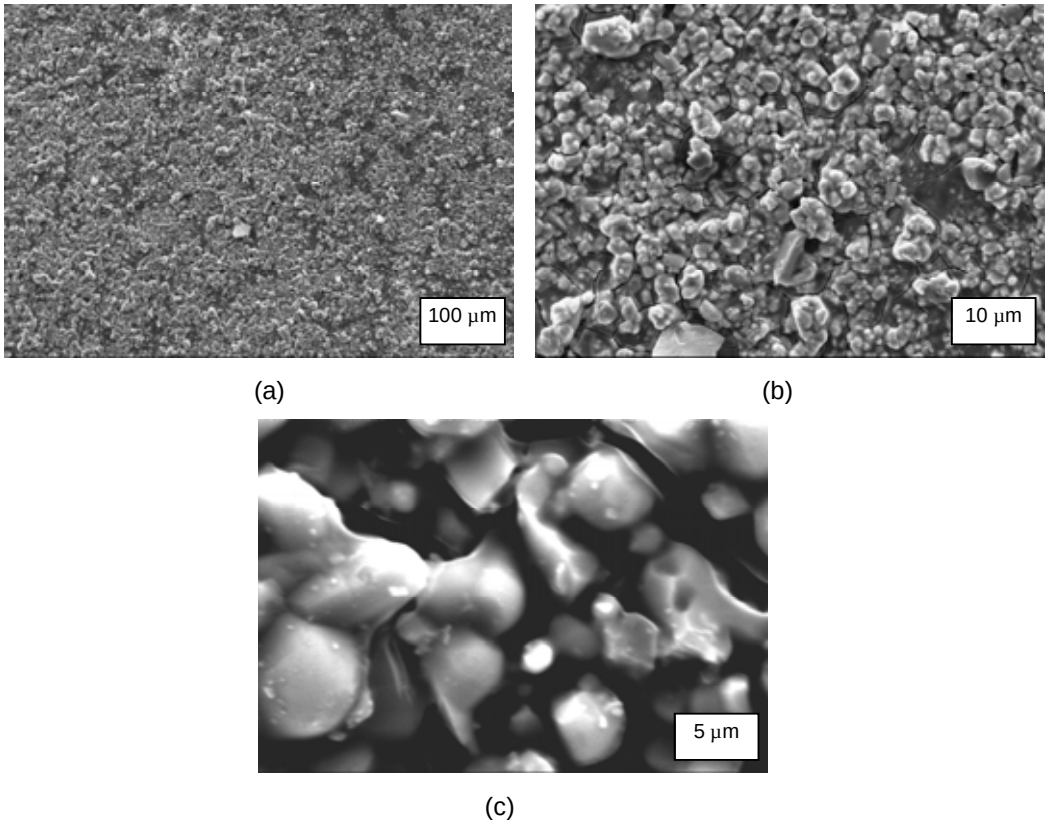

Figure 9. Microstructure observations of a coating prepared from ZrB_2/PHMS-OH/ethanol slurry, with lower polymer content than the formulation presented in Figure 8.

Most surprising is the fact that the silicon content according to EDS analysis almost disappeared completely in comparison to the same coating after the pyrolysis at 1000°C. This means that the Si was vaporized, presumably by the formation of gaseous SiO under the reducing conditions. Also noticeable, is the transformation of the sharp edges of the ZrB_2 particles to blunt, suggesting exothermic reactivity with the SiOC binder, although the ZrB_2 powder was expected to be thermodynamically favored and stable. This is a very unexpected observation and never observed in previous studies at SRI, in which the same SiOC precursor was heated at high temperature with and without "inert" fillers. The integrity of the post pyrolyzed coating is maintained up to about 1300°C. The mechanism of this high temperature reactivity has not been investigated.

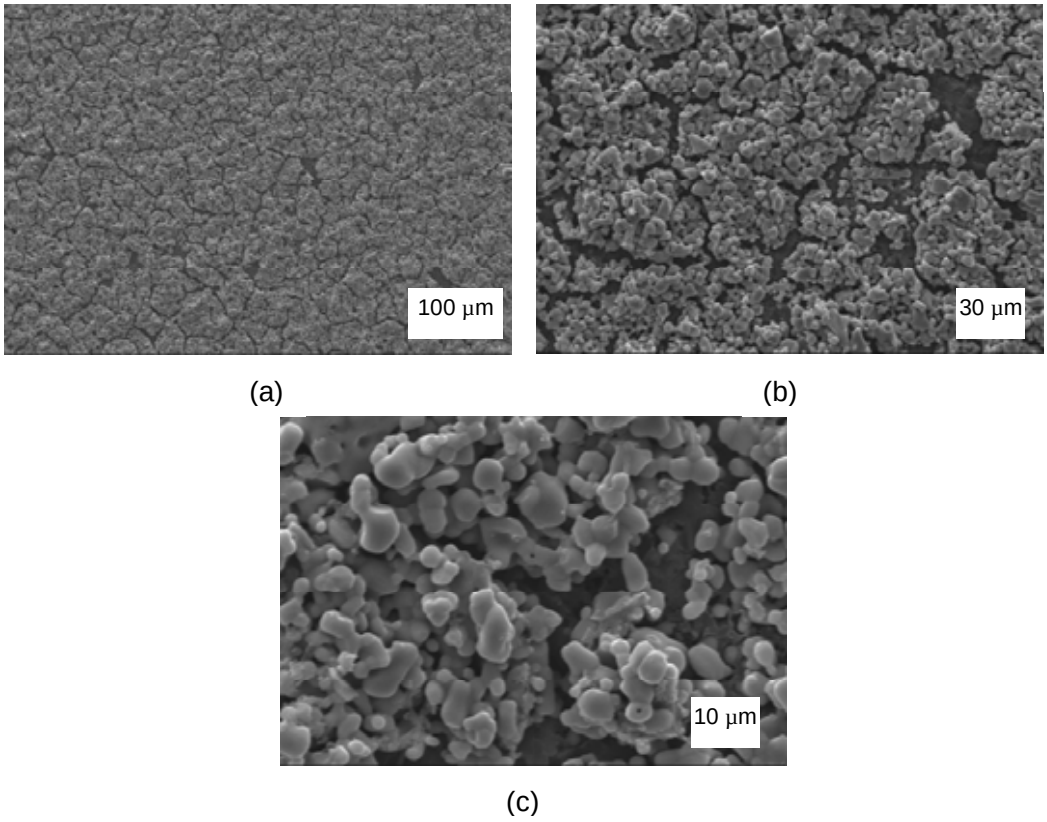

Figure 10. Microstructure observations of a coating made of ZrB_2/PHMS-OH/ethanol slurry heated up to 1500°C. Severe degradation has occurred.

A postulated mechanism to explain this phenomenon is shown in Reaction 1 but it was not possible to find an appropriate thermodynamic calculation that supports this reaction:

$$SiO_xC_y + ZrB_2 \longrightarrow SiO(g) + BO_z(g) + ZrBC \text{ or } ZrC_y \quad (1)$$

The conversion of ZrB_2 to ZrC and ZrBC is not thermodynamically favored. Yet, such "up-hill" reactivity has been observed during the exploration of the second coating approach. Assuming a reaction between the 2 phases it would be more likely to obtain the following reaction, that does not eliminate the Si content:

$$SiO_xC_y + ZrB_2 \longrightarrow BO_x(g) + ZrOB + SiC \quad (2)$$

Because of this unexpected limitation, the work with SiOC precursors was abandoned.

3.2.3.4 Slurry Containing Polymeric Precursors to SiC

Precursors to SiC do not contain oxygen (except the oxygen accumulated during processing and curing of polymethylcarbosilane. Therefore, the chemical reactivity observed with PHMS-OH at high temperature, is not anticipated. Two polymers were assessed. One was polymethylcarbosilane, $[-CH_3SiHCH_2-]_x$, the polymer used for making the Nicalon and Tyranno fibers. This polymer possesses a significant excess of free carbon derived from its molecular structure. It also picks up several % of oxygen during the conventional heat curing in air. The second polymer was allylhydridopolycarbosilane, $[-(CH_2=CH)SiHCH_2-]_x[-SiH_2CH_2-]_x$ (SMP-10), produced by Starfire Systems as a stoichiometric precursor to SiC, with almost no excess of carbon.

3.2.3.4.1 Polymethylcarbosilane Formulation with ZrB_2 Powder

Coatings based on polymethylcarbosilane (PMCS) as a binder were highly cracked and loosely bonded to the surface (See Figure 11). Observations revealed that the slurry did not bond well to the surface after curing, in contrast to coatings based on PHMS-OH and SMP-10. The loose bonding can be attributed to lack of good wetting or adhesion properties of PMCS due to its low surface tension. Formulations based on PCMS were abandoned and not studied further.

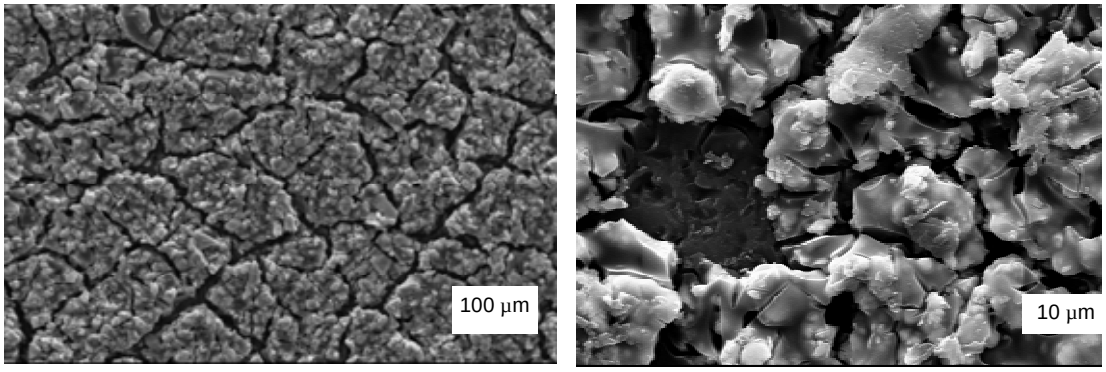

(a) (b)

Figure 11. Low integrity coatings obtained from ZrB_2/PMCS slurries.

However, this polymer is still a good candidate for matrix processing combined with Zr or Si particles that would react with the excess of free carbon in the polymer derived ceramic product. The advantages of using PMCS over SMP-10 in a matrix application is its air stability during the infiltration and curing processes, and its lower cost relative to SMP-10. It is also a

solid with a melting point and the low viscosity after melting allows a hot infiltration process. Its disadvantages include the excess carbon and the fact that low temperature impregnation such as in a lay-up process would require solvent while in the case of SMP-10 the polymer is already a liquid with low viscosity.

3.2.3.4.2 Early Stage Assessment of SMP-10 Formulation with ZrB_2 Powder

Coatings made by a formulation containing ZrB_2 and SMP-10 in a weight ratio of 4.39: 1.00 powder to polymer (77:23 volume ratio after pyrolysis) adhere very well to the SiC substrates in spite of slight cracking (Figure 12). The coatings contain a slight excess of polymer and therefore are sealed with a vitreous layer (except in the cracks). The cracks are shallow and probably generated because of segregation between the polymer and powder during the drying step, leaving a thin polymer layer on top of the powder/polymer blend. Pictures 12c and 12d reveal that a razor blade did not remove the coating but was abraded leaving a metallic smear at the coating surface (the lighter spots).

Once coatings of the above and similar formulation are heated to 1500°C, a major microstructure change is obtained, although no significant cracking is observed (Figure 13). The coating becomes very porous and can be scratched off the surface relatively easily. The polymer-derived binding phase has been depleted, though Si is still detected by EDS. It seems that the polymer-derived material is going through transformation from an amorphous phase to crystalline. However, we also observe whiskers (Figure 13c), indicating the formation of volatile silicon (possibly SiO) containing species that are redeposited at the surface. The ZrB_2 particles become blunt.

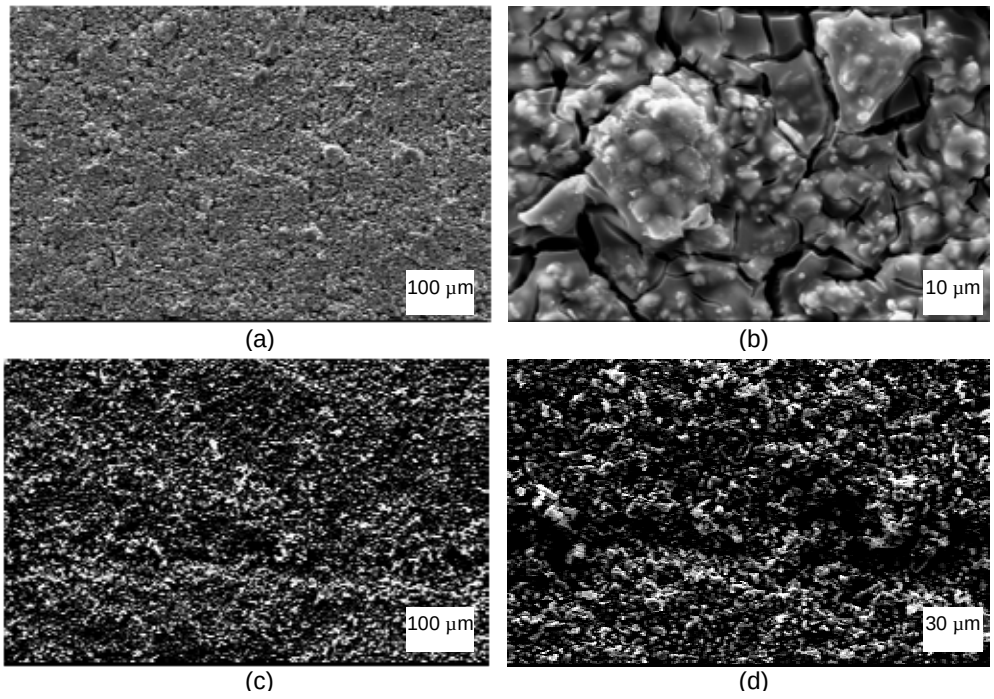

Figure 12. UHTC coatings generated from a mixture of ZrB_2/SMP-10 with strong bonding to substrate. Minor level of shallow cracks is found at the top of the coating, but they do not affect the adhesion to the substrate.

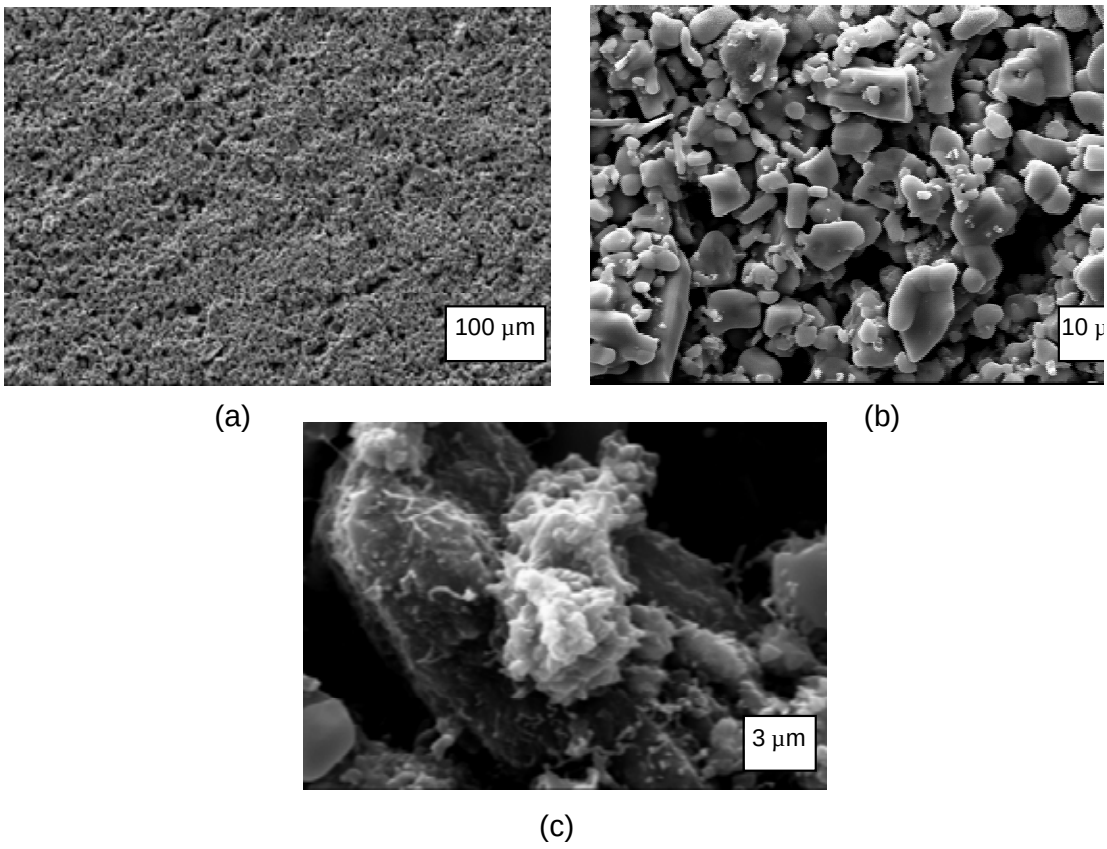

Figure 13. UHTC coatings generated from a mixture of ZrB_2/SMP-10 (excess level of polymer) after further heating to 1500°C.

3.2.4 Further Evaluation of the ZrB_2/SMP-10 Formulation

3.2.4.1 Coatings

The ZrB_2/SMP-10 slurry composition was selected for further evaluation as a potential approach for achieving the UHTC coatings. The development effort started with the assessment of the optimal ratio of powder to polymer to obtain up to 30 μm per layer. Such crack-free coatings have been achieved and microstructural evidence shows that they can be built up to 100 μm thick (as observed at the bottom of the dip coated specimens) without significant cracking. However, the formation of a 100 μm coating in a one step process is not expected to adhere well to the substrate due to high stress built-up at the interface. Also, a graded composition approach may be required.

The adjustment of the powder/polymer ratio required a significant effort to balance between the case of excessive level of polymer (resulting in significant coating "mud" cracks) and the case of insufficient level polymer (resulting in excessive porosity). The resultant optimal formulation consisted of a slurry that was still a liquid even after complete solvent removal. Therefore, it was difficult to mold it into a bulk specimen when the properties of the bulk were studied for their potential use as matrix formers.

Figure 14 shows the microstructure of such optimized 30 μm coating (see Figure 14c). The slurry has a weight ratio of 6.29:1.00 of powder to polymer (approximately 1:1 volume ratio during the slurry stage but 80:20 volume ratio after pyrolysis and heat treatment at 1500°C). The resultant pyrolyzed coatings had high integrity with no observable cracking. However, the trade off was a clear level of porosity. No evidence for amorphous binder filling between particles is observed, in contrast to the related coating shown in Figure 12.

It was therefore concluded that the potential to maintain stability of coatings derived from ZrB_2/SMP-10 above 1400°C with a single layer approach is unlikely because of the porosity as well as the typically strong oxidation activity across the first 100 μm deep layer observed during the oxidation of UHTCs. Corroboration of this conclusion was further confirmed during the oxidation studies. However, the ZrB_2/SMP-10 formulation was selected for further coating study. It was also selected as a candidate formulation for oxidation studies in a bulk form (as candidate for CMC's matrix processing.)

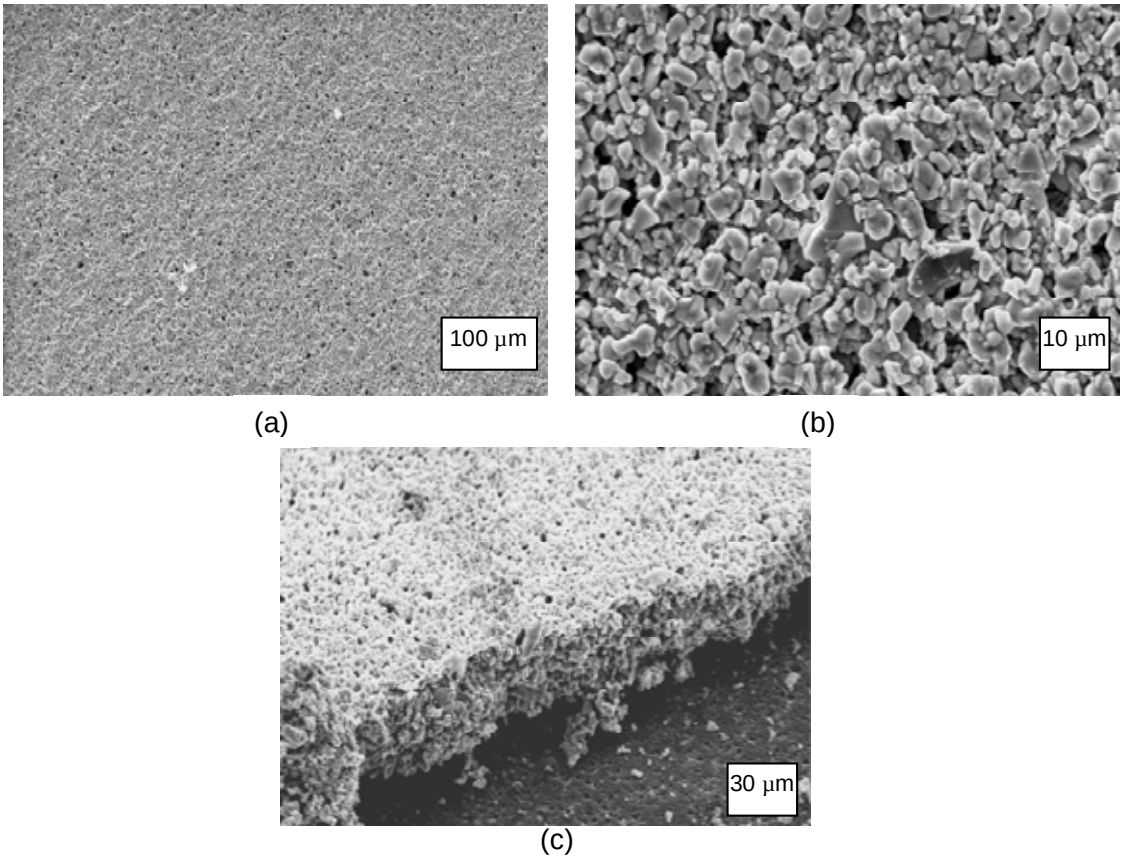

Figure 14. UHTC coatings generated from a mixture of ZrB_2/SMP-10 with optimal ratio of powder to Polymer.

Attempts to reinfiltrate the evolved porous layer with additional SMP-10 derived SiC phase were not successful, when a single filling step was practiced. Such reinfiltration process led to coatings that were highly cracked and easily delaminated after the pyrolysis step, as a consequence of the stress buildup by the polymer shrinkage during its conversion to ceramics. A way to bypass the stress formation is to process the reinfiltration stepwise with a dilute

preceramic polymer solution. This approach allows for the deposition of a thin layer at the pore surface within the base coating. This thin layer then shrinks in a preferential direction perpendicular to the coated surface of the pores. Therefore, the lateral stresses are not significant. However, there is a need to repeat this process several times. This sealing process was performed in this study up to 5 times for learning purposes and generating specimens for oxidation, but the practicality of this approach decreases with each extra cycle because of time/cost reasons.

An alternative but similar approach was then developed in which a 2 layer coatings of about 15 μm each were deposited. The first layer had a lower polymer-to-powder ratio to avoid cracking (the same coating presented in Figure 14). The second layer contains higher polymer-to-powder ratio (like the one represented in Figure 12). However, the liquid polymer partially migrates from the top layer and infiltrates into the pores of the base layer by a capillary force. The second layer is therefore designed to further seal the first layer and form a strong bond between the two layers as well. Assuming that the pyrolysis yield of the polymer is around 75 wt% the following volume ratios of ZrB_2:SiC are calculated:

1^{st} layer: ZrB_2 81vol%; SiC 19vol%

2^{nd} layer: ZrB_2 75vol%; SiC 25vol%

The overall coating is relatively dense, compared with previous results and it is difficult to observe the interface between the separately processed layers as illustrated in Figures 15 and 16. The double-layer coating bonds well to the surface with medium hardness manifested by the capability to scrape it with razor blade.

Microstructural analysis of the double layer cross section demonstrates good interface integration between the 2 layers even in very thick areas at the bottom of the dip coated specimens (Figure 16c; over 200 μm thick!). Only delamination is detected indicating that the adhesion to the surface has been decreased due to stress buildup but no perpendicular cracking is detected.

The hardness of the ZrB_2/SMP-10 coating is relatively low. Microhardness measurement of such coatings give values in the range 0.5 and 1.25 GPa, which is relatively low hardness due to the porosity of the coatings.

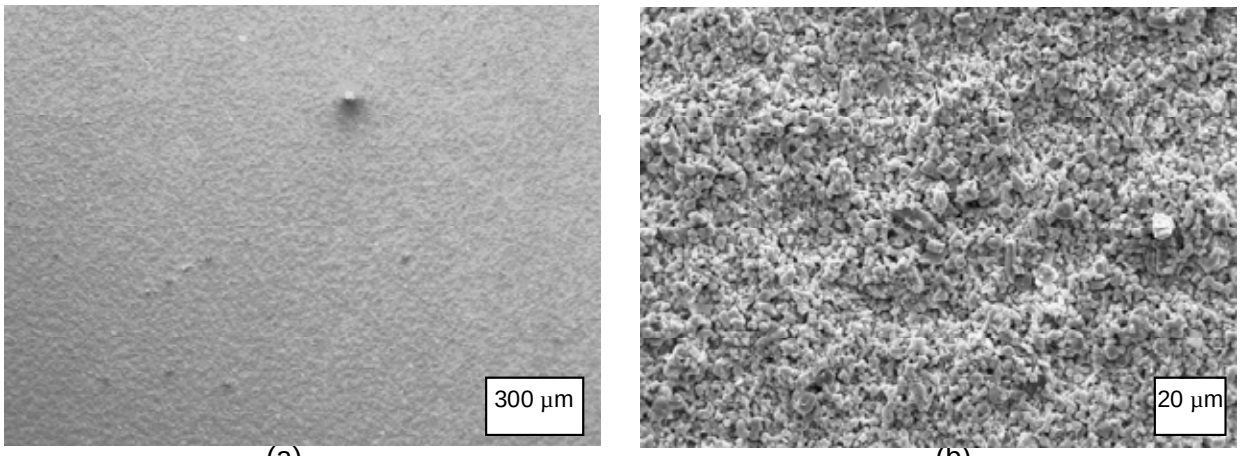

(a) (b)

Figure 15. Double coating of ZrB_2 with SMP10. The 1st layer contains lower amount of SMP10 followed by 2nd layer with higher amount. The coating shows high integrity with no cracks and no excess of polymer (like shown in Figure 12) is observed.

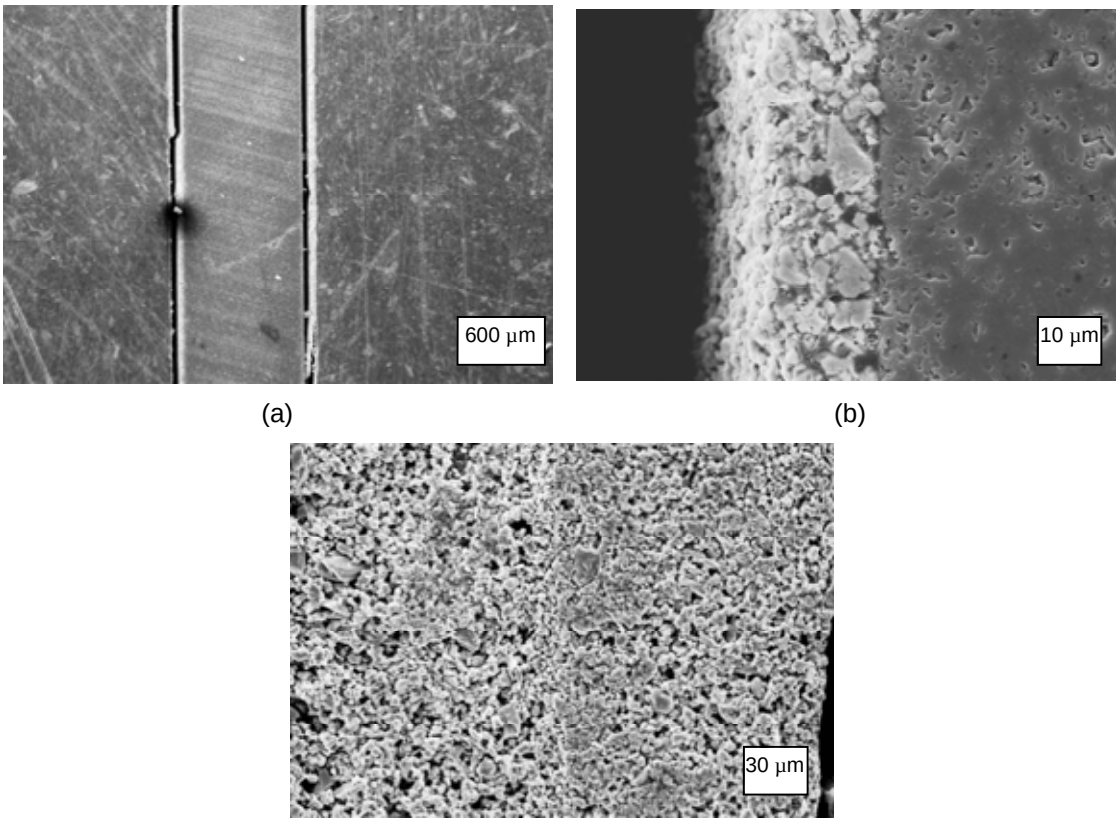

(a) (b)

(c)

Figure 16. Cross section of a double layer coating made of ZrB_2/SMP-10. The thick double layer in (c) shows excellent cohesion of the two layers and a clean interface. The layer on the left side is the top layer.

3.2.4.2 Evaluation of Bulk ZrB_2/SMP-10

Bulk material of the 2 formulations above were molded and cured for bulk oxidation testing. Figure 17 represents a bulk formulation with the higher binder content. The bulk material is dense with microscopic evidence for SiC binding phase between the particles. Shaping a molded structure based on this formulation was difficult because of its low viscosity even in the absence of a solvent. Nevertheless, some irregularly shaped products were obtained for evaluation under various oxidation conditions.

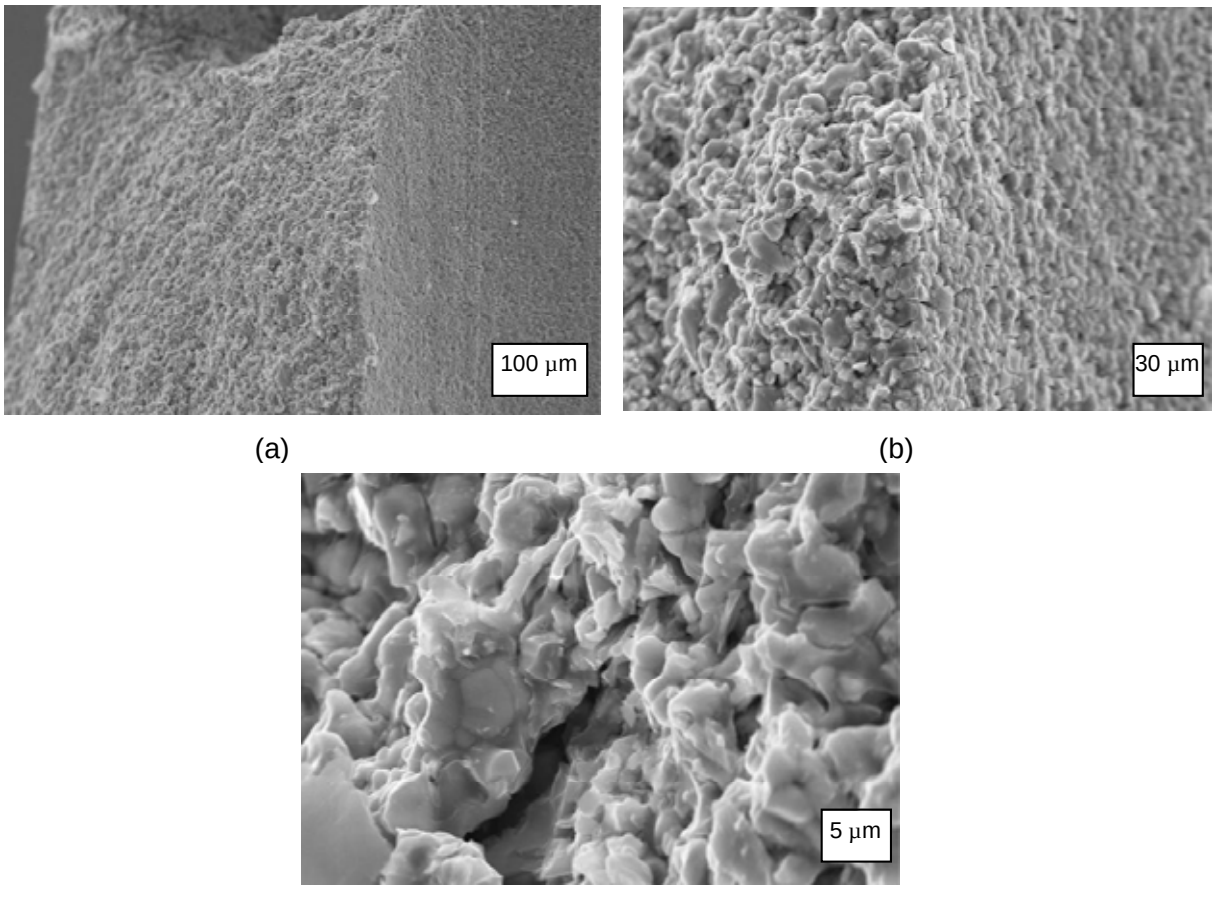

Figure 17. A bulk specimen of pyrolyzed ZrB_2/SMP-10 made of the same formulation that generates the top layer in the double layer approach. The bulk is significantly denser than the coatings.

3.2.5 Formulations Containing Polymeric Precursors to Carbon

The initial plan for using polymeric precursors to carbon was to let them react in-situ with either Zr or Si powder at elevated temperature. Initially, a polynaphthalene precursor was chosen, because it contains low level of oxygen (only after air crosslinking) and is increasingly used for producing meso carbon matrix for C/C composites. However, the solubility of the polymer was limited even in the most appropriate recommended solvent and its slurry stability was limited. In addition, it bonded very poorly to the SiC substrate and subsequently it delaminated and deformed easily.

Phenolic resins were selected as an alternative choice and were introduced after the polynaphthalene approach was abandoned. Two types of phenolic resins were studied, both produced by Schenectady International. Both resins possess soluble thermosetting characteristics. One resin consisted of 73% solids in ethanol (HRJ-14209). The other one consisted of 69% solids dissolved in water (SP-6877). Both provided good slurries and excellent adhesion to the substrate prior to pyrolysis. Eventually, the ethanol based resin was selected, because it seemed to provide slightly more stable slurries and gave slightly higher conversion yields to carbon during pyrolysis.

Although the formulations described below were not down-selected for further study after the initial exploratory phase, the concept of using phenolics as an excellent binder was later practiced heavily in the study of Approach 2, which is discussed later on in this report.

3.2.5.1 Formulations of Zr with Phenolic Resin

The purpose of this coating was to assess in-situ reactivity between Zr and C as an integral part of the coating development. In previous studies SRI has studied the reactions of Hf and C powders, that are activated well below 1500°C, under conditions that do not generate self-propagation uncontrolled reaction [20-22].

Coating made of Zr powder mixed with ethanol-dissolved phenolic resin (HRJ-14209) and pyrolyzed at 1000°C are porous but show very high integrity. No cracks are observed in spite of the coating thickness (around 30 μm) as shown in Figure 18. A razor blade scratching of the coating's surface (Figure 18b) reveals that the coating material remains bonded to the surface very well. Figures 18c and 18d indicate a significant interaction between the Zr particles and the polymer already at 1000°C, resulting in particle (grain) cracking.

The formation of Zr/Phenolic (HRJ) coating heated at 1500°C revealed a coating that was not cracked and was still bonded relatively well to the surface. However, these coatings are significantly porous and we have not observed a melting activity of the Zr powder similarly to previous observations in reactions between Hf and C powders at temperatures below 1500°C.

Not many changes in the gross microstructure have been observed between the coating heated to 1500°C and the coating after its pyrolysis at 1000°C (see Figure 19). Both have similar porosity and pore/grain size distribution. In both, the grains themselves possess submicron cracks, indicating reactions between Zr and C. The main difference is the presence of round “craters” in the particles at the higher temperature.

Figure 19b documents a razor blade scratch at the surface that did not go all the way through the coating. It suggests that the resin derived material is expected to be a robust binder by itself.

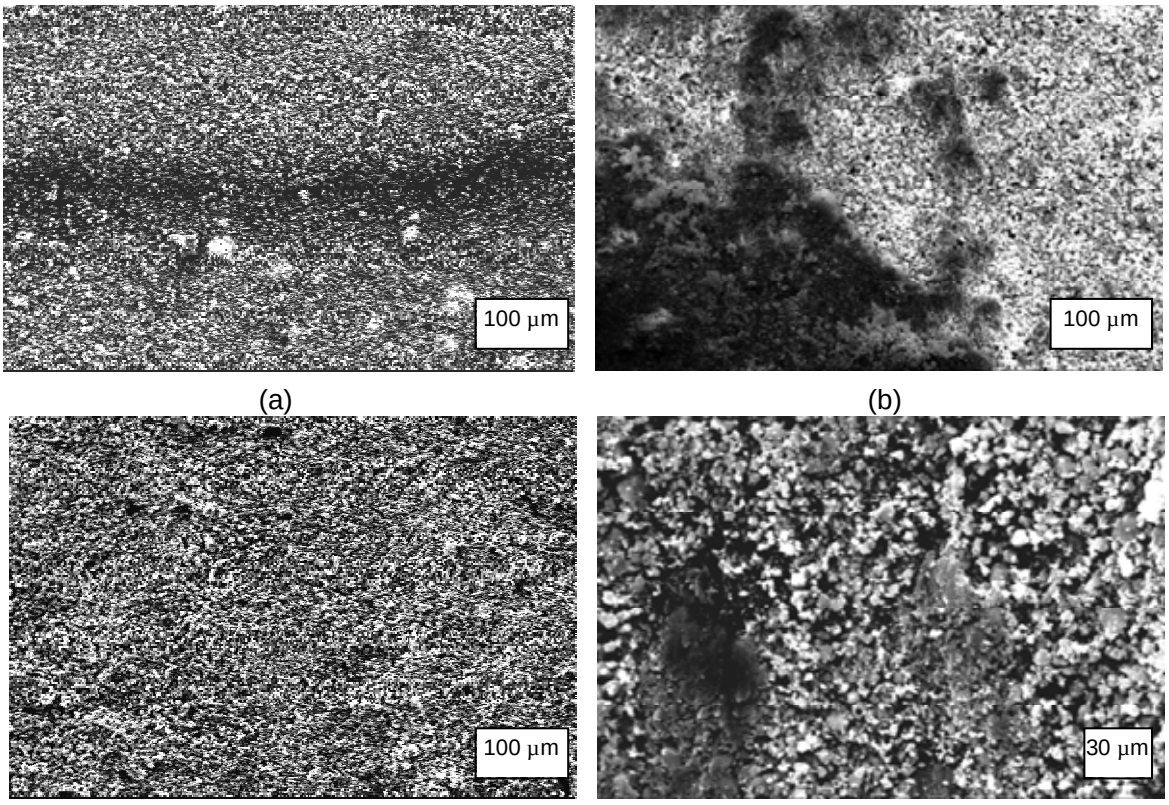

Figure 18. Porous but high integrity coating evolved at 1000°C from a slurry of Zr/phenolic resin formulation.

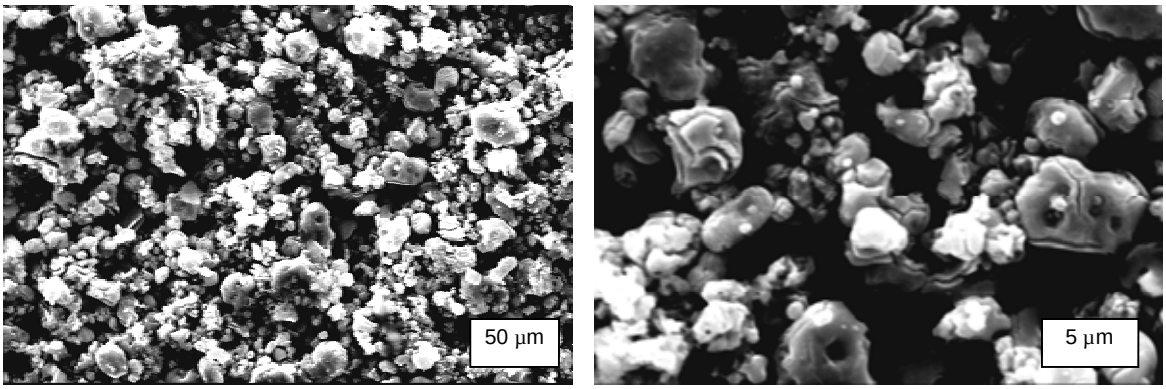

Figure 19. Porous but high integrity coating evolved at 1500°C from a slurry of Zr/phenolic resin formulation.

3.2.5.2 Silicon Powder with Phenolic Resin

In parallel to the reaction between Zr and polymer derived carbon, the reactivity of silicon powder with the phenolic resin was investigated in the form of coatings. Coatings were based on a slurry made of Si powder and phenolic resin in a weight ratio of Si:Phenolic = 4:1. This means that only 30 mol% of the silicon can react with the pyrolytic carbon. The rest is expected to melt and seal the coating. Figure 20 provides evidence that some reactivity occurs already after the pyrolysis stage at 1000°C. The formation of "blisters" at the particle surface is observed.

Once heated above the melting point at 1500°C the silicon indeed melts and forms a continuous coating (as shown in Figure 21). The coating is dense with no cracks and high integrity with individual crystalline islands. Some dendritic features are also observed (Figure 21c). Attempts to scratch the surface result in the abrasion of the razor blade but no removal of the coating.

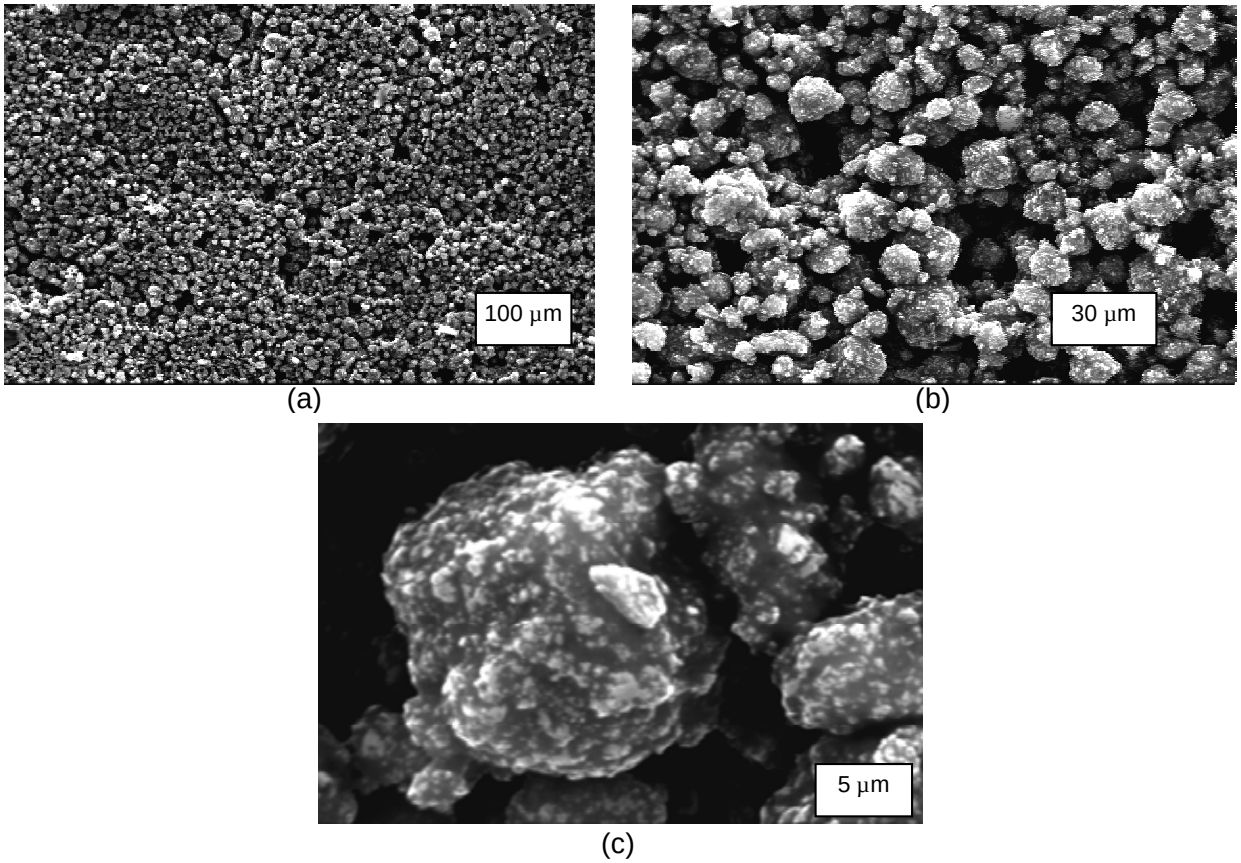

Figure 20. Coatings made of Si powder and phenolic resin derived carbon after the pyrolysis stage. Even at this low temperature, there is an evidence for chemical interaction between the 2 reactants.

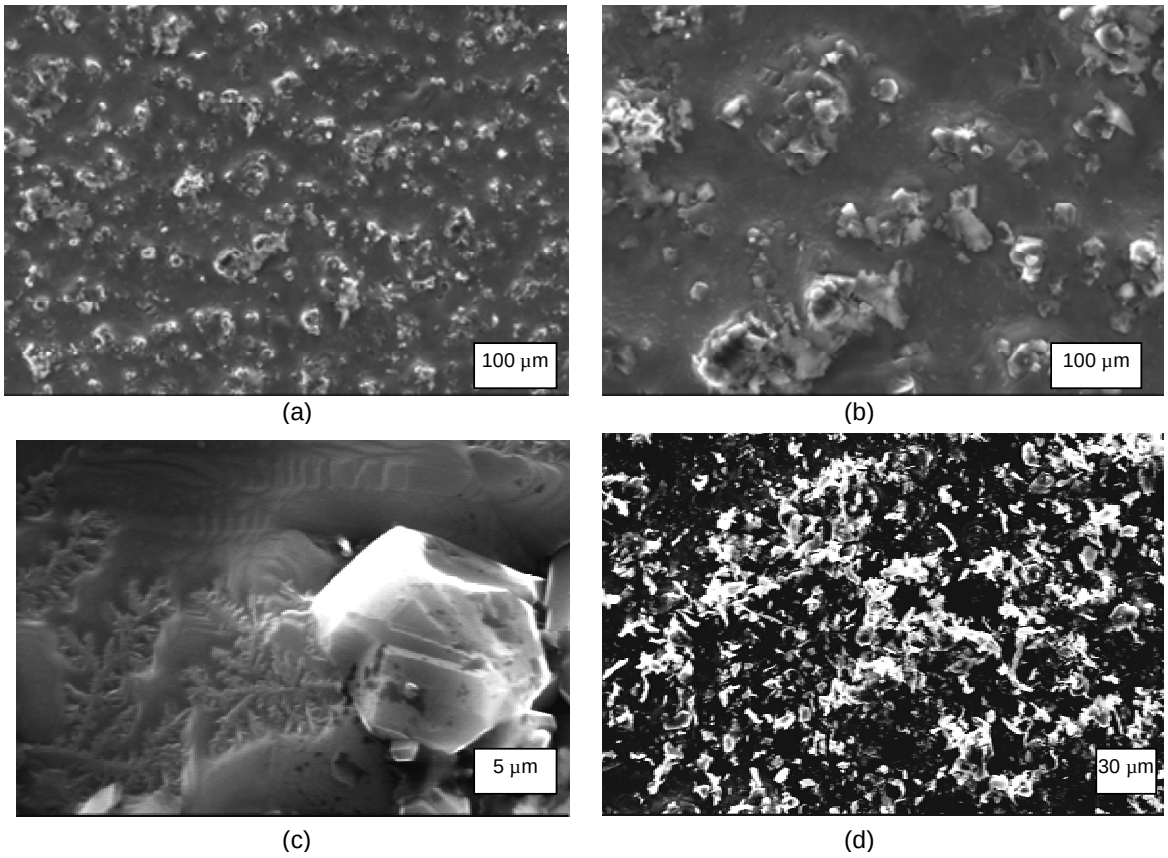

Figure 21. Coatings made of Si powder and phenolic resin derived carbon after heating at 1500°C.

The next step was to combine Si powder with ZrB_2 and phenolic binder in an attempt to obtain a high density coatings based on an in-situ RBSC. The polymer and silicon powder amounts were adjusted to fit a final composition of 80:20 volume ratio of ZrB_2 to SiC. The coating results were very disappointing. Very porous coatings were obtained as shown in Figure 22, which could be scratched with a razor blade off the surface. The postulated reason for this behavior is the solid phase reactivity of the Si particles with the surrounding carbon binder, which is coated around each particle. Consequently, a thin crust of SiC is formed before the Si actually melts. The SiC shell formation prevents the Si from flowing freely and further reacting with the phenolic-derived C leading to localized reaction bonding only.

Although this approach was not found to be useful in its direct formulation format, the observed RBSC served as the seed idea to establishing the second coating approach that has become the leading successful coating approach of the entire exploratory study.

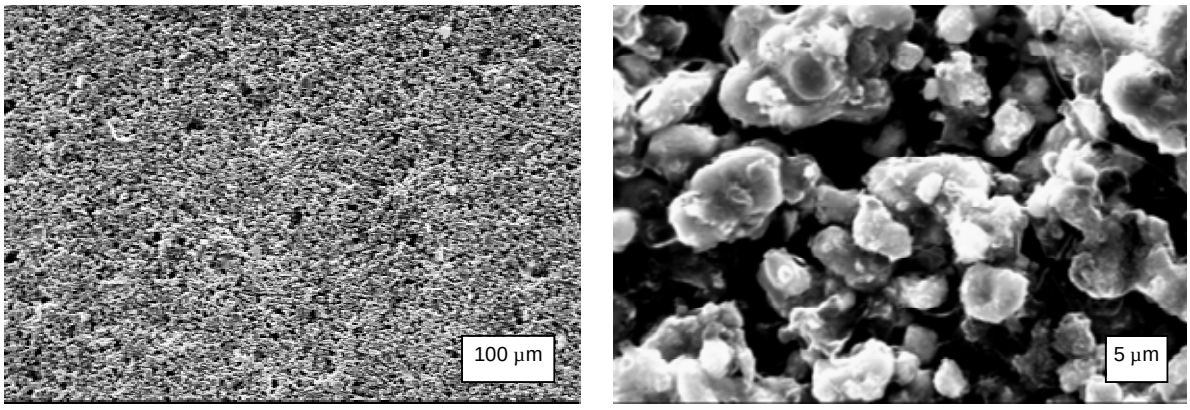

(a) (b)

Figure 22. Coatings based on ZrB_2 and Si powders formulated with phenolic binder leads to a very porous coating in spite of the anticipated melting of the Si and its reactivity with the polymer-derived carbon.

3.3 Approach 2: UHTC Coatings Based on RBSC

The second system under development is based on depositing first a layer of ZrB_2 or Zr powders bonded with phenolic-derived carbon and then exposing it to a molten silicon phase, which rapidly reacts with the carbon. A third step is required to eliminate the excess elemental Si.

The development began by searching for formulations, deposition, curing, and pyrolysis conditions for obtaining a first layer with high integrity by adjusting the ratio of the ZrB_2 powder to the phenolic polymer. Alternatively, formulations containing ZrB_2 and SiC powders with phenolics were also developed. The latter formulation was designed to form a UHTC coating with 40 to 60 vol% SiC, assuming that there would be a need to develop a graded coating composition to mitigate the differences in thermal expansion coefficient. Both formulation options led to coatings that adhered very well to the substrate with apparently good binding between the particles (Figure 23). These coatings are similar or better in their integrity and bonding to the surface than the similar slurry coatings achieved with SMP-10 after pyrolysis at 1000°C.

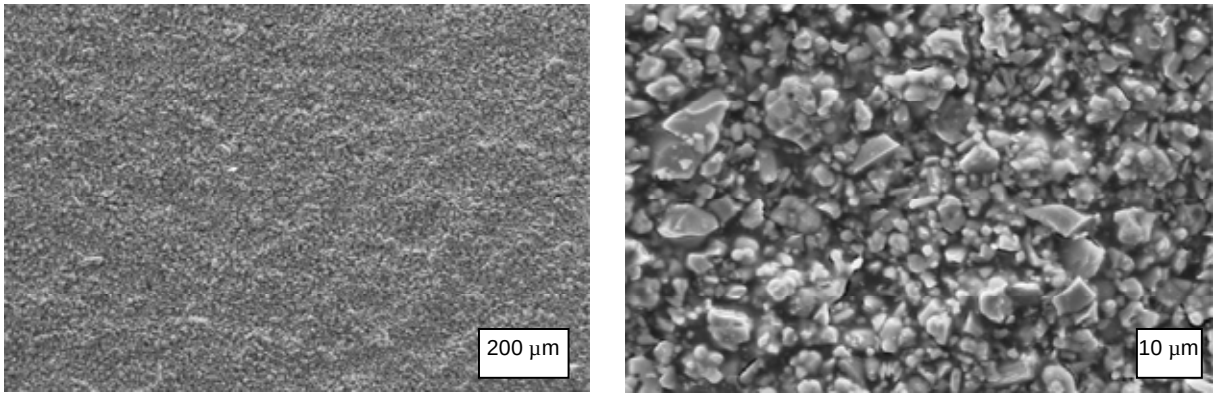

(a) (b)

Figure 23. Preform coating layer made of ZrB_2/C as the first step in forming UHTC coatings based on preform-RBSC, pyrolyzed at 1000°C.

This high integrity is attained in spite of the significantly larger weight loss of the phenolic resin during the pyrolysis of the phenolic resins, relative to other preceramic polymers assessed in this project. It is assumed that the tenacious bonding of the phenolic resin (polymer) to the powder at the polymeric stage to the substrate plays a major role in the post pyrolysis integrity of the coatings. These observations are in line with the previous observations about polycarbosilane and polynaphthalene that did not bond well to surfaces at the cured stage and eventually ended as loose and chalky coatings.

For obtaining a reliable process of the next step, it is preferred to heat the 1st layer (defined also as the "preform layer") to 1500°C prior to performing the second step due to high temperature volatilization from the 1st layer and the vapor redeposition on the silicon particles before they melt. Such redeposition was found to inhibit the melting of Si, probably by forming a SiC shell around the particles.

3.3.1 Establishment of Molten Si Infiltration

Next, it was necessary to establish a process to efficiently infiltrate molten silicon into the preform layer and react it with the carbonaceous material throughout the thickness of the preform coating. This step has required a significant effort of adjustment because of current lab furnace limitations. Nevertheless, the long-term objective is to develop a process using a system consisting of a dipper and a furnace assembly that would allow submerging composites coated with the preform layer into a molten Si pool. Alternatively, it would be possible to operate the siliconization in a larger furnace where the specimen can be positioned flat and covered with the desired amount of silicon powder in a coating form.

In the absence of such furnace capability alternative routes were practiced. First, an approach of depositing a 2nd layer, consisting of Si powder, slightly bonded by a phenolic resin, was taken. The amount of phenolic resin was adjusted to react with only 10 mol% of the Si, assuming that only local microcrystalline SiC will be formed and the rest of the Si will flow into the first the preform coating layer easily. There was clearly a good interaction between the two

layers at 1500°C leading to a dense coating with mechanical integrity significantly greater than obtained with any of the preceramic polymers (Figures 24 and 25).

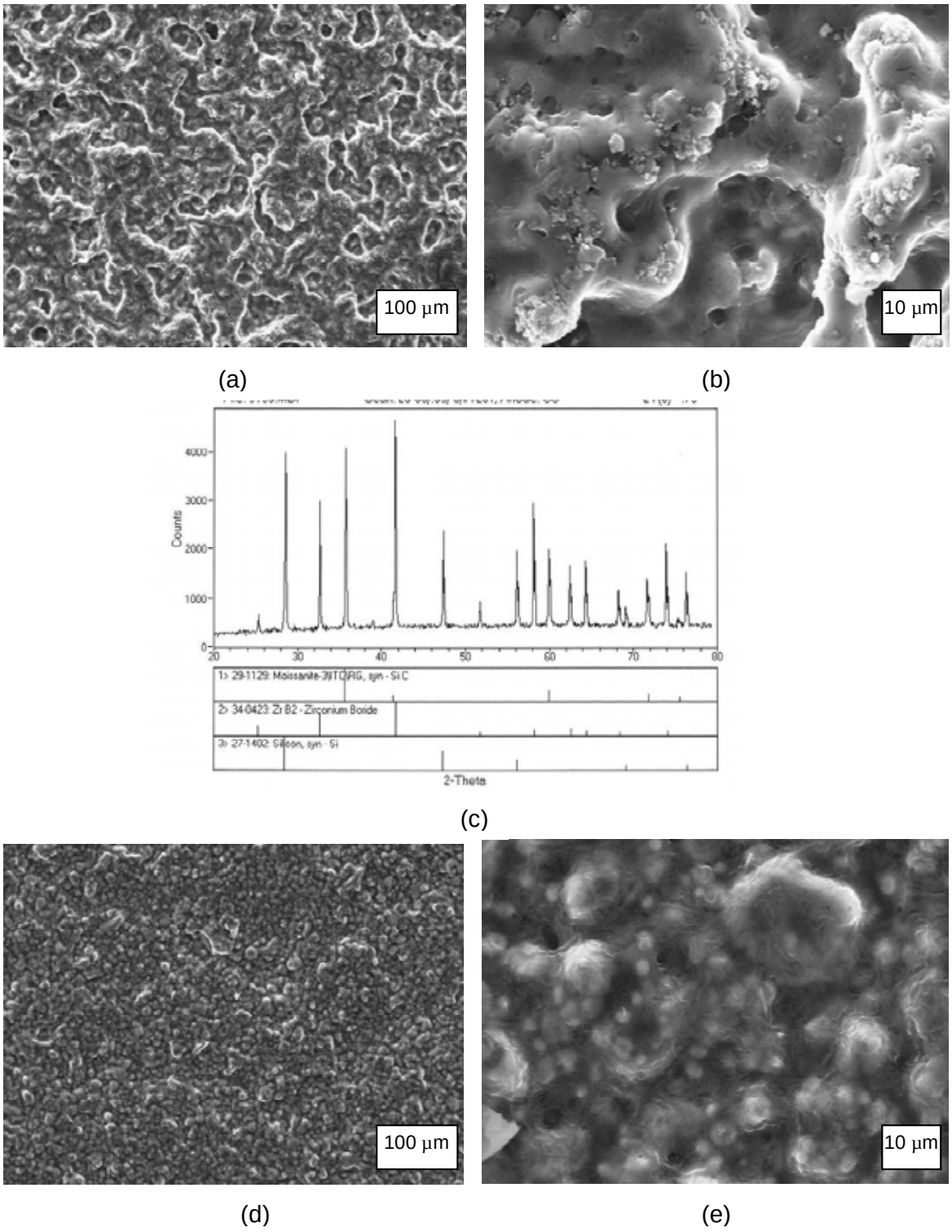

Figure 24. 1st layer and 2nd layer on top; 2nd layer: Si (1 mol): Phenolic (C is about 10 mol% of the Si level in the 2nd layer).

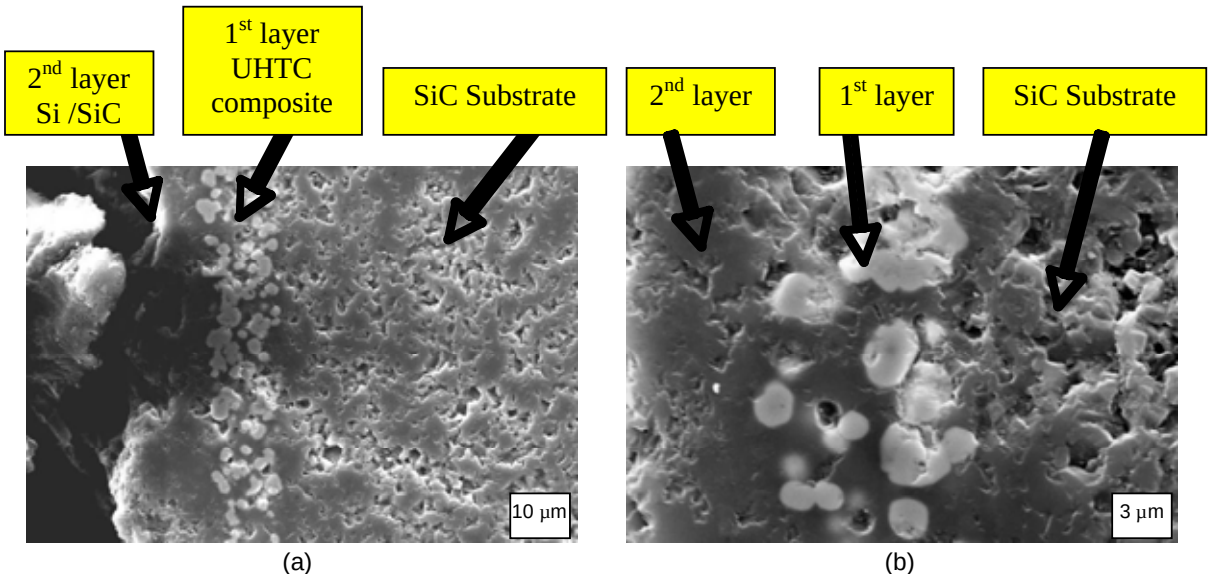

Figure 25. Cross-section of the combined 1st and 2nd layer RBSC coating process. A porous top layer is remained, which contains only silicon based material (both Si and SiC).

The SEM analysis reveals that a significant portion of the top layer with the Si remained as a second top layer and a significant excess of Si detected by XRD (see Figure 24c). However, it is clear from SEM, EDS, and XRD analyses that a significant reaction bonding occurred. The top SiC layer is more porous as a result of the molten Si migration to the preform layer. Thus, a potential way to practice this coating approach in real application will be to remove such a porous layer by mild grinding, if it is found to be advantageous to (a) use the Si powder coating technique as a practical approach or (b) the top SiC layer provides an additional protection function.

An important observation was the phenomenon of upward migration (against gravity) of the molten Si across the surface of the preform coating. The silicon layer was originally deposited only on the lower half of the ZrB_2/C coating. Yet, the pictures in Figure 24d and 24e show a clear coverage of Si, confirmed by EDS, indicating the wicking of Si through the entire area covered by the carbon-containing layer.

3.3.2 Approaches to Eliminate Excess Si

After establishing the capability to process dense UHTC coatings via RBSC, we searched for methods that would eliminate the top layer and also remove any elemental silicon remained within the composite coating layer.

Table 3 describes different approaches that were examined for generating high integrity ZrB_2/SiC thick coatings with no free Si. Both gas and solid phase techniques were evaluated. Gas approaches to include the reactions of the Si excess with a gaseous precursor to carbon, nitrogen and oxygen at lower temperature. A few examples are described below.

Table 3. Steps, Variations and Attempts to Eliminate Excess Si in Approach 2 Processing

#	Procedure/ Purpose	Observations
1	**1 layer**: ZrB_2 powder (0.66 mol ratio), Si powder 1.0 mol ratio) Phenolic (~1.00 mol ratio of C), heated to 1500°C; *For generating in-situ SiC by reacting Si with polymer-derived C*	Base approach prior to the multi-step method development. Good integrity but coating can be scratched with a razor blade. SEM reveals no significant cracks or coating defects but the coating is relatively porous due to the structure evolved during the reaction between the Si powder and polymer-derived C at 1500°C.
2	**1st layer**: ZrB_2 (8.17mol ratio), phenolic (~1.0 mol ratio), heated to 1000°C; **2nd layer**: Si bonded with phenolic heated to 1500°C	The 1st layer is very uniform with no cracks and mild porosity. The second layer was deposited only on 3/4 of the 1st layer by the dip technique. **Excess of Si is detected**. A Si-containing layer is formed as a **"top layer"**. Si wicked and also covered all the area of the 1st layer that was uncoated with the slurry of the 2nd layer. **Conclusion: Si can significantly migrate to a carbonaceous area during the RBSC**
3	Coating made according to #2 embedded into carbon black powder and heated again at 1500°C. **Purpose: converting excess silicon to SiC.**	**The elemental Si disappeared** and a sharp XRD pattern of SiC is generated. There is still a significant top layer of SiC only. The surface is also covered with whiskers.
4	**1st layer**: ZrB_2 (8.17 mol ratio), phenolic (~1.0 mol ratio), heated to 1000°C; The specimen was placed vertically on top of Si chips in a BN boat and heated to 1500°C.	The concept here is to use the wicking properties of the molten Si during the RBSC. The Si wicks at 1500°C throughout the entire coating. SEM indicates the migration of Si 2cm upward. There is still a layer of Si on top but it is much thinner, except the area where the sample was standing in the molten Si.
5	Coating made according to #4 embedded in carbon black and reheated at 1500°C.	The top SiC layer is eliminated or almost completely eliminated. The Si was converted to SiC. This process became the leading concept for further development.

Table 3. Steps, Variations and Attempts to Eliminate Excess Si in Approach 2 Processing (Continued)

#	Procedure/ Purpose	Observations
6	**1st layer**: ZrB_2 (8.17mol ratio), phenolic (~1.0 mol ratio), heated to 1000°C; **2nd layer**: Si bonded with phenolic heated to 1500°C; **3rd layer**: ZrB_2 (8.17mol ratio), phenolic (~1.0 mol ratio), heated to 1500°C;	A 3rd layer approach for further reacting a carbon source with the excess of Si. No major reaction is observed between the top layer and the excess of Si. However, the top layer bonds well to the 2nd layer but can be still scuffed of the surface by a razor blade. The migration of molten Si to the top layer creates an intermediate layer with porosity.
7	**1st layer**: ZrB_2 (8.17mol ratio), phenolic (~1.0 mol ratio), heated to 1000°C; **2nd layer**: Si bonded with phenolic heated to 1500°C; **3rd layer**: ZrB_2 (8.17mol ratio), phenollic (~1.0 mol ratio), heated to 1500°C; **4th layer**: Si bonded with phenolic heated to 1500°C; **Step 5:** Followed by reheating in carbon black powder at 1500°C.	Thick coating formation by repeating the process of #2 followed by the process of #5 at the end of the second processing cycle. The overall coating bonds strongly to the surface and has no cracking though it was heated already 4 times to 1500°C and it was about 60 μm thick. The top layer is partially covered with a glassy crust and partially with whiskers. The coating structure clearly shows a multilayer coating with internal layer of SiC.
8	Process of #2 followed by a coating with 20 wt% solution of Phenolic pyrolyzed at 1000°C and then heated at 1500°C.	Another approach for eliminating the free silicon. Only the top layer can be scratched by a razor blade. SEM is performed after removal of top layer. Some areas still have remains of the reacted phenolic layer (XRD reveals only ZrB_2 and SiC.
9	Process #2 treated in **air** (oxidation) at 1000°C for 10h.	An alternative approach to eliminate the excessive silicon by selective oxidation. No significant microstructural change from the coating before oxidation. No oxide phases are observed and the Si pattern is still strong as detected by XRD. *To be repeated at higher temperature.*

Table 3. Steps, Variations and Attempts to Eliminate Excess Si in Approach 2 Processing (Continued)

#	Procedure/ Purpose	Observations
10	Process #2 treated in **air** (oxidation) at 1400°C for 1h. *Alternative approach to convert Si to SiO_2.*	An alternative approach to eliminate the excessive silicon by selective oxidation. Severe oxidation occurred including the oxidation of ZrB_2, leading to coating deformation. No further investigation of this approach was done. It should be further explored in future studies.
11	Process #2 treated in $\mathbf{N_2}$ (nitridation) at **1400°C for 1h**. *Alternative approach to convert Si to* $\boldsymbol{Si_3N_4}$**.**	An alternative approach to eliminate the excessive silicon by selective nitridation. A glassy layer is formed with "ice" cracks or embedded whiskers in this layer. The ZrB_2 was also nitrided. ZrN and BN are observed by XRD.
12	Process #2 treated in a gas mixture of **2000 ppm propylene, 2000 ppm ethylene, 2000 ppm acetylene**, at1500°C for 3h. *Alternative approach to convert Si to SiC.*	A carbon crust is formed. When removed, SEM and XRD analyses confirm the conversion of the free Si to SiC.
13	Process #4 and #5 with **one additional step**. Prior to the embedding of the sample in carbon the specimen is placed vertically on top of a layer of carbon powder and heated at 1500°C to "drain" molten excessive silicon accumulated at the bottom of the specimen.	This process provided a dense 30 micron UHTC coating with almost no top layer of SiC. It became the leading approach for the rest of the study.
14	Thick coating formation The process of #4, #5, and #13 with a modification of step #4: The ZrB_2/phenolic was repeated 3 times with only a curing step at 120°C between dipping.	A high integrity coating, dense and 100 µm thick. Some areas at the bottom are 300 µm thick. Excellent adhesion. This process was used for generating specimens at the final stage of the oxidation effort.

A 2 layer processed coating (1^{st} ZrB_2/C, 2^{nd} Si/C; #2 in Table 3) was heated in nitrogen at 1400°C in an attempt to nitride the free Si. A glassy layer was formed with "ice" cracks or embedded whiskers in this layer as shown in Figure 26. A very complex phase formation was detected by XRD analysis, including the formation of ZrN and BN as shown in Figure 26c.

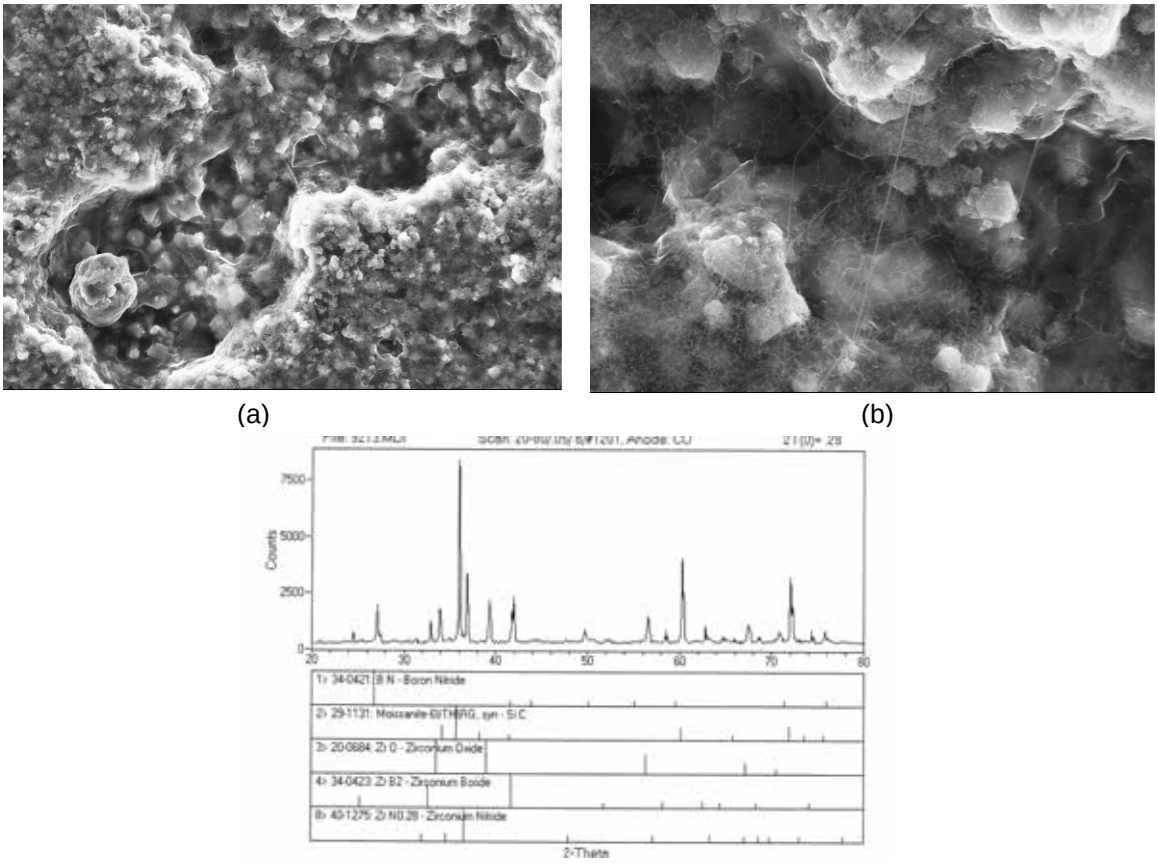

Figure 26. The microstructure and XRD pattern developed during nitridation of siliconized coatings.

Figure 27 shows a similar two-layer coating that was treated in air at 1000°C to oxidize the excess of Si. No significant change in the microstructure is developed. The free Si is still observed by SEM (Figure 27a and 27b). No oxide phases are observed and the Si pattern is still strong as detected by XRD analysis (Figure 27c).

The same approach was taken but the oxidation was performed at 1400°C. Under these conditions the coating was completely deformed due to severe oxidation. The coating is white and easily removed from the substrate surface. Clearly, all the ZrB_2 and the already developed SiC phase were oxidized. This approach deserves additional assessment in future development. Potentially, oxidation at lower temperature (in the solid phase) will be required to prevent the attack of the oxygen on the ZrB_2 and SiC phases. However, the diffusivity of the oxygen under these conditions is expected to be limited.

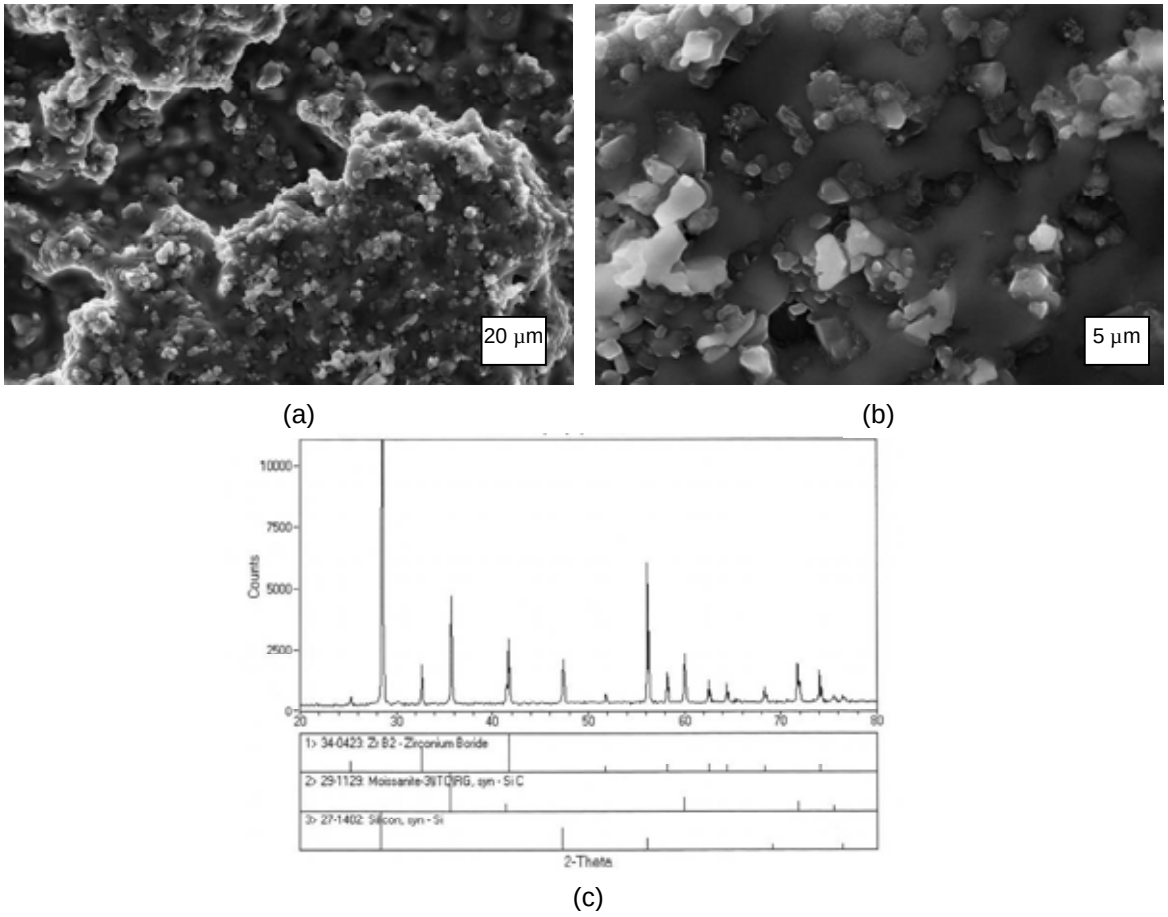

Figure 27. A two-layer coating prepared according to Process #2 in Table 3 after treatment in air at 1000°C.

A different approach was evaluated in which a third layer of ZrB_2/C was deposited in order to allow the free silicon from the second step to react with the freshly developed carbonaceous material. This three-layer process consists of 1st -- ZrB_2/C, 2nd -- Si/C, and 3rd -- ZrB_2/C layer depositions all heated to 1500°C, individually (Process #6 in Table 3, Figure 28). The porous top layer indeed absorbs the free silicon from the coatings below but new porosity is evolved inside the bottom layers as shown in Figure 28c and Figure 28d. The top layer shown in Figure 28a and Figure 28b contains high level of porosity.

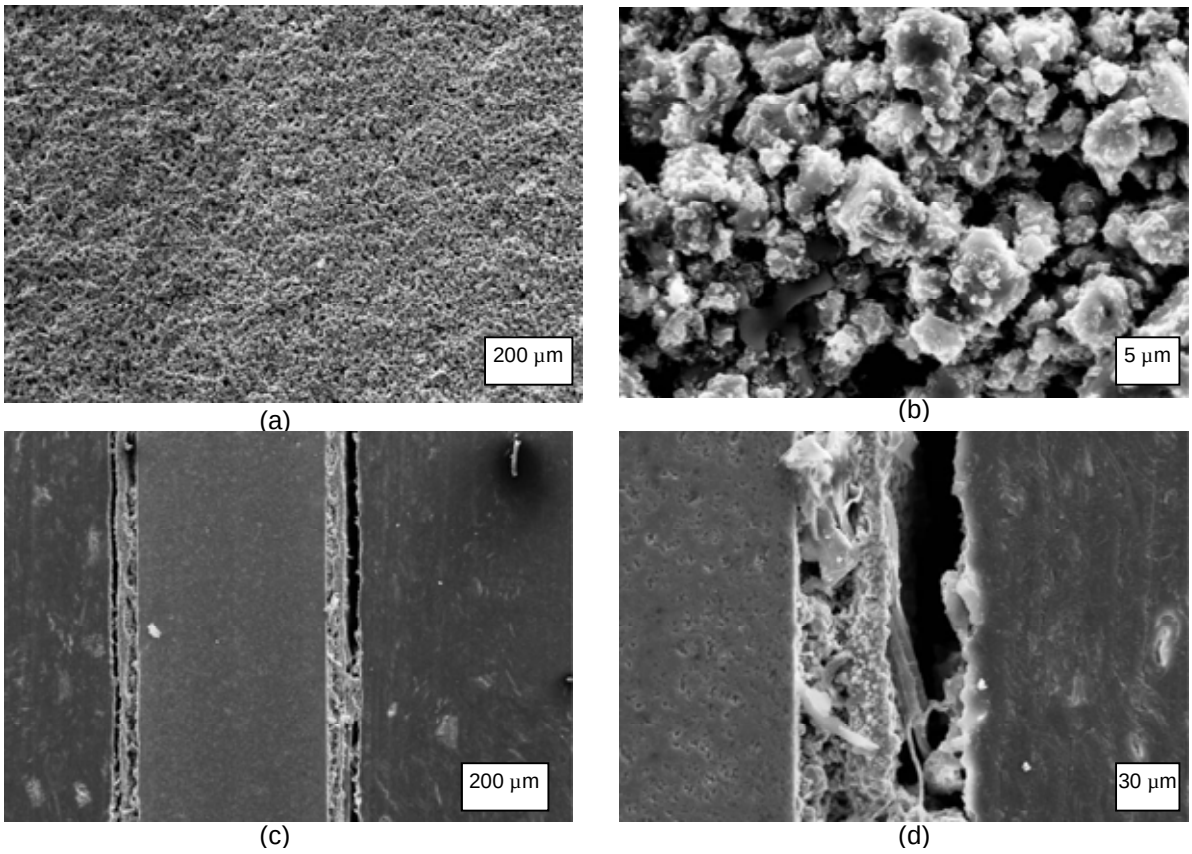

Figure 28. A third layer of ZrB_2/C on top of a two-layer coating; porosity is generated due to the partial migration of Si from the middle to the top layer.

The deposition of a carbon layer as a means to eliminate the Si was also explored. A phenolic resin coating was deposited (Approach #6, Table 3) on top of the Si layer by dipping the coating in 20 wt% phenolic solution in ethanol (Figure 29). No free silicon was detected by the XRD analysis of the surface and more SiC was determined.

The microhardness of such coatings is in the range of 3.4 to 10.8 GPa, which is comparable to the hardness of glass. The large variation is attributed to the roughness of the coatings as well as for areas, which are covered with a thin SiC layer versus areas where the composite microstructure is exposed.

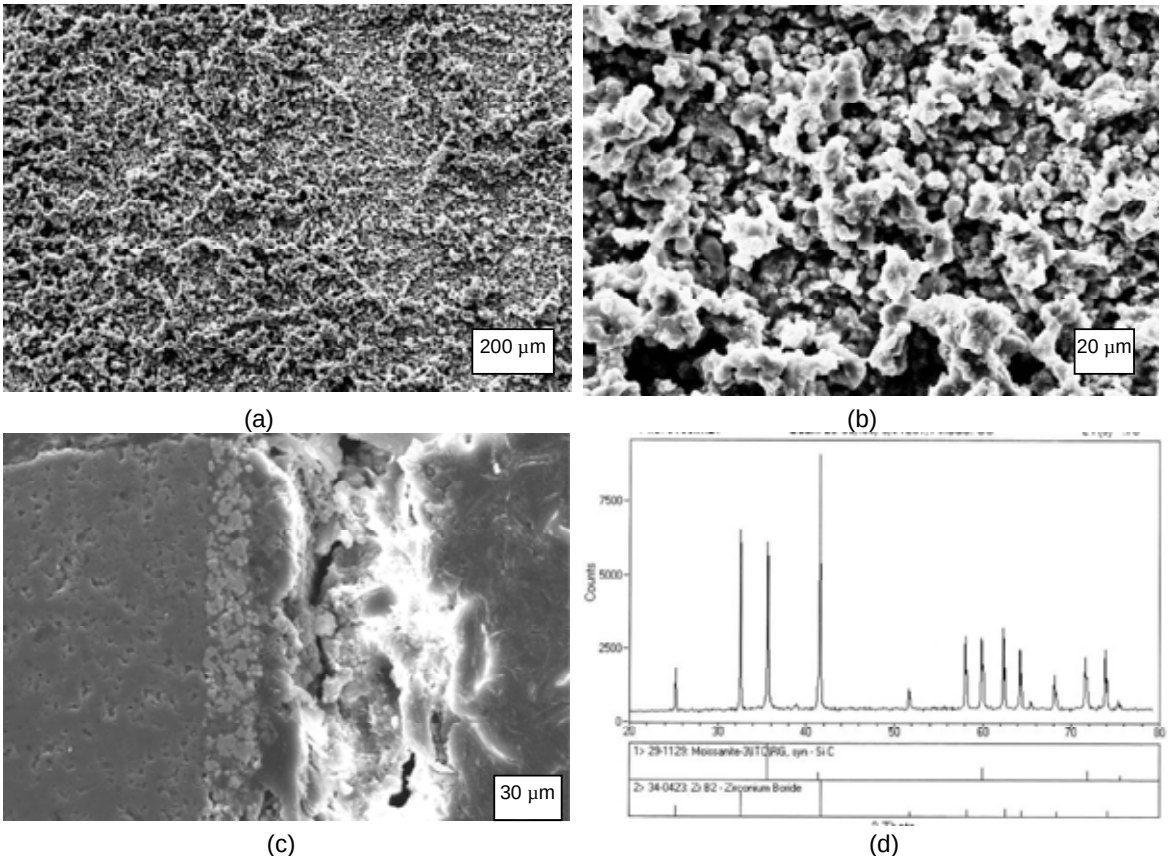

Figure 29. Three layer coating consisting of ZrB_2/C (1st layer), Si/C (2nd layer), and a 3rd layer of dipped 20% phenolic coating heated to 1500°C.

The best and rather simple approach to eliminate the free Si was to simply cover the siliconized specimen in black carbon powder and reheat it at 1500°C. This method results in the elimination of free Si without creating a porous layer. The coating thickness was typically 30 to 40 µm. The surface is ragged and, in addition, some SiC needles are formed as illustrated in Figure 30. However, the surface roughness is only 1 to 5 µm in depth, less than the roughness of a typical CVI C/SiC. The distribution of the Zr and Si phases are homogeneous considering the irregular size and shape of the original commercial ZrB_2 powder used in the study. This powder is 325 mesh in size and the dominant particle size range is 5 to 15 µm. In future studies it will be important to study the effect of the ZrB_2 particle size on the characteristics of the coatings.

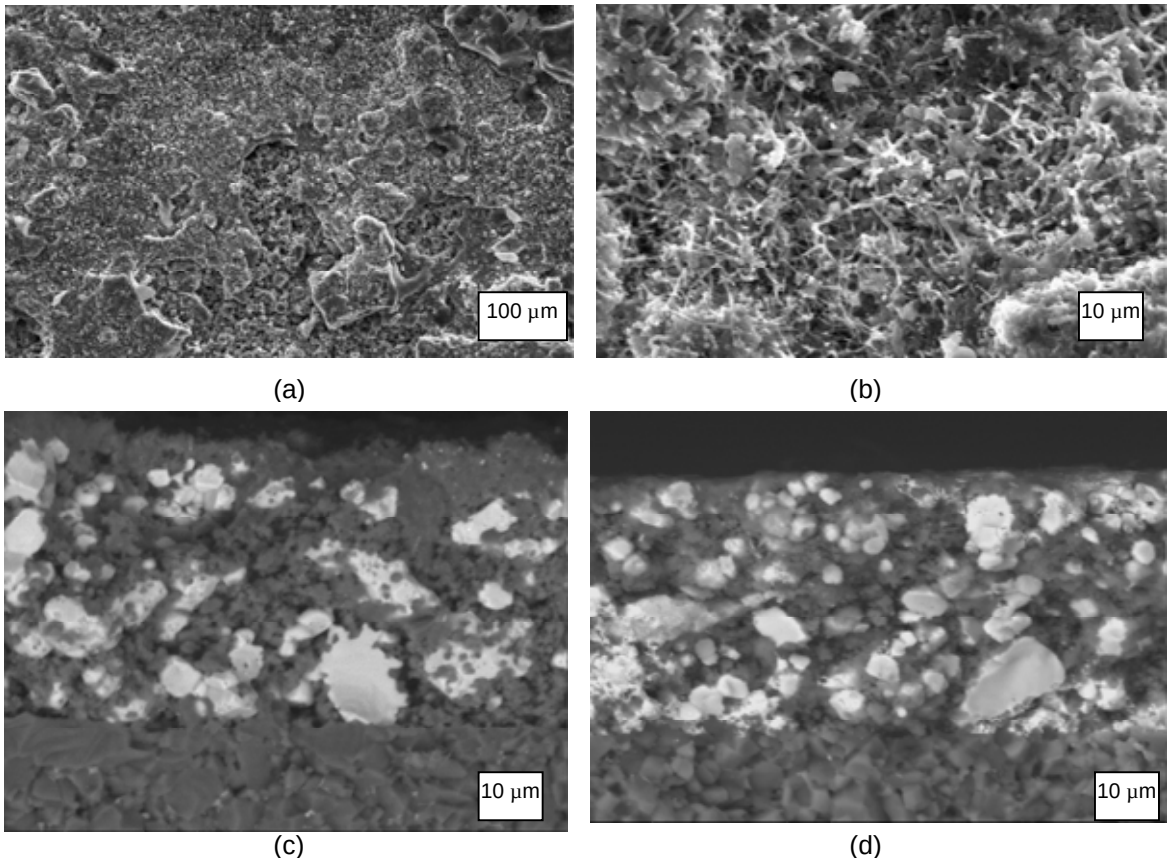

Figure 30. Coatings produced by a three-step process: (1) ZrB_2/C preform coating; (2) Si infiltration by the wicking process; (c) reheating covered by carbon powder. The cross-section pictures are taken in a back scattering mode to contrast the Zr-containing phases from the Si-containing phases.

In addition to the elimination of the free silicon, the phase analysis of these coatings reveals a very interesting phenomenon of converting part of the ZrB_2 to ZrC. This transformation must be attributed to the reaction of the boride with the phenolic derived carbon, but the molten silicon may be involved in the mechanism. Therefore, it seems that kinetic and concentration effects take a significant role. The conversion of the boride to carbide as shown in Reaction (3) is unfavorable thermodynamically. However in the presence of low oxygen level the following Reaction (4) is spontaneous at 1500°C.

$$ZrB_2 + C \longrightarrow ZrC + 2B \qquad \Delta H_{1500°C} = 139.0 \text{ kJ}; \Delta G_{1500°C} = 107.5 \text{ kJ} \quad (3)$$

$$ZrB_2 + C + "O_2" \longrightarrow ZrC + 2BO \quad \Delta H_{1500°C} = 136.0 \text{ kJ}; \Delta G_{1500°C} = -195 \text{ kJ} \quad (4)$$

In some cases a small level of zirconium silicides, $ZrSi_2$, was also detected, which is even a more thermodynamically unfavorable. The silicide phase was never detected after step 3 (the carburization of the Si). Figure 31 shows the evolution of the XRD pattern after each of the three basic steps of the RBSC approach. These reactivities need to be further studied in a future fundamental research.

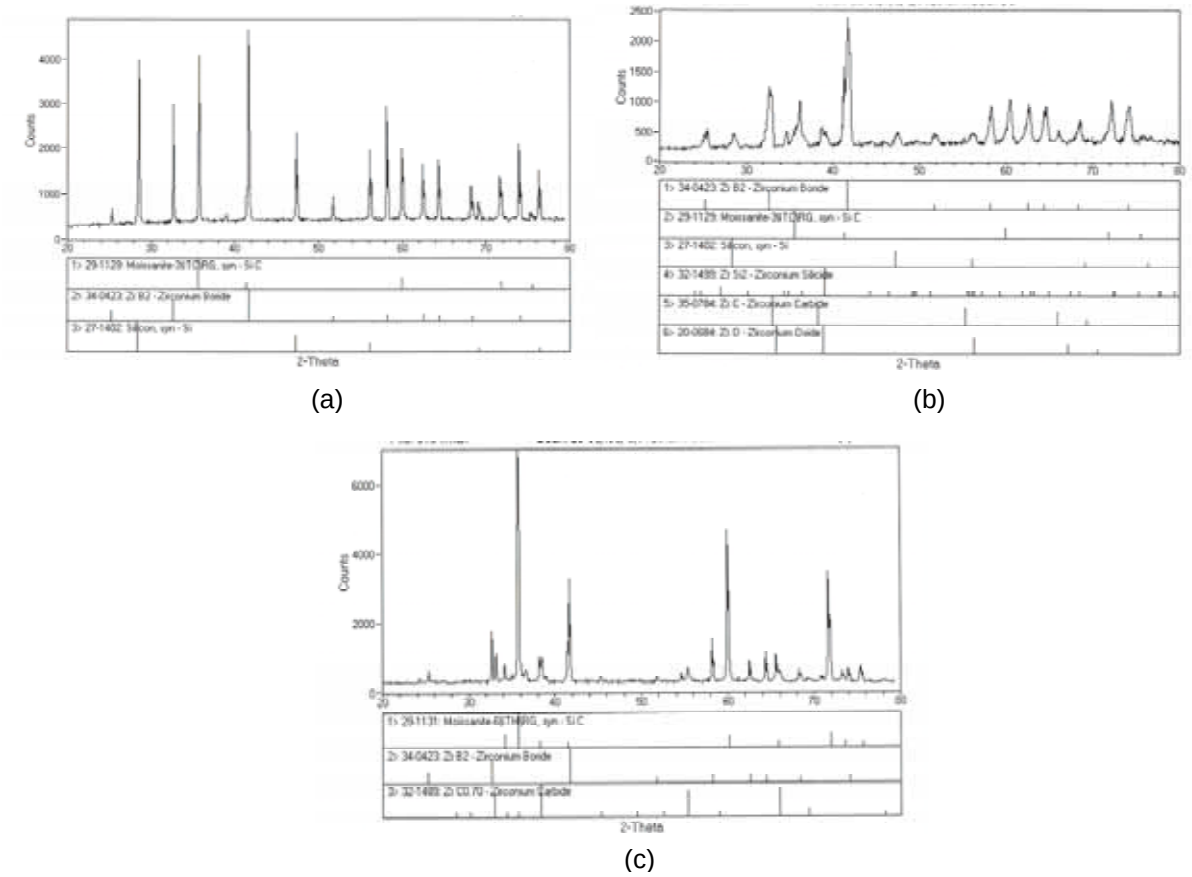

(a) (b)

(c)

Figure 31. XRD pattern of coatings processed by the RBSC approach; (a) and (b) are two variations in phase development after the siliconization step; (c) shows the pattern after reacting the excess of carbon.

3.3.3 Thicker Coating Development

Several recent oxidation studies of similar UHTC particulate composites reveal that major reactivities occur during high temperature oxidation across the first 100 µm of the bulk material [70,73,74]. The initial coatings developed by the preform coating approach were 30 µm thick. Since the coating approach is based on a dipping technique in slurries with varied viscosities, the major factor affecting the final thickness is the thickness of the deposited ZrB_2/phenolic slurry during the 1st step. Potentially, if layers thicker than 30 µm are deposited in a single step, defects such as bubbles due to solvent volatilization and cracks due to the coating

shrinkage and mismatch between the coefficients of thermal expansion (CTE) of the coating and the substrate are commonly generated.

If the issues of CTE mismatch and stress formation are ignored, there are several potential ways to increase the thickness:

(a) Repeat the entire process twice.

(b) Generate a thick preform coating (100 μm thick) and then continue the next steps in a single operation.

(c) Perform the same approach as in (b) but also alter the preform composition.

(d) Perform the same approach as in (b) but also incorporate elemental Zr or Hf to form a ZrC or HfC phases.

A 2 cycle processing of the 3 step process was investigated first. The initial SEM analysis was very positive as illustrated in Figure 32. A 60 μm layer has been obtained with very good bonding to the surface and no cracking of the coatings. Notice that there is a thin interface layer between the 2 coatings, which is the residual layer of SiC carbide obtained during the first layer deposition. This SiC layer may be advantageous by forming an intermediate barrier and as silicate forming "reservoir". However, it may increase the stress formation especially if a silica layer is locally formed.

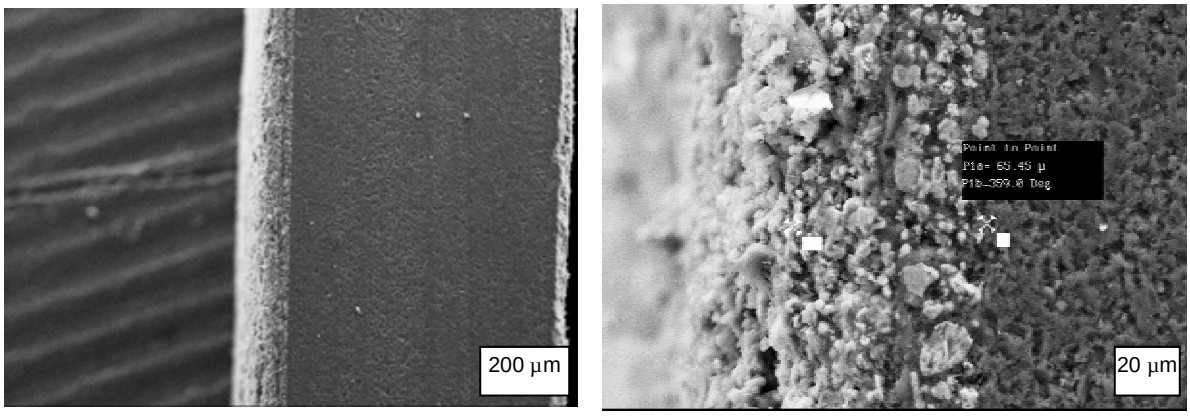

(a) (b)

Figure 32. A 60 μm coating is obtained by 2-cycle processing of the three-step preform- RBSC-carburization approach.

Figure 33 represents a three layer coating made by this approach. The overall thickness is about 100 μm. There is no delamination or significant cracking observed across the cross section of the coatings. The coating seems to be dense and Si can be detected in all three layers. No thin layers of SiC developed during the siliconization of each layer were observed in this case. There is very little evidence for the interfaces between the three layers.

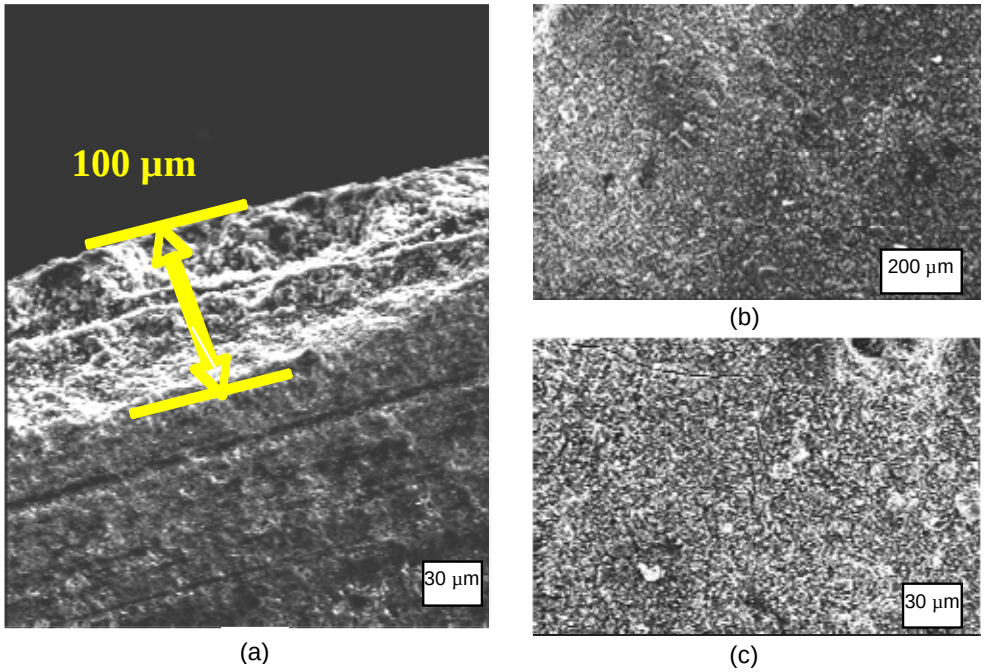

Figure 33. A 100 µm coating is obtained by 3-cycle processing of the three-step preform- RBSC-carburization approach.

A second approach to achieve thick coatings was assessed in parallel. A thick ZrB_2/C preform layer was processed by depositing 3 layers of ZrB_2/C of the standard slurry used to form a single layer. Initially each layer was cured and pyrolyzed but in order to eliminate processing steps, an attempt was made to form the thick preform layer by just curing the coatings after each layer deposition. The curing was performed in a conventional open oven at about 100°C prior to the deposition of the next layer.

After pyrolyzing the preform layer the coatings still maintained good integrity probably due to the generated porosity that mitigated the stresses generated by the shrinkage of the pyrolyzed phenolic resin. The preform coating was efficiently infiltrated by molten Si throughout its thickness by applying the same wicking approach developed for the 30 µm coatings (i.e., vertically placing the preform-coated specimen on top of Si powder.) The efficient infiltration of the Si was evidenced by EDS analysis.

Also, the carburization process obtained by embedding the coated specimens in carbon black powder was found to be efficient and a dense coating was obtained. No free Si was detected by XRD analysis. Figure 34 represents a coating achieved by forming the thick preform layer. This coating is 100µm thickness. Figures 34a and 34b exhibit an area of the coating, where all three layers are bonded well to each other is shown. Figure 34c shows an area in which the bonding between the first and the second layer possesses a local gap. The three layers are clearly observed. In addition there is a top layer of SiC. Figure 34d shows the coating's surface indicating that no cracking is observed in the thick coating.

The microhardness of the thick UHTC coatings was measured with values in the range of 10.6 to 40.7 GPa. These values are well within the range of hot pressed SiC. The large range is again attributed to the irregular surface texture and areas that are covered with additional SiC

layers versus exposed composite areas. It is possible that the roughness causes significant inaccuracy in the microhardness test results but clearly, the above values are well above the values obtained for other coatings described earlier in this report.

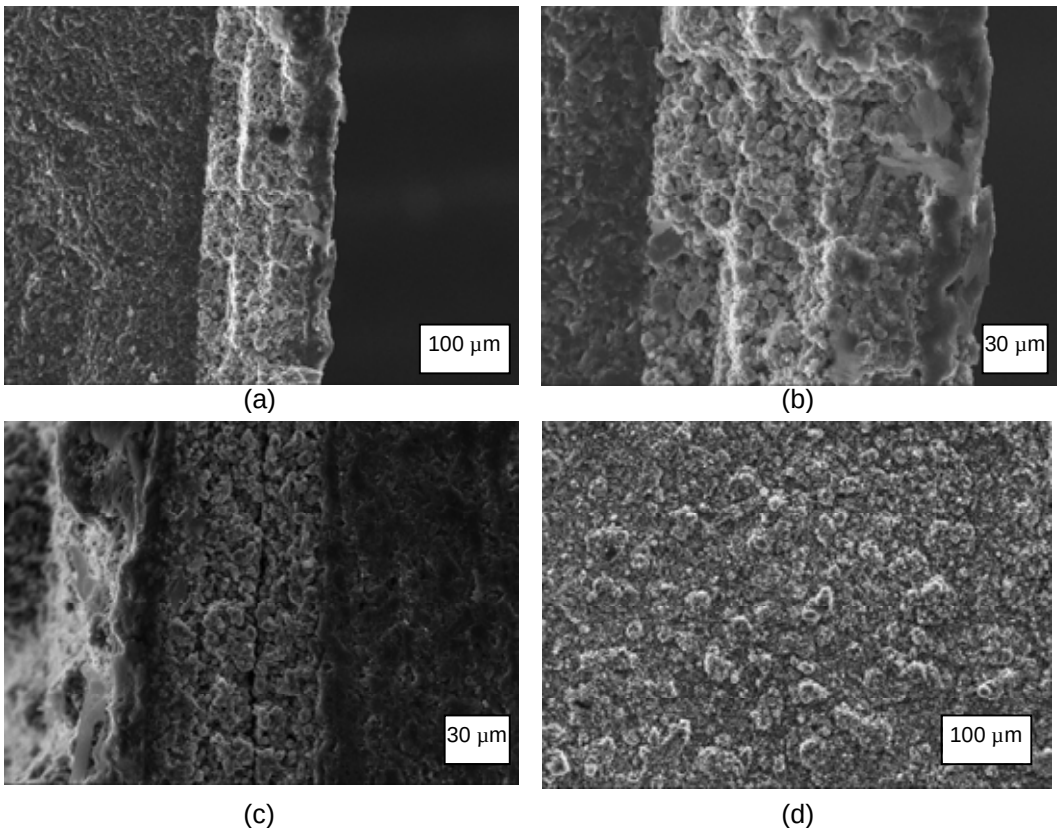

Figure 34: A 100 µm UHTC coatings obtained by (a) depositing three layers of ZrB_2/phenolic, (b) pyrolysis, (c) siliconization and (d) carburization steps.

3.3.4 Detailed Microstructure Analysis of Preform-RBSC coatings

The infiltration of molten Si into a ZrB_2/C preform layer is anticipated to provide primarily only one new phase – SiC, assuming that all the Si was converted. Yet, repeatedly we have observed the formation of a new Zr phase – ZrC as shown in Figure 35a. The intensity of this phase relative to the pattern ZrB_2 is varied from sample to sample, suggesting that its formation is kinetically driven. In some cases the carbide line are larger than the diboride. In a few cases (but rarely) a $ZrSi_2$ phase was also detected (Figure 35b), thus we cannot rule out that $ZrSi_2$ serves as an intermediate for the formation of the carbide. Both the formation of ZrB_2 and $ZrSi_2$ are unexpected, because the Gibbs energy calculations and the enthalpy of these reactions are endothermic and not spontaneous. Alternative mechanisms may occur such as described earlier in Reactions (3) and (4).

Detailed microstructure analysis reveals several intriguing aspects. First, the Zr based material has converted from irregularly shaped particles to a more "sintered" morphology with crystalline-like grains. The Zr containing particles are not homogeneous and contain lighter and darker areas as shown in Figure 36.

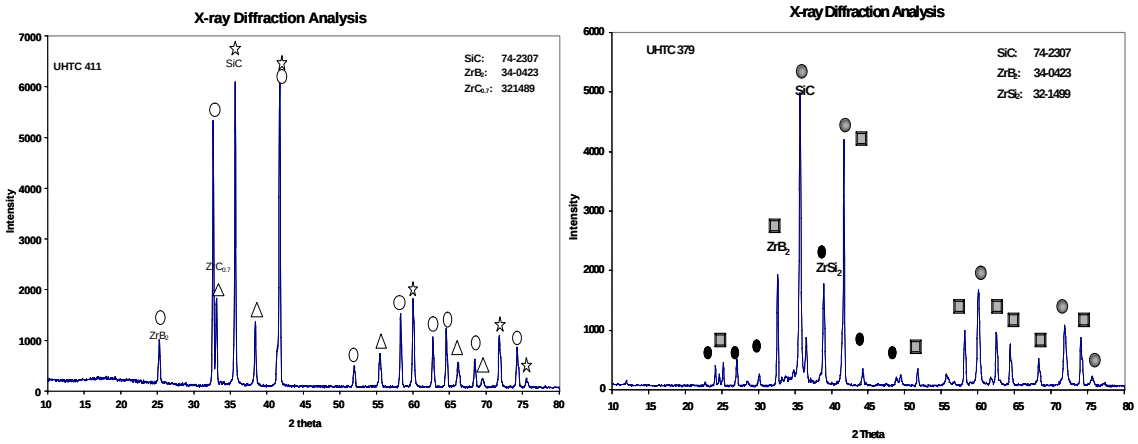

(a) (b)

Figure 35: XRD analyses of preform-RBSC coatings reveal the formation of new Zr compounds phases – (a) ZrC, (b) $ZrSi_2$.

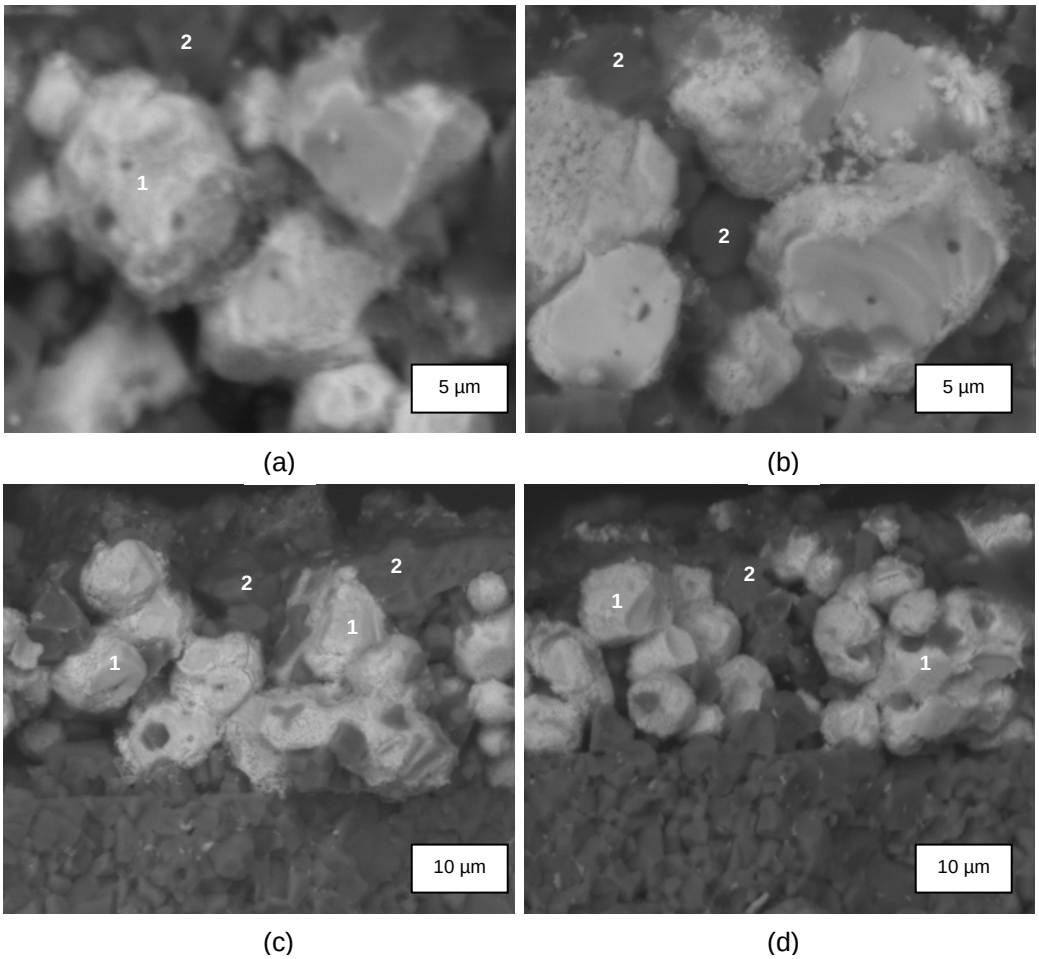

(a) (b)

(c) (d)

Figure 36: Significant changes in microstructure of the original ZrB_2 particles. Some are "sintered" to each other. Some contain darker inclusions.

The different area shades numbered in Figure 36 were analyzed by EDS. Area 1 is Zr rich with C and B. The carbon level is much higher to be assigned just to the Si peak, which probably comes from an adjacent SiC grain (Figure 37). This area may be the microstructural evidence for the presence of a zirconium carbide phase. Area 2 represents a typical SiC grain surrounded by the Zr-containing materials.

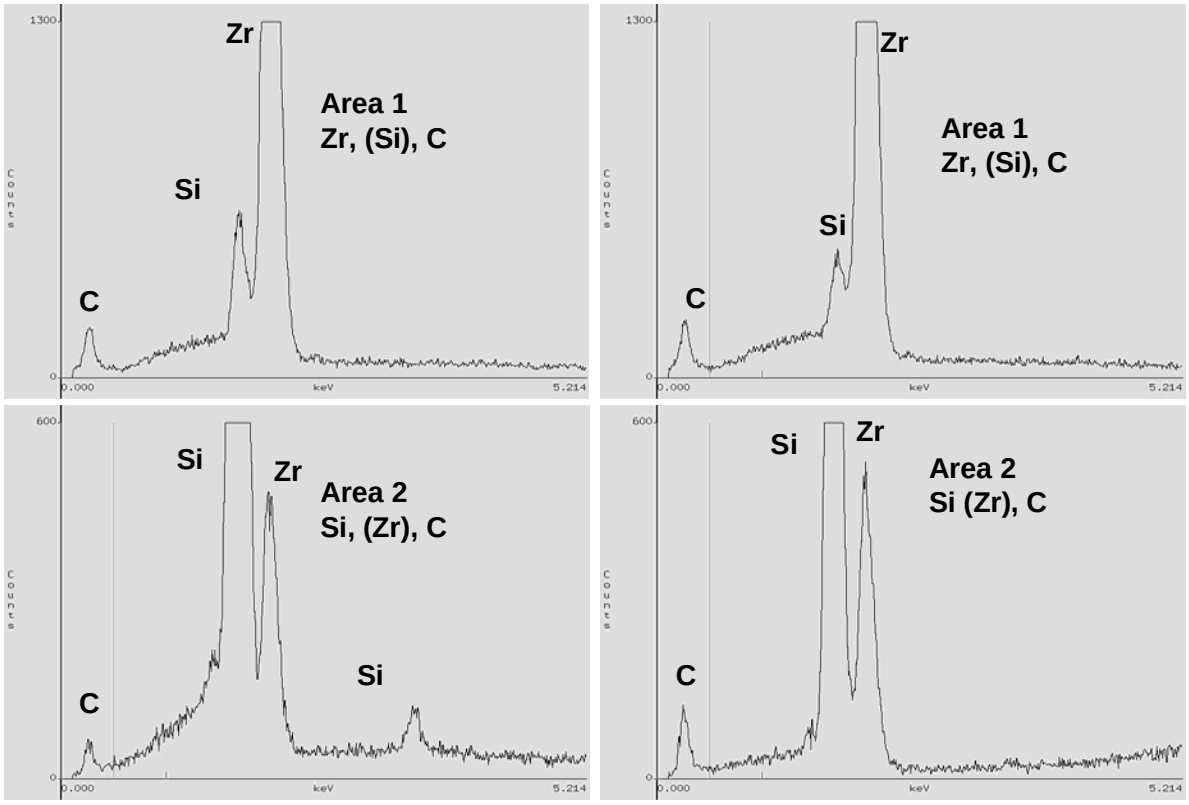

Figure 37: EDS analysis of marked spots in Figure 36.

When a $ZrSi_2$ phase is observed, the microstructure is different as shown in Figure 38. The EDS analysis of Area 1 indicates Zr rich phases including containing C, B and low level of Si (Figure 39). This region contains ZrB_2, and ZrC since the level of C is greater than expected for SiC by the ratio of the C/Si peaks. The dark spots represented by Area 4, is found to be an inclusion of free carbon rich in oxygen. Area 2 is assumed to be $ZrSi_2$ as corroborated by XRD. Area 3 is clearly a SiC phase, with low-level inclusion of oxygen.

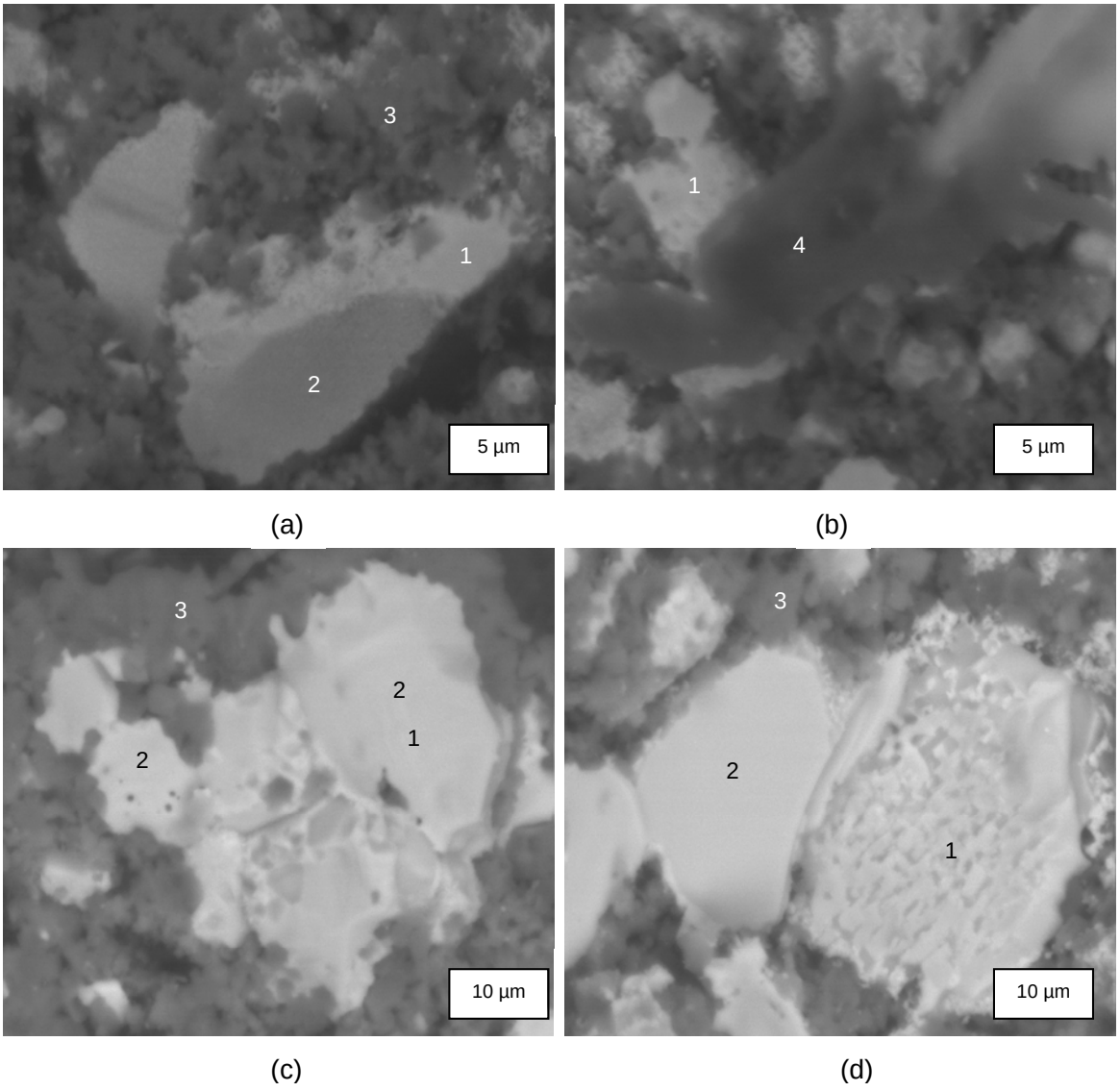

Figure 38: Microstructure of coating developed by the RBSC approach that possesses a $ZrSi_2$ phase.

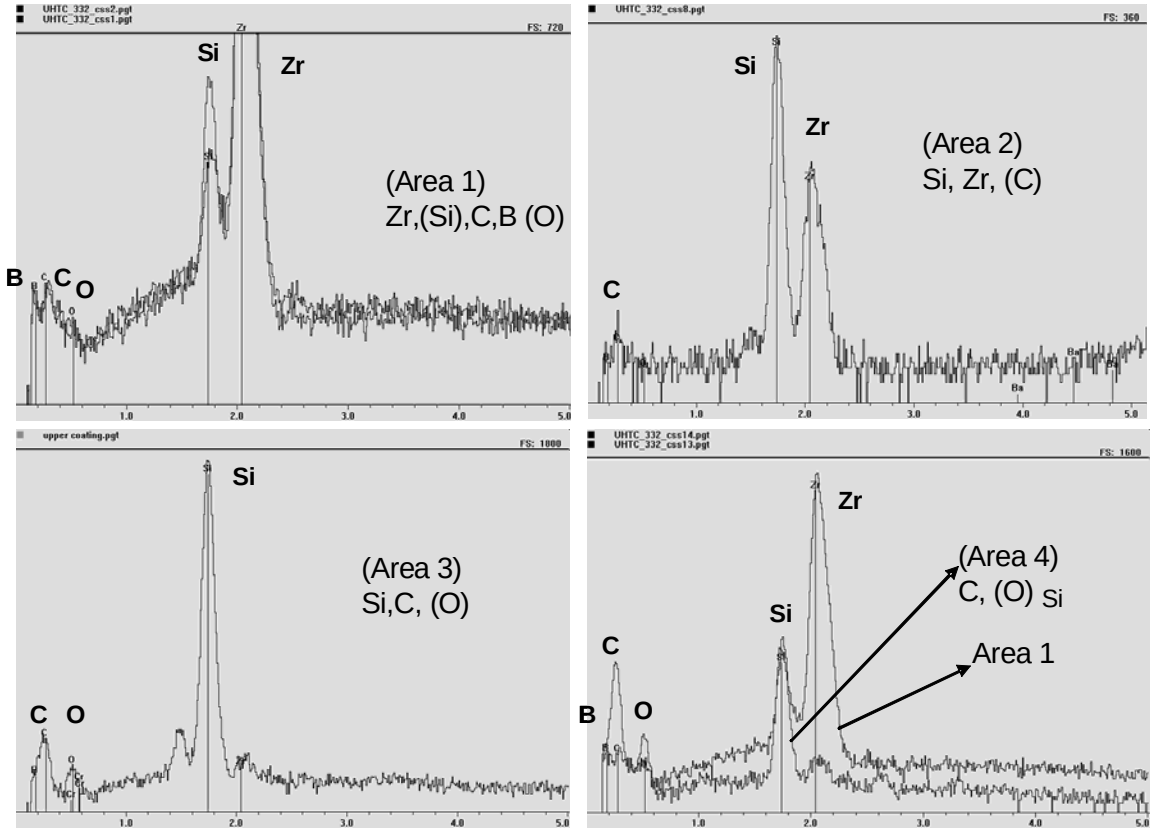

Figure 39: EDS of the numbered spots found in Figure 38.

3.3.5 Coatings on Carbon Fiber Reinforced SiC Composite

The final goal of the developed coatings is to protect either C/SiC or SiC/SiC composites. A limited number of 25 x 10 x 3 mm specimens made of C/SiC composite material (total of 36 specimens produced by GE) were received from NASA Glenn Research Center at the beginning of the project but remained unused because of their very limited quantity and the complexity of their surface, which led to the decision of using monolithic SiC as the preferred substrate through the entire exploratory phase. However, a few of the promising preform-RBSC processes were experimented on such composite specimens at the end of the project as shown in Figure 40. The C/SiC composite already possesses a SiC coating, known as "seal coat", which is 30 to 50 µm thick. The dip coated UHTC slurry conforms very well to the highly irregular surface of the composite, forming good cohesion to the substrate. The UHTC coating is dense and planarizes the coarse textured surface of the composite, derived from the original fabric topology.

A similar coating, shown in Figure 41, demonstrates the good coverage of the coating on top of the complex surface, which consists of dip square holes as well as SiC micro nodules generated by the CVD process. Figure 41b indicates that the composite coating (a) conforms very well to the native SiC layer as shown in Figures 41c and 41d. Figure 41d indicates that the native SiC coating exhibits some cracking by itself before the UHTC coating processing. These cracks

are "designed" to mitigate the mismatch of CTE and prevent delamination due to thermally induced stresses. At high temperature the cracks are physically sealed by expansion. Figure 41b also reveals that debonding of the coating due to mechanical damage obtained during the cutting of the specimen for the SEM analysis is more likely to occur between the bulk composite and the seal layer, rather than between the SiC and the UHTC coatings.

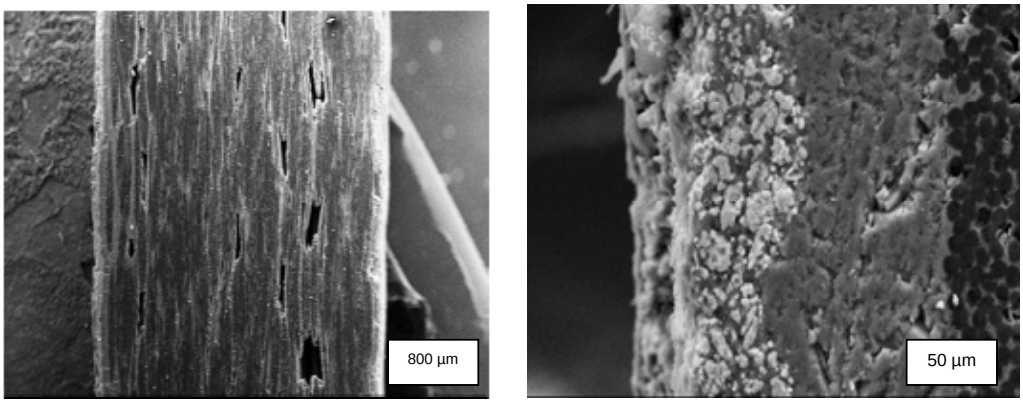

(a) (b)

Figure 40: A 30 to 50 µm thick UHTC coating obtained on top of a CVI composite of C/SiC produced with a SiC seal layer.

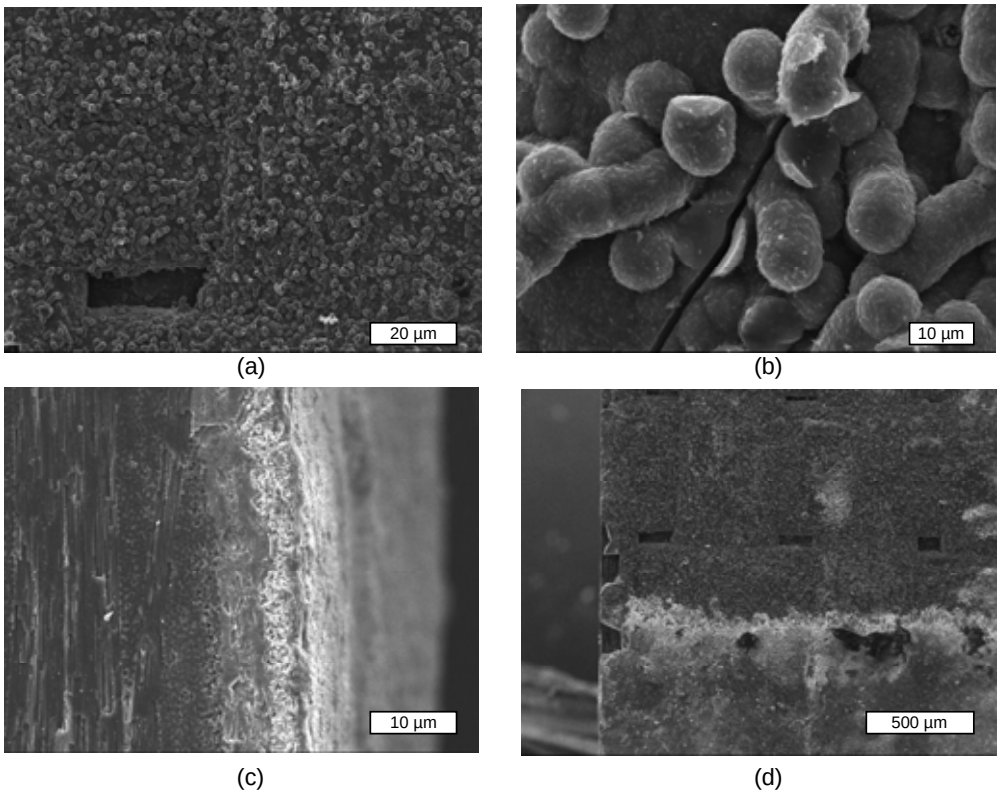

(a) (b)

(c) (d)

Figure 41: A UHTC coating obtained on top of a CVI composite of C/SiC planarizes the seal layer and follows the crack pattern of the originally deposited SiC.

Thicker coatings were also deposited successfully on top of the fiber-reinforced composite by performing the 3-layer process of cured ZrB_2/phenolic slurry. The coating bonds very well and planarizes the surface, as shown in Figures 42a and 42b. Some of the ZrB_2/SiC coating clearly covers the cracks generated in the seal layer, as illustrated in Figure 42b. Some cracks are shown in the UHTC layer, especially in areas that are very thick as shown in Figures 42d and 42e, which again continue the original cracks of the seal layer. Other intriguing observations are the capability to form coatings that are over 200 μm thick as shown in Figure 42d and the capability to form a good bonded coating directly to the cross section of the composite material which is not covered by a SiC layer (Figures 42d and 42e). This is an important observation, since the coating covering the cross section is deposited over a combination of 2 dissimilar materials (SiC and C) that are heterogeneously dispersed and possess gross voids.

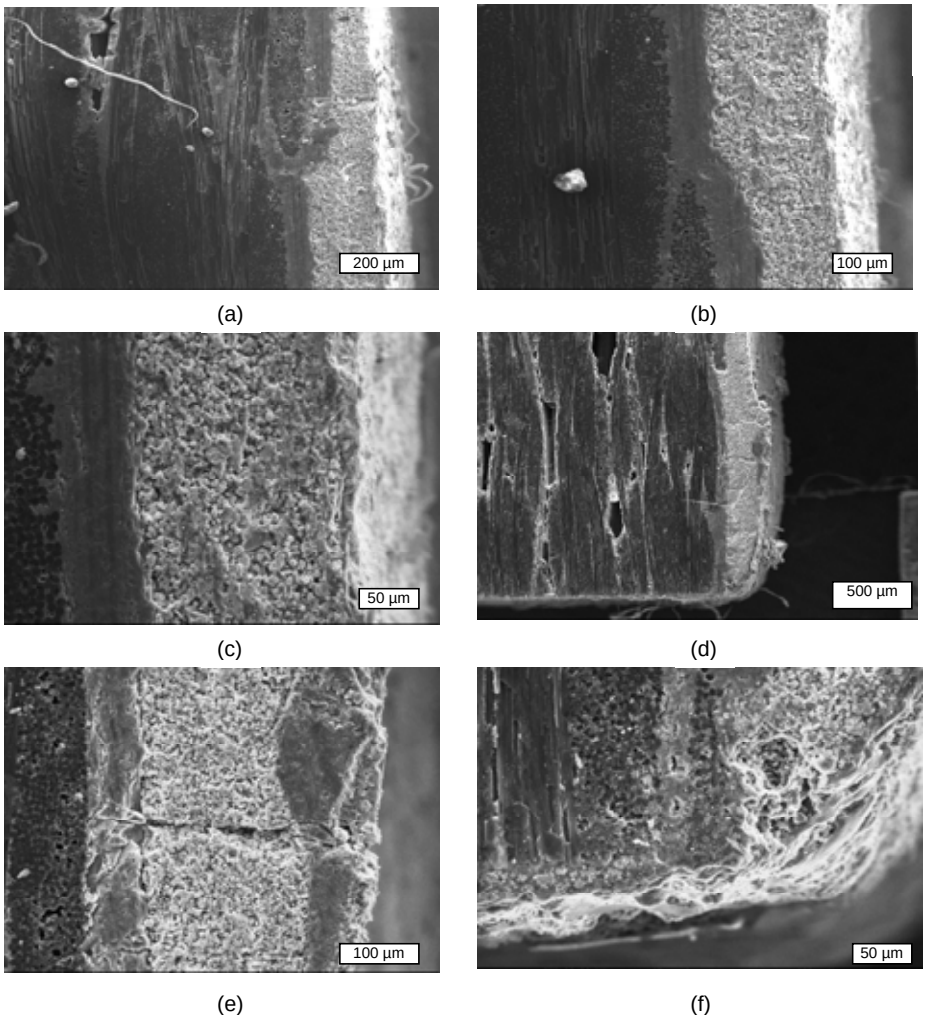

Figure 42: A 100 to 200 μm UHTC coating is demonstrated on top of a C/SiC composite specimen.

3.3.6 UHTC Coatings Consisting of other Compositions

Early oxidation studies of the preform-RBSC derived coatings indicated the formation of a glassy phase with a low melting point. A potential reason for this behavior is the formation of a low melting point borosilicate glass. These observations prompted an exploratory study of processing UHTC coatings with compositions containing lower level of boron. Additional reason for such line of investigation was to demonstrate the capability of altering the composition of the ZrB_2/SiC composite coatings using the preform approach to demonstrate its generic capability.

3.3.6.1 ZrB_2/HfO_2/SiC UHTC Coating Composition

HfO_2 was selected as the first additional phase to be incorporated as powder into the preform formulation to assess this line of research. Its selection is based on the fact that hafnium oxide has higher melting point as well as higher phase transformation temperature than ZrO_2 (around 1800°C). An additional reason for selecting this phase as the secondary phase was "scientific", i.e., to allow the tracking of the effect of an oxide phase in the overall composite coating, by distinguishing it from the evolved Zr based phases.

Initial attempts for generating the ZrB_2/HfO_2/SiC coating revealed that there may be a problem in infiltrating the molten silicon during the second step, since the evolved coatings was more porous than obtained with the base formulation as shown in Figure 43. It was assumed that wetting of the HfO_2 particles by the molten Si was not as efficient as the wetting of the ZrB_2 particles. Improvement of the infiltration was achieved after adding a step of dipping the preform coating in 10% phenolic solution assuming that a thin layer of carbon on top of exposed HfO_2 particles would enhance the wettability of the molten Si and allow its capillary infiltration into the micron-size pores of the preform. The results, shown in Figure 44, suggest that a slight improvement has been achieved. However, the derived coating was thinner than with previous formulations. Further study of processing this formulation revealed an unexpected phenomenon. There was a complete rearrangement of the Zr/Hf phases under the processing conditions.

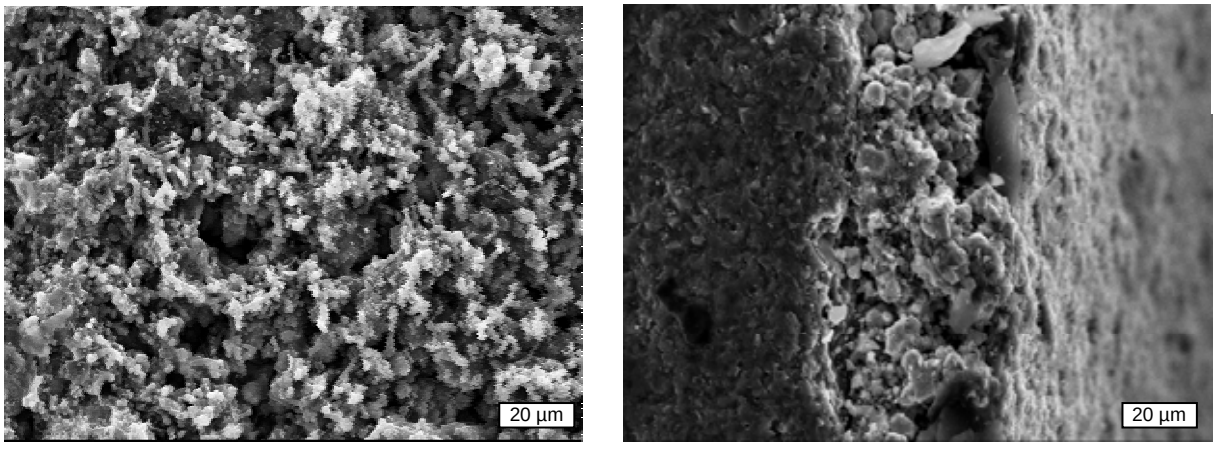

(a) (b)

Figure 43: A porous UHTC coating obtained with ZrB_2/HfO_2/SiC composition.

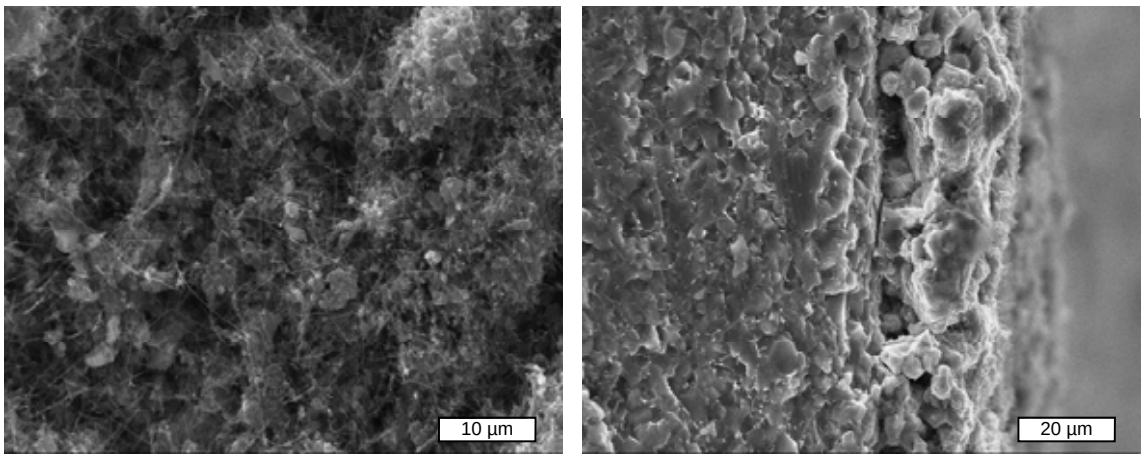

(a) (b)

Figure 44: A 20 µm ("thin") ZrB_2/HfO_2/SiC coating with improved density.

Figure 45 illustrates the morphological rearrangement that occurs with the HfO_2 formulation. The Zr/Hf phases seem to form microstructure resembling a sintering process. This rearrangement involves also trapping of SiC particles within the Zr/Hf based grains. The EDS analysis of the marked spots in Figures 45c and 45d detects areas in which both Zr and Hf present in the same location (Figure 46, Area 1). The EDS analysis does not show any significant level of oxygen as anticipated in this formulation. The XRD analysis reveals an almost complete disappearance of the HfO_2 phase, which typically provides very strong XRD lines. One postulated mechanism to explain these observations is a potential reaction between the HfO_2 and molten Si or the C to form volatile SiO or CO, which forms reactive Hf species that interact with the ZrB_2/ZrC phases. Nevertheless, these reactions are not favorable thermodynamically by simple calculations.

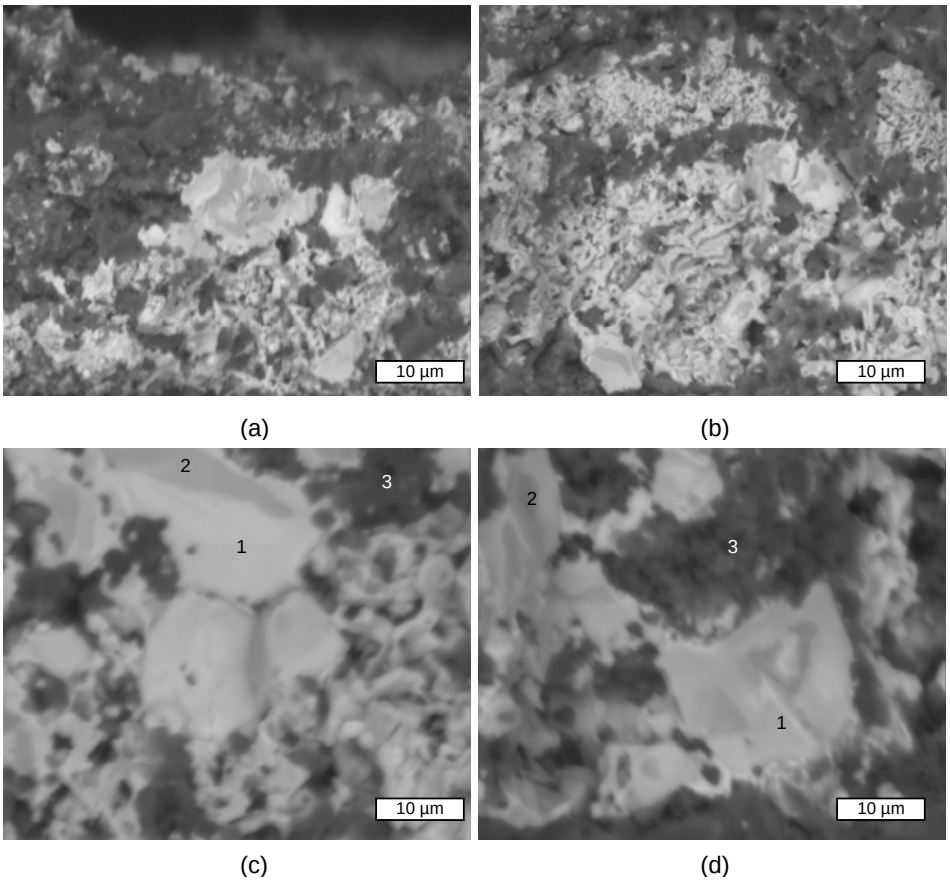

Figure 45: A rearrangement of the ZrB_2/HfO_2 phases obtained in a ZrB_2/HfO_2/SiC coating.

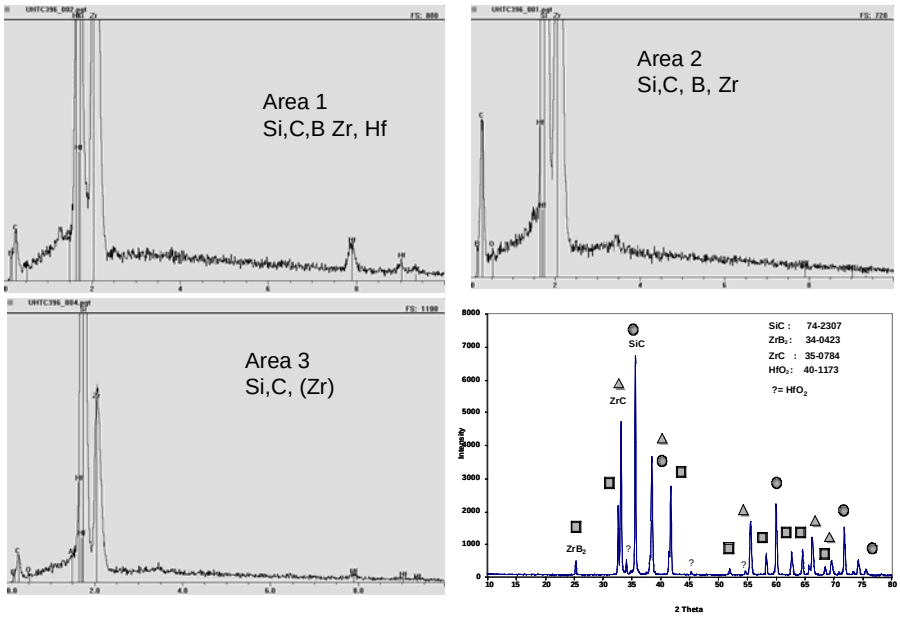

Figure 46: EDS analysis of spots marked in Figure 45.

3.3.6.2 ZrB_2/HfC/SiC UHTC Coating Composition

A similar attempt to introduce additional phase to the ZrB_2/SiC composition was achieved by incorporating HfC powder into the preform formulation. The reactivity of the HfC with the Zr phases was even more profound than above. A significant rearrangement of a crystallite-shaped pattern was observed. These grains contain either Zr or a mixed Zr/Hf phase. Some of these grains seem to sinter to each other as shown in Figure 47. SiC small grains can be found trapped inside the rearranged Zr/Hf phase. The XRD pattern reveals only ZrB_2, ZrC and SiC phases. No evidence for the presence of crystalline HfC is detected by XRD analysis. The EDS analysis of the marked areas is shown in Figure 48. Area 1 contains Si and Hf and potentially can be a hafnium silicide phase. Area 3 contains Zr, Hf, Si and C and can be a mixed phase or two phases fused to each other. Indeed the grain in Area 3 contains different shades.

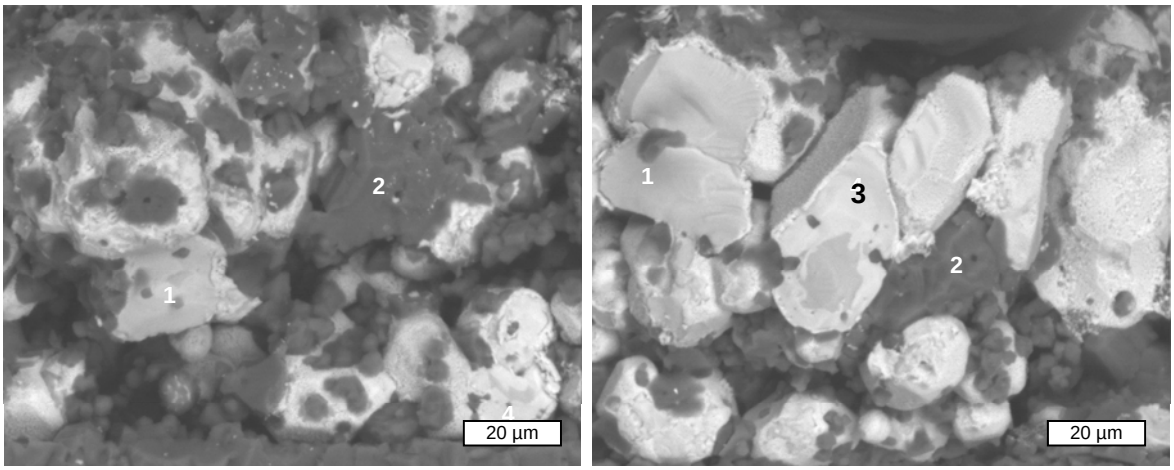

(a) (b)

Figure 47: A complete rearrangement of the Zr and Hf phases is observed in a coating based on ZrB_2/HfC/phenolic.

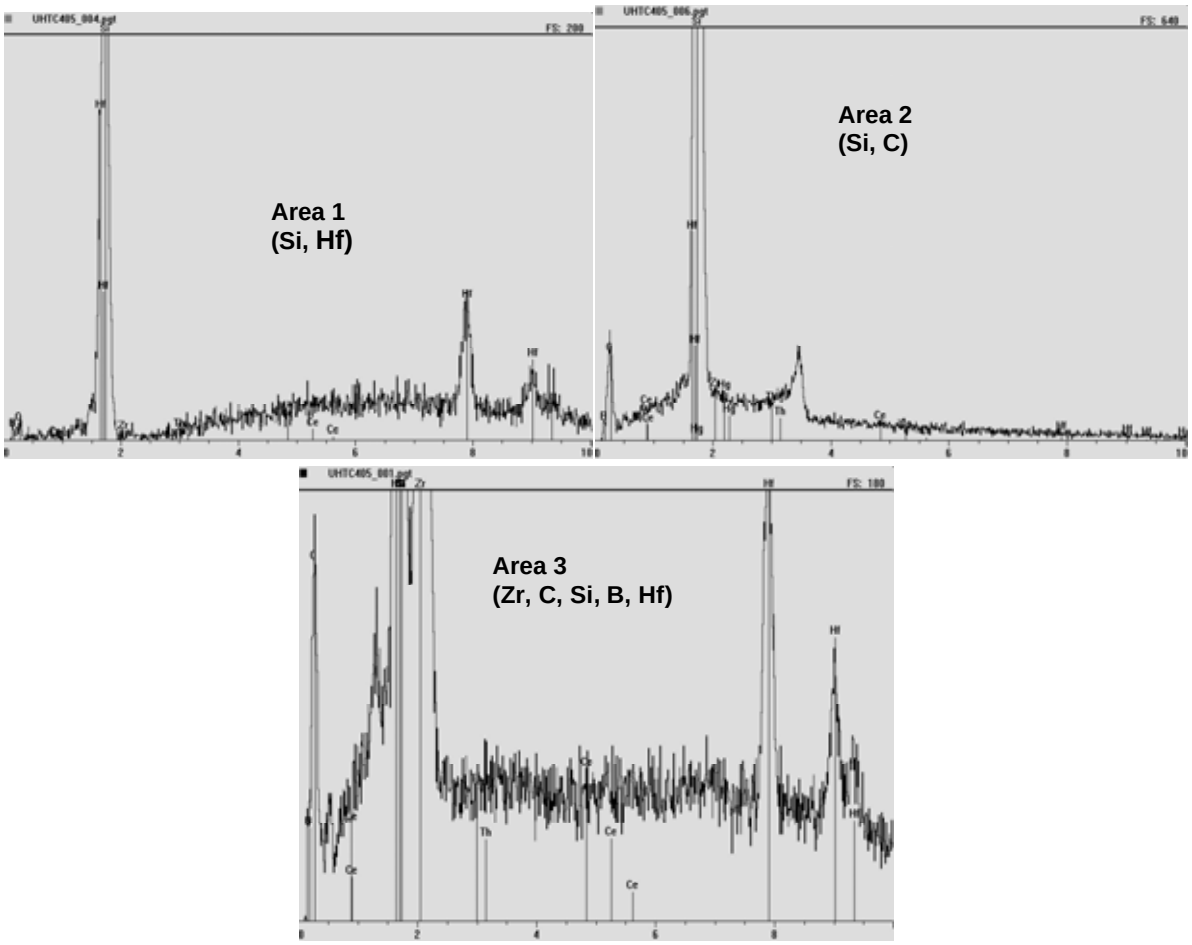

Figure 48. EDS analysis of areas marked in Figure 47.

3.4 Oxidation Study

3.4.1 Furnace Oxidation Testing: Test Procedures and Upgrades

Various coatings and a few promising slurry derived bulk materials were assessed for their performance under various oxidation conditions during the course of the project. A series of furnace oxidation studies at temperatures up to 1500°C were performed with flowing gas mixtures under: i) 21% O_2 in Ar (air equivalent mixture) at 1 atmosphere (760 Torr) total pressure, ii) a variety of reduced O_2 partial pressures in Ar at 1 atmosphere total pressure, and iii) high velocity (10's m/s) and low total pressure (~ 0.0026 atmospheres or 2 Torr) flow of 87% O_2 in Ar, with or without the presence of atomic oxygen generated by the microwave discharge source.

To reach the sufficiently high temperatures, SRI's low-pressure/microwave testing capability was augmented by adding two resistively heated tube furnaces to the existing test setup - a SiC heating element furnace (T_{max} = 1300°C) and a $MoSi_2$ heating element furnace (T_{max} = 1650°C). One-inch diameter alumina furnace tubes were used for almost all the

experiments. The microwave discharge and vacuum manifolds were mounted to movable stages so that they can rapidly be coupled to either furnace. The new configuration allowed testing under low-pressure dissociated oxygen atmospheres in one furnace, while simultaneously performing atmospheric pressure oxidation or stability experiments in the other. The current setup is shown in Figure 49.

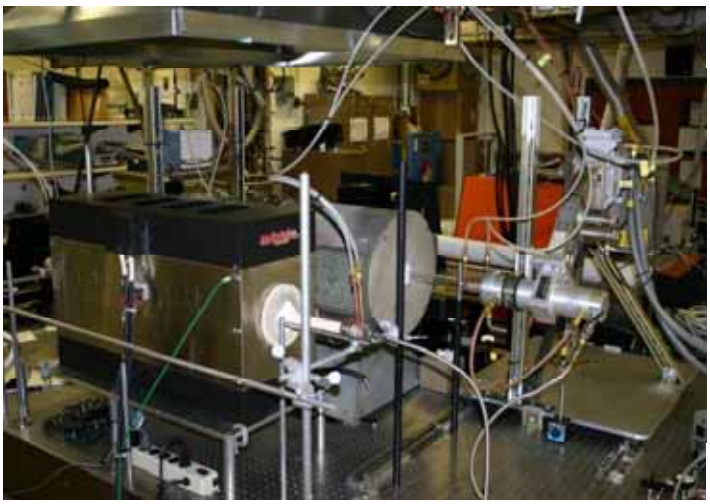

Figure 49: Current furnace oxidation testing setup.

Alumina stages were used for the oxidation test specimens at the beginning of the project. However, the oxidized specimens adhered to the stages very strongly due to the formation of a molten oxide glassy phase. To mitigate this problem, stages from hot-pressed SiC were constructed, upon which coated test samples could be placed with minimum contact, as shown in Figure 50. An improvement in preventing adhesion was obtained, but still not a perfect solution. Oxidized specimens occasionally stuck to the stage and occasionally blow off the stage under the fast flow conditions of the discharge experiments.

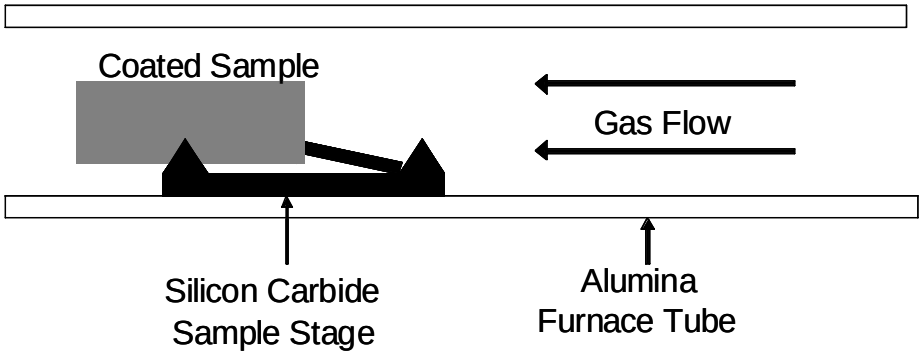

Figure 50: Coated test specimen in tube furnace.

Both the stages and samples were weighed before and after each oxidation test, to assess major transfer of mass from the test specimen to the holder, or in case the specimen could not be completely debonded from the fixture. The weight change of the holder provided also a control factor to assess whether active or passive oxidation has occurred. If both the test specimen and the holder gained or lost weight, it was a clear indication that the oxidation conditions were passive and active, respectively. Under the high-temperature conditions, especially in the low pressure experiments, aluminum was identified at sample surfaces during the post oxidation analysis (by EDS analysis), indicating a slight material evaporation-redeposition activity of the alumina furnace tube itself.

The basic purpose of these oxidation tests was to compare the oxidation resistance of different coating formulations and thicknesses processed by the various approaches used in the study under similar test conditions. Another purpose was to compare the performance of a single coating formulation/process/thickness under different test conditions. The primary comparative evaluation of the oxidized specimens consisted of (1) the change of sample mass, (2) overall microstructure deformations, delaminations, and phase segregation, (3) depth of oxide layer, and (4) difference in oxide composition and morphology as a function of position in the coating and cross-sectional depth. Microstructural characterization was primarily based on SEM observations, variations of elemental compositions were analyzed by EDS, and overall phase changes were analyzed using XRD.

3.4.2 Arc-Jet Testing: Upgrade Attempts

The original plan was to study the performance of the coatings in a laboratory-scale arc-jet apparatus that was built at SRI. The primary experimental protocol consisted of exposing different UHTC coatings to similar plume conditions. A second experimental protocol involved subjecting a coated sample to multiple rapid heating and cooling cycles by inserting and withdrawing the sample repeatedly from the plume. The goal of both types of tests was to assess and compare the stability of different coated materials in the same supersonic, reactive flow stream.

As mentioned previously, the original apparatus assembled at SRI suffered from a significant stream contamination problem. This problem was traced to the degradation of the Hf or W insert serving as the electron source in the cathode within the arc-jet nozzle. Figure 51 shows a cut-away of this pin. This pin is a commercial part manufactured for oxygen cutting torch equipment, in which stream contamination is not a serious issue. Degradation of the pin insert problem is exacerbated by flowing oxygen directly past the cathode when supplying argon-oxygen gas mixtures to the nozzle, as illustrated in Figure 52b.

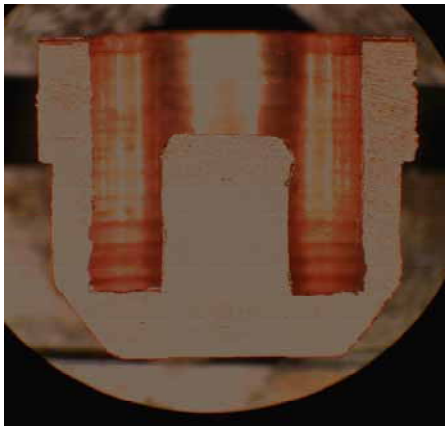

Figure 51: Arc Jet cathode.

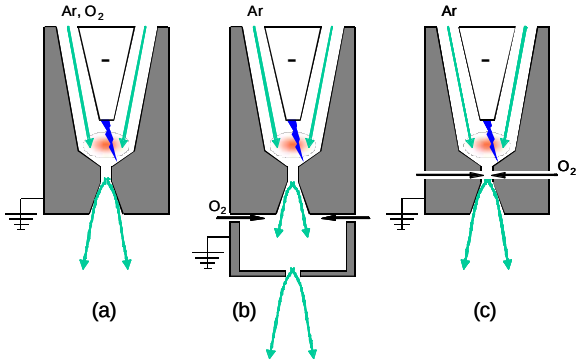

Figure 52: Different O_2 injection schemes.

Several approaches were taken at the beginning of the project to clean up the arc-jet stream by modifying the nozzle assembly via the addition of the oxygen downstream of the cathode. One attempt was based on attaching a small mixing chamber to the end of the nozzle, as illustrated in Figure 52b. The actual modified nozzle is shown in Figure 53.

Unfortunately, this modification failed to produce an energetic plume. It seems probable that the added thermal mass of the mixing chamber together with the turbulence-enhanced convective heat transfer between the gas stream and the walls cooled the gas substantially. Based on their color, samples exposed to this plume did not reach temperatures above ~ 600°C, which is not of much use for this study. This limitation was not overcome within our attainable operating parameter space (gas compositions, pressures, flow rates).

Figure 53: Mixing chamber injection.

Figure 54: Nozzle throat injection.

Another attempt was based on direct injection of the oxygen within the nozzle throat. This scheme is illustrated in Figure 52c and the actual hardware is shown in Figure 54. The idea behind this design was to avoid adding thermal mass and cooling the gas stream. Tests with this configuration returned basically the same argon plume as in the unmodified nozzle. However,

no difference in the energetics of the gas stream could be detected, as evidenced by color changes in the plume or the temperature responses of test specimens, when oxygen was injected. For this design, the problem appears to be a total lack of mixing between the injected O_2 and the main argon stream; i.e., the oxygen is apparently swept along the surface of the nozzle throat, never penetrating into the core.

A final modification of the direct injection nozzle was made, in which a small lip was added near the exit of the throat to generate local turbulence, in the anticipation that it would encourage mixing, without the opportunity for enhanced convective cooling before the stream exits the nozzle. However this modification also proved unsuccessful.

At the end, a decision was made to run the arc-jet in the original mode, where surface contamination is unavoidable but the stream is at least capable of generating high heating levels in a low-pressure, high-shear flow environment. Within the limitations imposed by stream cleanliness, these tests were intended to check coating adhesion and stability under convective heating and surface shear flow in a reactive gas environment. Unfortunately, during these experiments the arc-jet suffered a catastrophic electrical short and data were obtained for only a single coated specimen. Given the time and expense already invested in the arc-jet modification effort, a decision was made to discontinue this testing approach in favor of oxidation studies in the tube furnace – discharge system.

3.4.3 Initial Oxidation Studies

The oxidation study began by evaluating the threshold oxidation of ZrB_2/SiC coatings in parallel to the uncoated SiC test specimens. The initial tests were performed under atmospheric pressure with a blend of 21% O_2 in Ar. The temperatures of the tests were 1250, 1400, and only then the research effort focused on 1500°C oxidation. Low-pressure tests were performed serially under molecular or partially dissociated oxygen using the furnace – microwave discharge apparatus. This testing was performed at a relative low pressure of ~2 torr (0.0027 atm) with an input gas mixture of 87%O_2-13%Ar under rapid flow conditions (10's m per second).

Under most of the test conditions throughout the evaluation, oxidation under atmospheric pressure conditions can be characterized as passive with weight gain associated with the oxidation. At very low pressures, both oxygen and discharged oxygen (O/O_2 mixture) demonstrated active oxidation. However, it was difficult to separate the effects of low oxygen pressures and discharge activation on observed mass changes since a combination of mass loss by evaporation of BO_x species occurs simultaneously with the weight gain due to the formation of ZrO_2. Additionally, there is some ambiguity in partitioning total mass loss between coating, substrate, and stage (when samples stick).

From the literature, SiC passive-active oxidation transitions are experimentally found within the 1-10 Torr O_2 and 1200-1600°C pressure-temperature space. The transition boundaries for the coating formulations may differ from those for the substrate. To sort this out, a test series was performed at a later stage of the study, in which the oxygen partial pressure was systematically varied at fixed temperature and compared with the resulting mass change and surface microstructure between uncoated and coated specimens. The mass change results of this study are summarized in Figure 55.

Because oxidation rates may vary on "upward" or "downward" facing surfaces, and on coated or uncoated parts of the test sample, we report total mass changes after oxidation. Since

coated samples and test conditions are nominally identical, the total mass change is the most representative measure for comparison. For mass change per area averaged over the entire test sample, the values in Fig. 55 can be divided by ~8.3 cm^2.

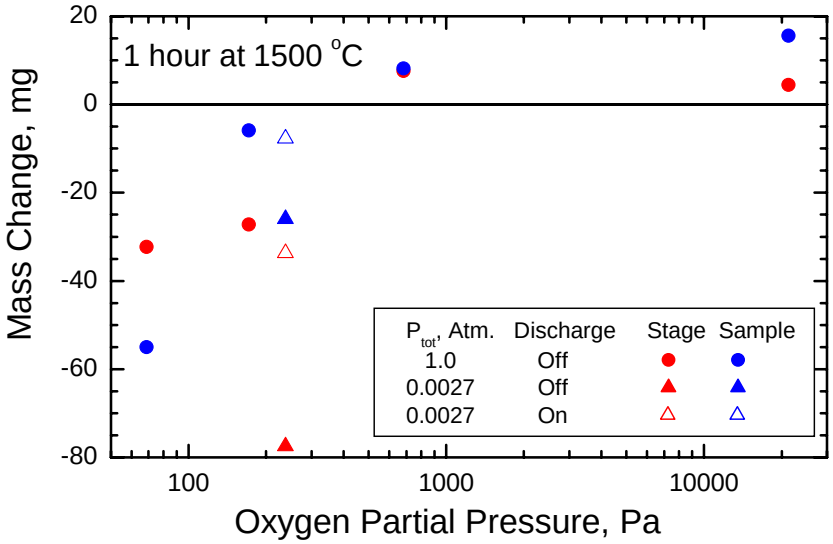

Figure 55: Mass changes for SiC samples coated with a ZrB_2/SiC (30 μm thick; prepared by Approach 2, blue symbols) and SiC stages (red symbols), as a function of oxygen partial pressure.

Figure 56 shows that at 1500°C and 1 atmosphere total pressure (solid circles), the transition between active and passive oxidation (as determined by net mass loss or gain) lies somewhere in the 1 to 5 Torr (~150 to 700 Pa) range, for both the stages and coated samples. This oxygen partial pressure range is consistent with previous experiments with SiC at this temperature, as shown in Figure 1, previously.

The solid triangular symbols show mass loss under low *total* pressure conditions in the presence of molecular oxygen. In this regime the gas flows are considerably faster (factor of 10 or so) than in the atmospheric pressure tests, continuously sweeping away the evolved volatile oxides. Under such fast flow conditions, boundary layers above samples are thinner lowering gas diffusion limitations and preventing the build up volatile oxides to equilibrium concentrations near the surface. Thus, the transition pressure is expected to fall to lower values at a fixed temperature, or to occur at lower temperatures for a fixed oxygen partial pressure. This is indeed what is observed for both the coated sample and stage.

When the discharge is activated under the same low pressure – high flow conditions (open triangles), mass loss is still observed for both the sample and stage. However, the magnitude of these mass losses are significantly reduced. While only limited and indirect data were generated, the results are consistent with the findings of Balat [35] suggesting that atomic oxygen favors SiO_2 formation on SiC under temperature and pressure conditions where oxidation by O_2 favors SiO formation. Note that the flow above the sample is only *partially* dissociated, so that both O and O_2 are present when the discharge is activated, and competing surface oxidation reactions are probable.

3.4.4 Oxidation of System 1: ZrB_2/ SMP-10

Coated specimens with about 30 μm thick coatings derived from the formulation of ZrB_2/SMP-10 slurry were oxidized under atmospheric pressure using a 20% O_2 in argon. At 1250°C there is a very small weight gain of about 0.6% including potential weight gain from the area of the uncoated SiC specimen. As shown in Figure 56, a thin glassy phase is formed at the surface of the coating embedded with some micron sized crystalline phases.

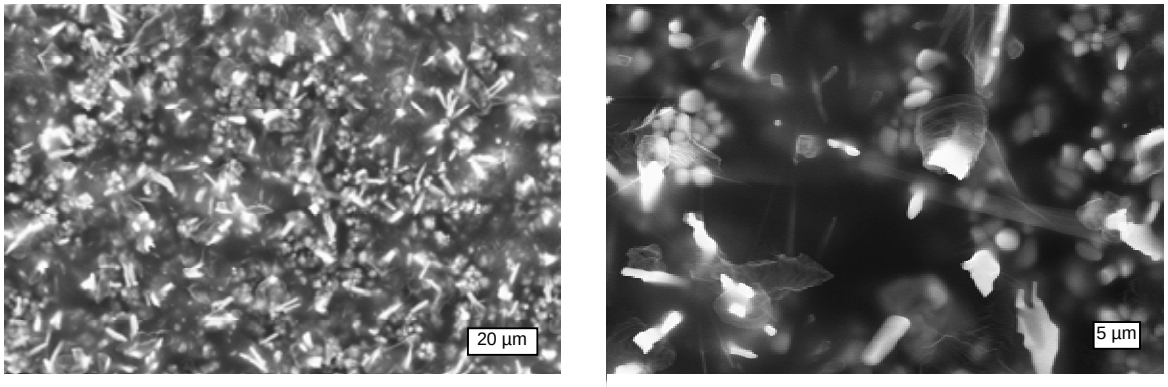

(a) (b)

Figure 56: Surface oxidation and passivation of a coating derived from ZrB_2/SMP10 and oxidized in 20% O_2 in Ar (1 atm) at 1250°C.

At 1400°C the weight change is still insignificant but major microstructural changes occur. The coating turns to be creamy in color but still bonds sufficiently to the substrate. The SEM analysis reveals the formation of dendritic spikes as well as lamellar structures growing out of a glassy surface (see Figure 57). These spikes are attributed to monoclinic ZrO_2 as detected by XRD. The presence of small SiC and ZrB_2 phases in this coating is still detected by XRD, suggesting that the coating oxidation is not completed. The minimal weight gain is attributed to a combination of oxygen pick up and on the other hand volatilization of BO and maybe even SiO species. It is possible that the formation of a molten glassy phase plays a role as a flux in the formation of this microstructure. Gas-liquid-solid reactivity may be another explanation.

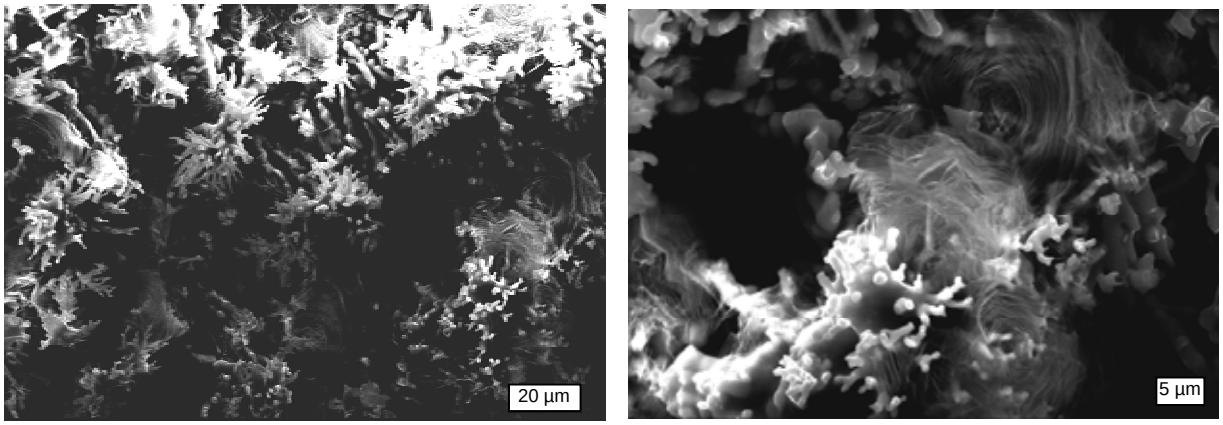

(a) (b)

Figure 57: Surface oxidation and passivation of a coating derived from ZrB_2/SMP10 and oxidized in 20% O_2 in Ar (1 atm) at 1400°C.

Coatings made of formulations based on System 1 are porous and therefore expected to be easily oxidized. During their oxidation at 1400°C under atmospheric pressure (20% oxygen in argon) the coatings are sealed as shown in Figure 58. Clearly, the polymer-derived ceramic phase (the amorphous gray area) is oxidized and expands, although the overall weight change of the oxidized sample is very low. Analysis of the cross section reveals that indeed the oxidized coatings become dense. However, there are two other intriguing observations. One is the oriented growth of ZrO_2 dendrites out of the coating plane (z directions). It is assumed that the Zr-containing phase close to the substrate is still ZrB_2 because this phase is still present in the XRD of the sample (Figure 59). The other significant observation is the delamination of the coatings, which can be associated with a combination of coating expansion and the low viscosity oxide glass, which is formed during the oxidation (Figure 60).

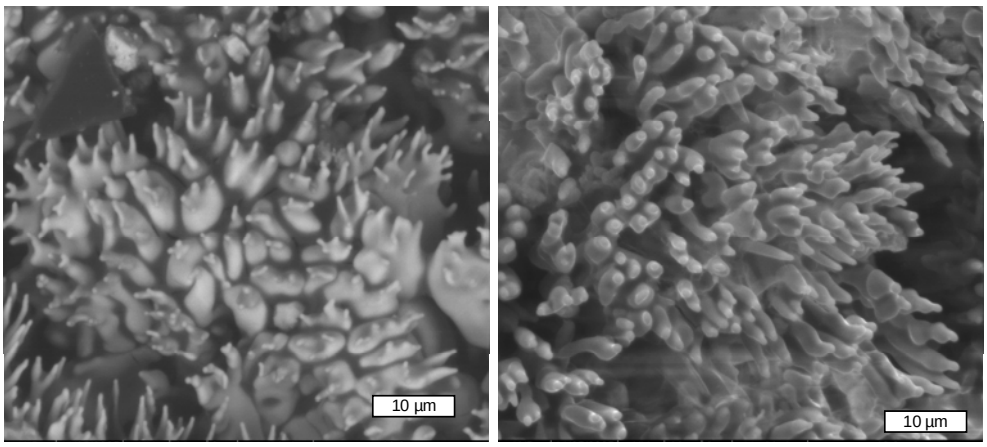

(a) (b)

Figure 58: Dendritic surface obtained during atmospheric oxidation of ZrB_2/SMP-10 coating at 1500°C.

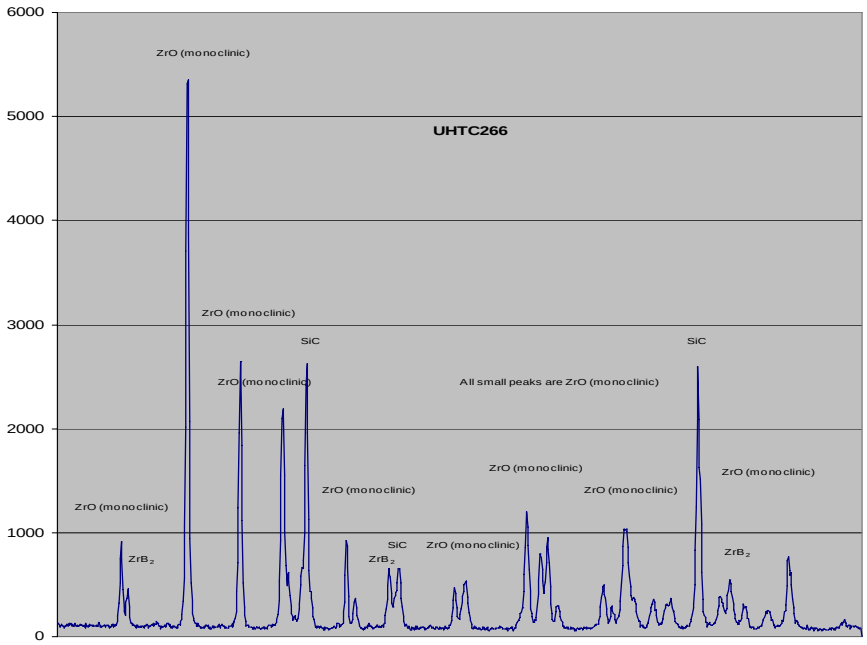

Figure 59: ZrB_2 and SiC phases still exists at or close to the surface after significant oxidation of a ZrB_2/SMP-10 coating over SiC specimen.

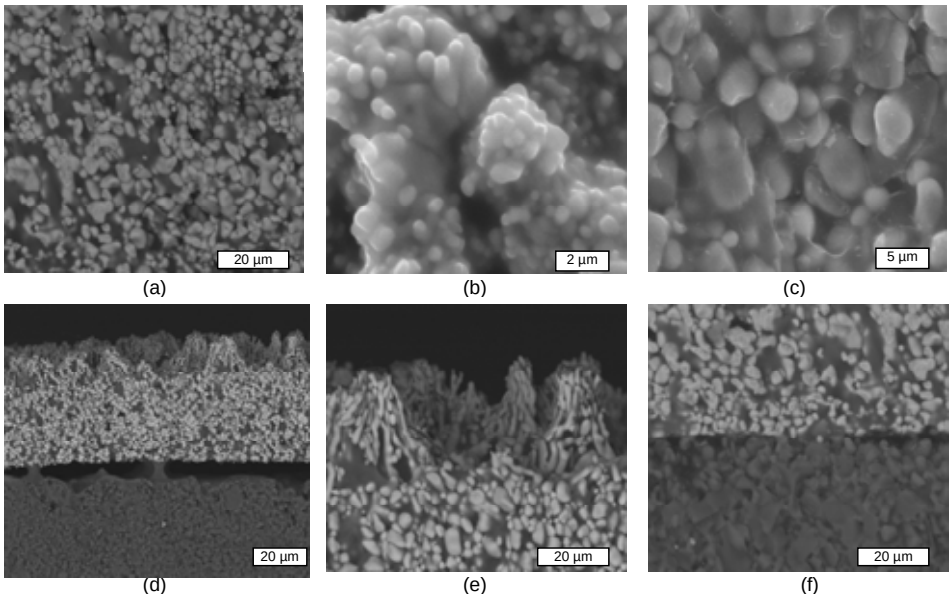

Figure 60: Oxidized ZrB_2/SMP-10 coating over SiC specimen. The delamination at the interface may be the result of excessive oxidation of the substrate itself versus the coating oxidation.

Bulk material made of the same formulation as the above coating was also tested. The bulk specimens were prepared by casting fluidic solventless slurries in a mold, curing them in inert atmosphere (with unavoidable large bubbles) followed by pyrolysis at 1000°C. In this case,

a white oxide scale is formed only at the surface of the specimens even when oxidized at 1500°C at atmospheric pressure for 1h (20% O_2 in Ar). A tested specimen gained significant weight, indicating passive oxidation. The formation of a 30 to 50 micron thick oxide layer is observed. A dark material is found under this layer as shown in Figure 61.

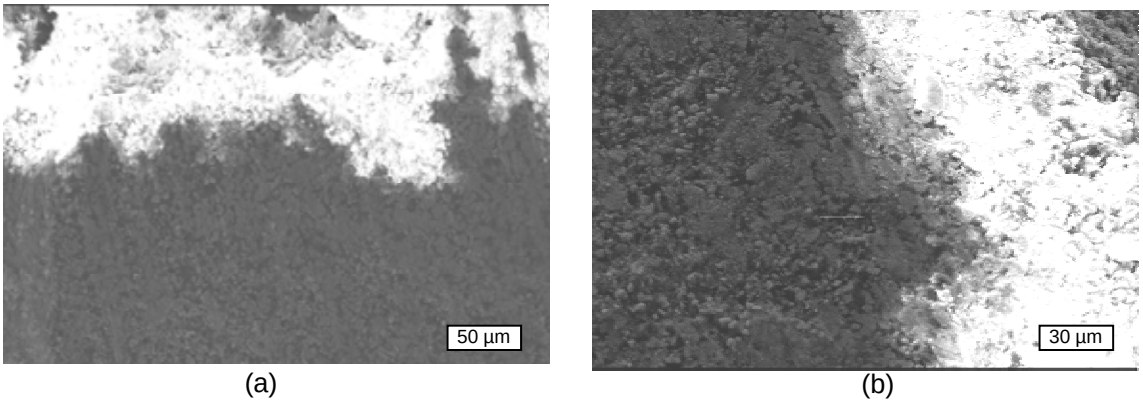

(a) (b)

Figure 61: Bulk specimen made of ZrB_2/SMP-10 develops a 30 to 50 µm of oxidation layer at 1500°C but no significant oxidation underneath. The oxidation layer seems to seal the bulk material underneath.

The top surface is also dendritic similar to the features observed at the surface of the oxidized coating discussed above (Figure 62). However, the cross section of the material reveals densification of both the oxide layer and the bulk. It is highly possible that the sub-oxidation layer material was densified and maintained high integrity due to partial oxidation of the matrix material forming a passivating SiOC material with expanded volume. This expansion may be responsible for the sealing effect. Also, the microstructural rearrangement of the external oxide layer can form a sealing that prevent oxygen diffusion.

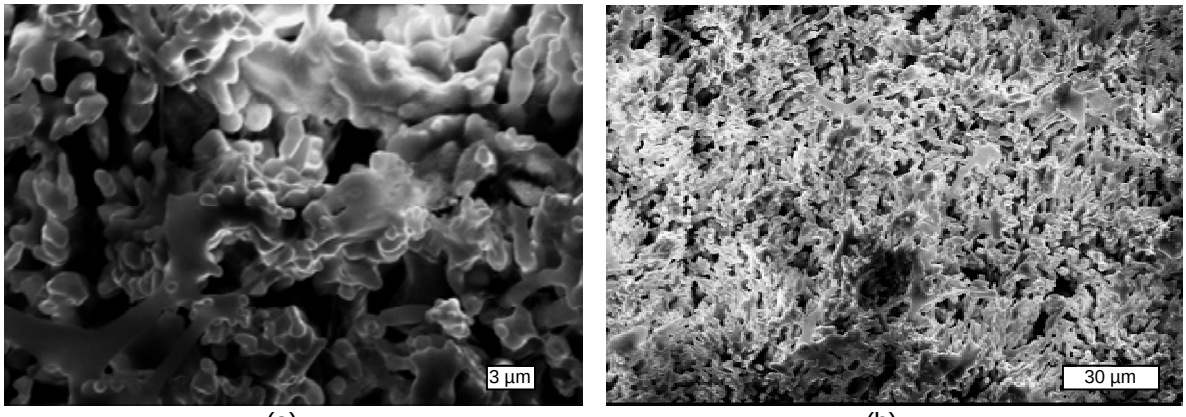

(a) (b)

Figure 62: Dendritic surface formed at the scale of a bulk ZrB_2/SMP-10 material at 1500°C and 1 atm of 20% oxygen in Ar.

Figure 63 exhibits further analysis of a similar bulk material cube (5 x 5 x 5 mm) oxidized at 1500°C for 1 h at atmospheric conditions of 20% O_2 in Ar. In spite of the original porosity of the sample the material is sealed during the early stages of oxidation. The oxidation is passive in its nature with an overall weight gain of 12%.

At the surface of the cube specimen there are 2 major areas of microstructures. One is a crystalline phase containing primarily Zr and O (Figure 63, Area 1). The ZrO_2 crystallites are topped with coral-like dendrite formation suggesting a growth from the subsurface to the surface area assisted by a liquid phase. That liquid phase may be the same as shown in Area 2, which has flown to topological "valleys" formed during the evolution of the dendritic structure. Another reason for the phase separation is low wettability of the evolved ZrO_2 microstructure by the glassy phase.

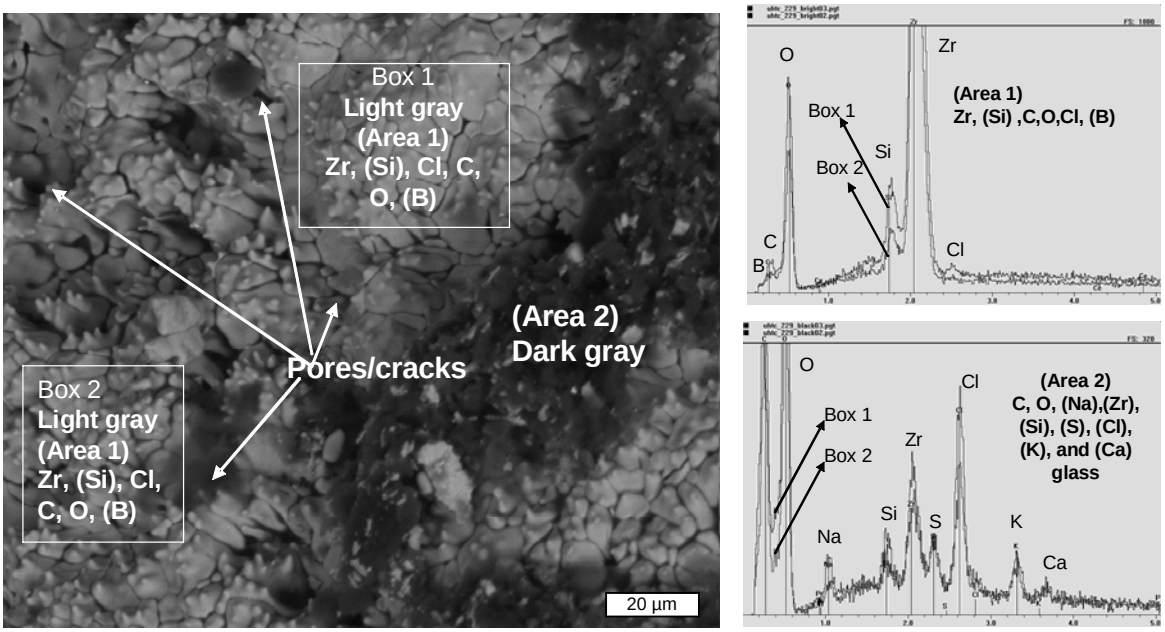

Figure 63: Further analysis of an oxidized bulk specimen at 1500°C and atmospheric conditions. The enhancement of the dendritic morphology of the surface may be related to contamination of Na, K and Ca salts in the porosity of the material during the cutting of specimens for oxidation testing.

The glassy phase contains also Na, K, Cl, and S. These contaminants were incorporated during the cutting of the bulk molded material to test specimens, when cooling water has penetrated and trapped in the original porous structure. This contamination may assist the dendritic growth at the surface. In future studies of such porous materials it is recommended to ultrasonicate the samples in deionized water several times followed by alcohol prior to oxidation in order to exclude such contamination.

Another intriguing observation is the presence of significant levels of carbon in the glassy phase. In addition, ZrB_2 is still a significant phase in the overall structure and its XRD spectrum is stronger than the evolved ZrO_2. The large presence of the oxygen peak according to the EDS analysis suggests the presence of significant amount of boron in Area 2. There is no good

explanation for the very large presence of carbon, unless it is associated with a secondary formation of carbonates of the alkali and alkali earth contaminants.

The analysis of the oxidation of the ZrB_2/SMP-10 formulations led to the conclusions that the coatings made of these formulations will not be very useful to protect SiC-based substrates in their current processing approach. Yet, these formulations, which generate low viscosity slurries, even in the absence of solvent, are very good candidates for developing slurry-based UHTC matrix materials for fiber reinforced composites. Further investigation in that direction was not conducted, since it was not the focus application in this study.

3.4.5 Oxidation of System 2: ZrB_2/SiC via Preform-RBSC

3.4.5.1 Oxidation under Atmospheric Pressure

Coatings formed by Approach 2 were initially evaluated at 1250°C in 20% O_2/Ar at atmospheric pressure. The weight gain under these conditions is negligible. The coating stays bonded to the surface and maintains its black color but becomes slightly shiny. The uncoated SiC area is also shiny. SEM of the coatings reveals the formation of a glassy phase between the ZrB_2 crystallites (see Figure 64). The glassy phase probably provides improved sealing of the surface. No delamination or major defects are detected. In some areas, a minor level of whiskers starts to grow from the surface.

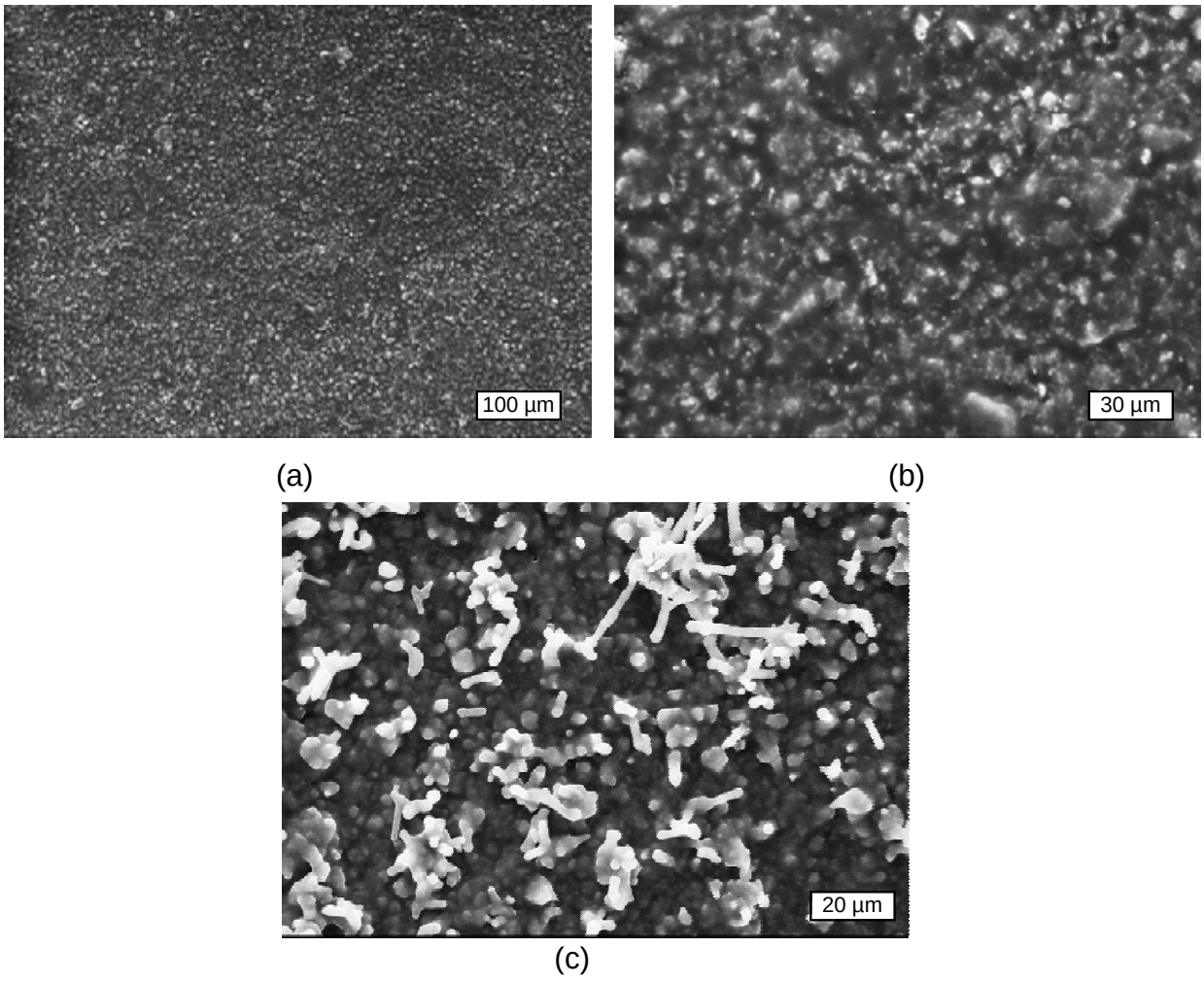

Figure 64: Oxidized coating made by the preform-RBSC approach at 1250°C under atmospheric pressure (20% O_2 in Ar).

At 1400°C the coatings are still relatively stable under the same conditions. The coating's microstructure reveals that a thin glassy layer is formed, which is not covering the entire area. Some submicron crystallites are detected under the glassy phase. Some of the crystallites are exposed after some of the glassy layer is delaminated, most likely due to CTE mismatch during cooling. The XRD pattern reveals the presence of a significant level of ZrB_2 phase and medium presence of SiC phase. Monoclinic ZrO_2 (Baddeleyite) is the only detected oxide phase with peaks significantly smaller than the two other phases. Figure 65 represents features shown in this oxidized sample.

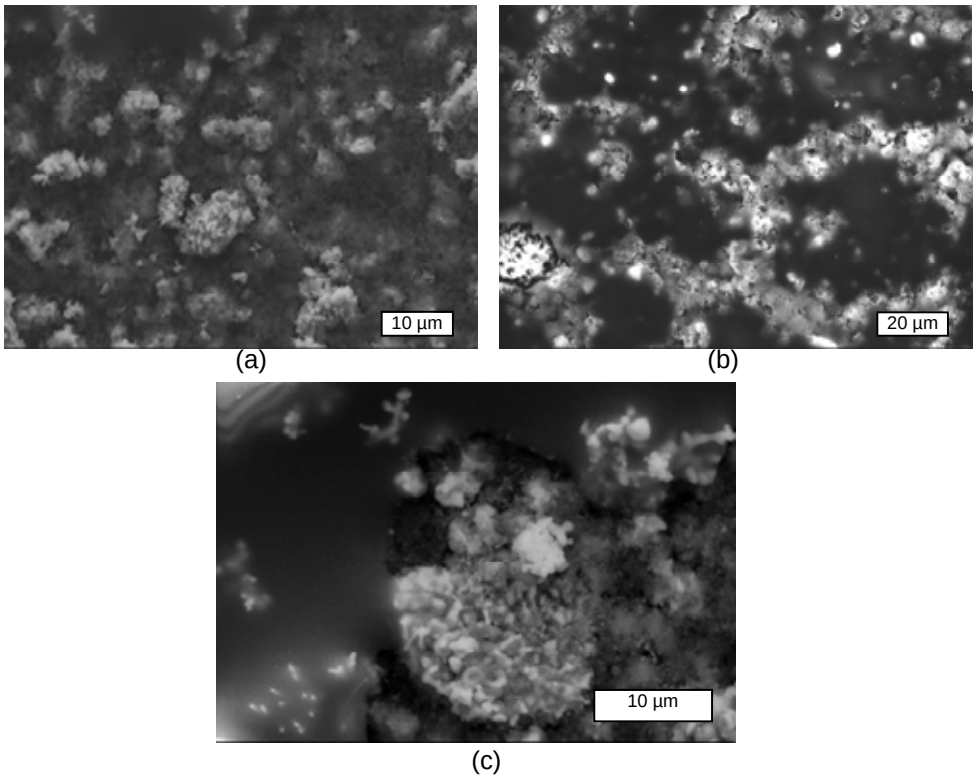

Figure 65: Oxidized coating made by the preform-RBSC approach at 1400°C under atmospheric pressure (20% O_2 in Ar).

Figure 66 represents a similar coating oxidized at 1500°C by atmospheric 20% O_2 in Ar. The microstructure shows areas, where no glassy layer is observed (Figure 66a and 66b) as well as areas close to the uncoated SiC substrate where a thick glassy layer has been formed (Figure 66c and 66d). The glassy layer does not wet the SiC substrate well. It is possible that the glassy layer was formed by the uncoated SiC and flowed down to the coated area.

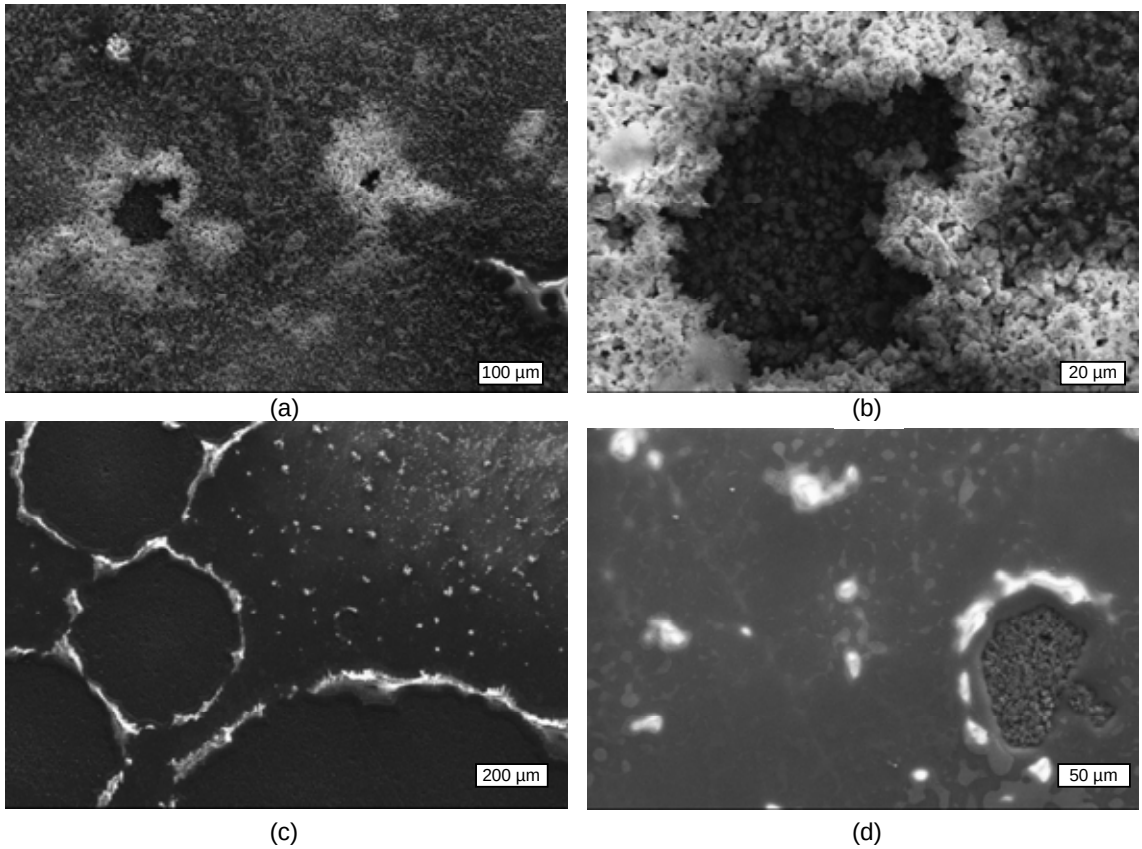

Figure 66: Oxidized 30 µm coating made by the preform-RBSC approach at 1500°C under atmospheric pressure (20% O_2 in Ar).

3.4.5.2 Oxidation under Low Pressure

Oxidation performed at low pressure leads to a much more active oxidation associated with an overall weight loss of the coated specimens as well as the base SiC material. The conditions at which such active oxidation occurs consisted of either O_2 or O_2/O partial pressure of 2.06 torr (275 Pa) in the presence of 0.74 torr (100 Pa) of Ar at 1500°C. In fact, a mixed active and passive oxidation behavior is still detected under these conditions and the microstructure includes areas resembling the two modes of oxidation.

Figure 67 shows that under these conditions in the presence of molecular oxygen (O_2) the coating is swollen during the oxidation forming bubbles, 10 µm in diameter. Holes in the coating are also noted. The evolved microstructure is very inhomogeneous and includes crystalline ZrO_2 areas with glassy phase regions in between. The crystallites are partially oriented in the z direction suggesting a progressive growth of the ZrO_2 from the "bulk" of the coating. The adhesion of the coating to the substrate is maintained. The XRD phases of this oxidized specimen show primarily monoclinic ZrO_2 with a small SiC phase, probably present in the substrate itself (Figure 68). All the original ZrB_2 phase was eliminated. An additional peak

was assigned to quartz. In addition, a thin glassy layer was formed on top of the coating. The viscosity of this layer must be low at 1500°C, evidenced in the formation of large bubbles with thin walls, which burst during the heating or cooling stages of the oxidized specimen as indicated in Figure 69.

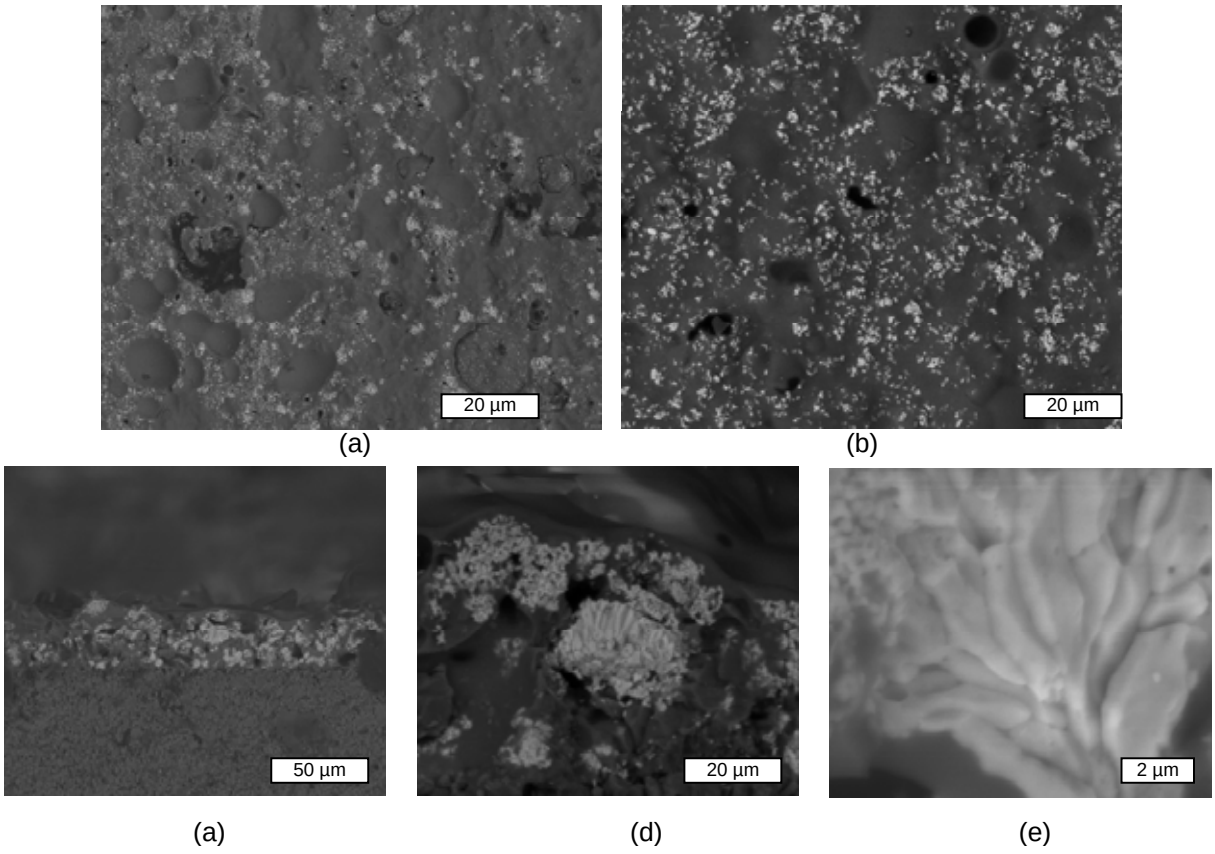

Figure 67: Oxidized 30 µm coating made by the preform-RBSC approach at 1500°C in O_2/Ar under low-pressure conditions. (a) and (b) represent the surface microstructure; (c)-(e) represent a cross section area.

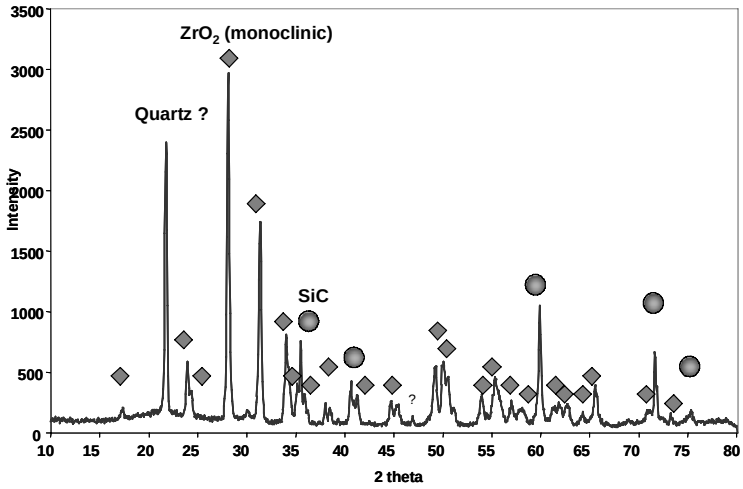

Figure 68: XRD of oxidized preform-RBSC coating under low-pressure conditions.

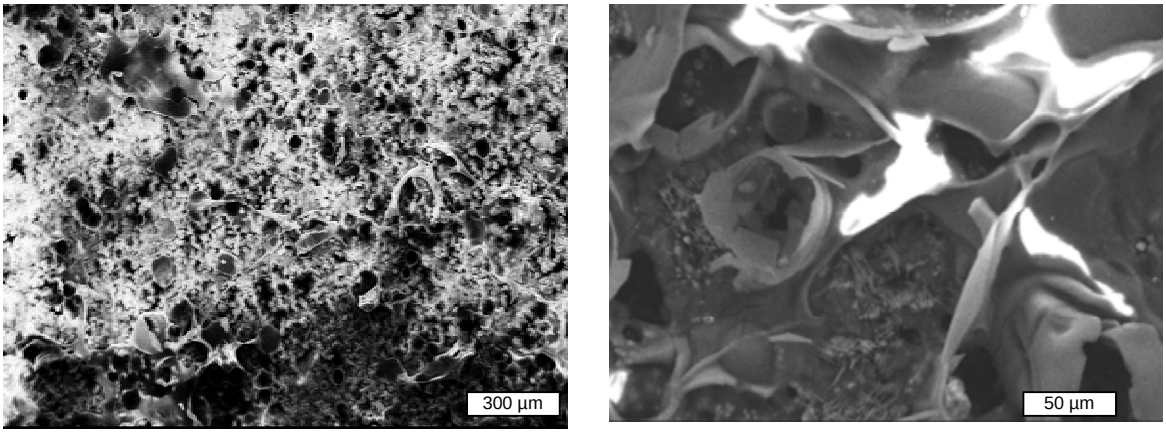

(a) (b)

Figure 69: Thin-wall bubbles formed at the surface of an oxidized coating under low-pressure conditions.

Oxidation of a similar coating in the presence of atomic oxygen (O/O_2 mixture generated by microwave discharge) under the same pressure and temperature conditions of the specimen described above shows a more massive oxidation, in spite of the minimal change in the overall weight of the specimen. Figure 70 shows thick bubble formation, 100 µm in diameter. The entire coating bloats and rises above the surface. Notice that a layer of composite coating is still bonded to the substrate surface underneath the bubbles. Also, the oxidation penetrates the substrate itself causing large bubble-like pores in the SiC material. An inner glassy phase possessing primarily Si and O is evolved. The XRD pattern of the oxidized coating is very similar to the one observed in Figure 68.

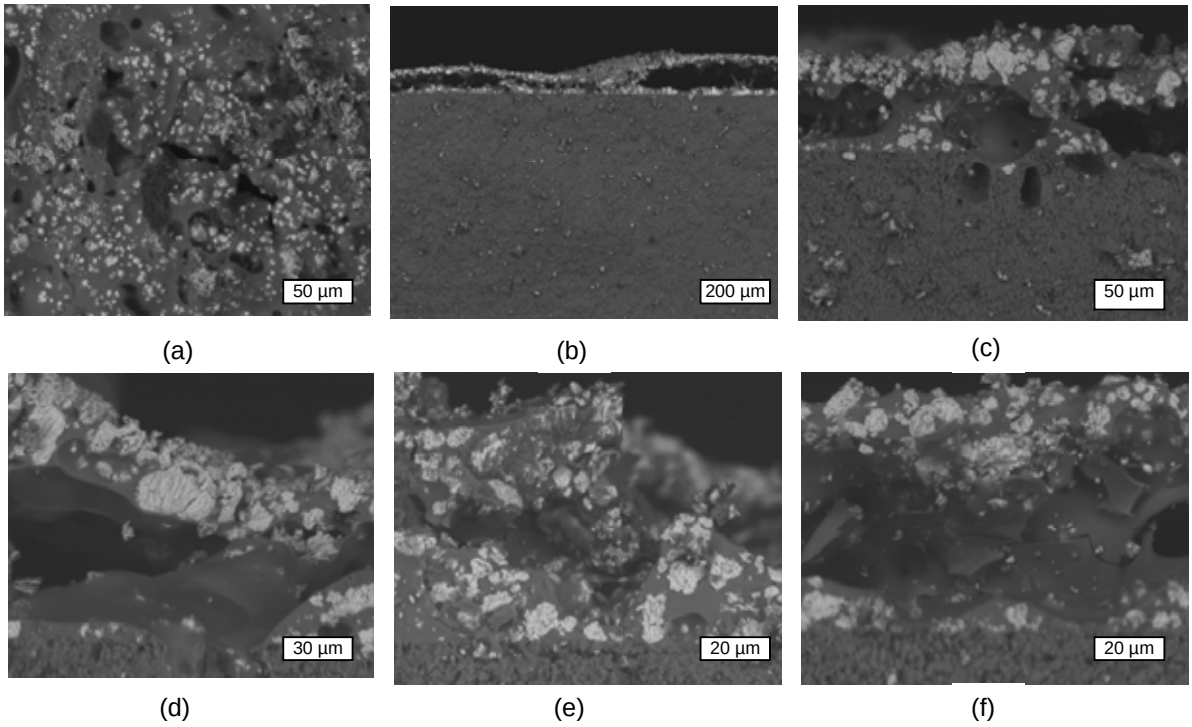

Figure 70: Oxidized 30 µm coating made by the preform-RBSC approach at 1500°C in $O/O_2/Ar$ under low-pressure conditions.

The oxidation studies led to a tentative conclusion that the boron level in the composite is too high causing two simultaneous effects: (1) evaporation boron suboxide species from the external area of the surface and (2) reaction the evoled boron oxide with the oxidized SiC at the coating-substrate interface forming a low viscosity glass at the operating temperature. The enhanced active oxidation under the coating leads to the formation of a glassy interface, which is liquid at 1500°C causing bubbles in the substrate itself and localized delamination of the coating. Consequently, a small effort was performed in parallel to the main development of ZrB_2/SiC coatings at the end of the project to develop UHTC compositions that contain less boron. This effort has been described earlier.

Another more obvious conclusion was the need to form thicker than 30 µm coatings. Oxidation studies of UHTCs in recent years show that an oxidation scale of 100 to 150 µm is developed at the outer surface of the bulk materials, with segregation of elements as a function of depth. Various distinct oxidized layers with different compositions were observed in these studies [70,73,74]. This layer formation during the oxidation suggests major reactivities at the first outer 100 to 200 µm of the bulk UHTC, eventually leading to a protective configuration in an equilibrium stage. Similar reactivity is anticipated to occur in UHTC coatings. An effort to produce 100 µm thick coatings was been therefore performed.

3.4.5.3 Oxidation of Thick Coatings

A set of coatings that are 100 to 120 µm thick were tested for their oxidation behavior at 1500°C. These coatings perform much better than the 30 µm thick coatings. Figure 71 illustrates the difference between the surface of such thick coatings before (Figures 71a and 71b) and after oxidation (Figures 71c and 71d) in atmospheric 20% O_2/in Ar. Figure 72 compares the cross section of these coatings before and after oxidation. A glassy phase consisting of silica is developed at the top 5 to 10 microns. In this case, the silica layer flows and seals the coating. The coating underneath the glassy layer maintains high integrity. The uncoated area is oxidized much more severely with the formation of a silica layer that breaks and flakes off the surface after the specimen is cooled down, as shown in Figure 73.

Experiments with thick coatings under more reducing conditions were performed at 1500°C in atmospheric pressure but very low partial pressure of oxygen. The coating develops again a SiO_2 layer, which is slightly thicker than observed under higher oxygen levels. Although the top silica layer seals the surface, defects in the form of deep holes are observed (Figure 74a). These holes are associated with large holes created at the interface between the coating and the substrate. These oxidized holes are partially present in the SiC substrate material itself as shown in Figure 74b. Therefore, the silica top layer may be partially formed in this case by gaseous or liquid oxidized silicon that migrates from the substrate to the top layer. The round shape of these underlayer holes suggests the existence of local oxidation associated with a molten phase. Such local oxidation may occur locally, if a deep crack or a defect exists in the coating prior to the oxidation.

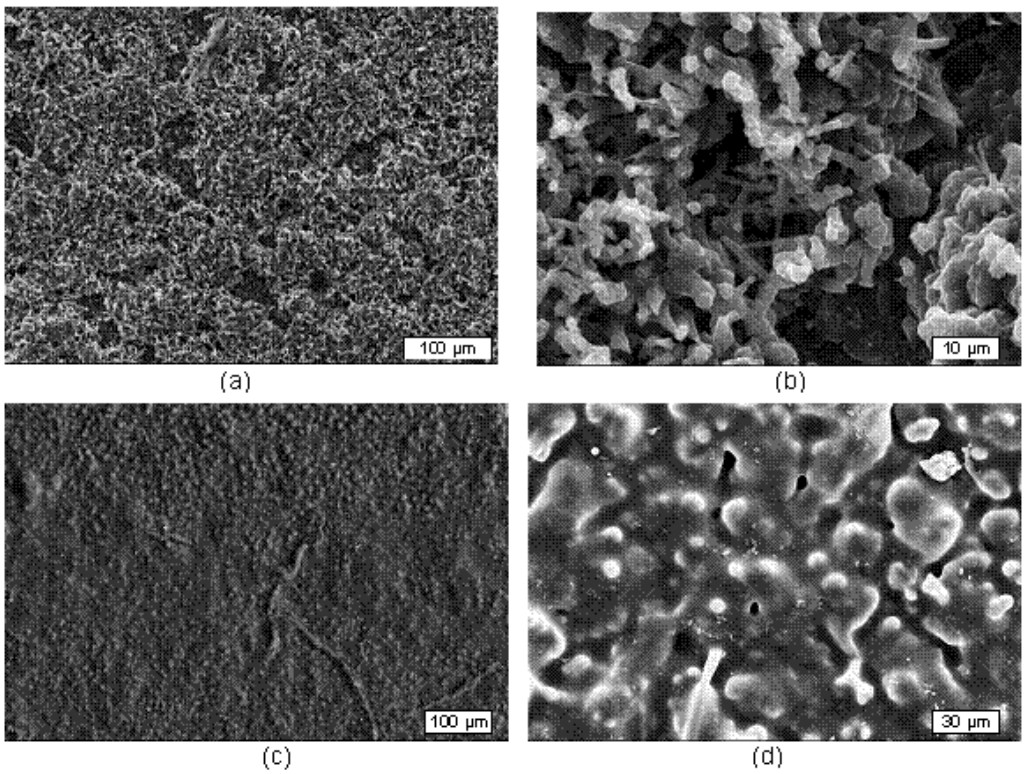

Figure 71: Comparison between the surface of 100 µm coatings before [(a) and (b)] and after [(c) and (d)] oxidation at 1500°C under atmospheric pressure (20% O_2 in Ar).

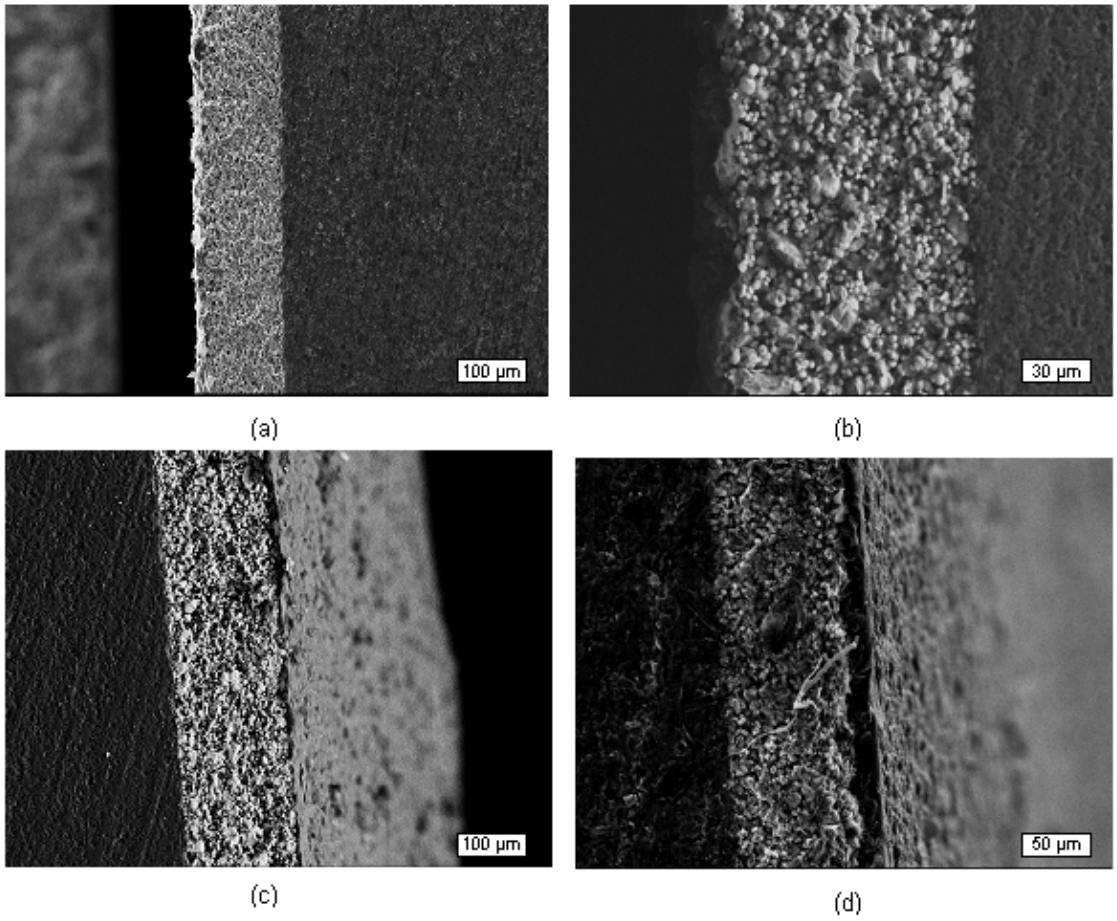

Figure 72: Comparison between the cross sections of 100 µm coatings before [(a) and (b)] and after [(c) and (d)] oxidized at 1500°C under atmospheric pressure (20% O_2 in Ar).

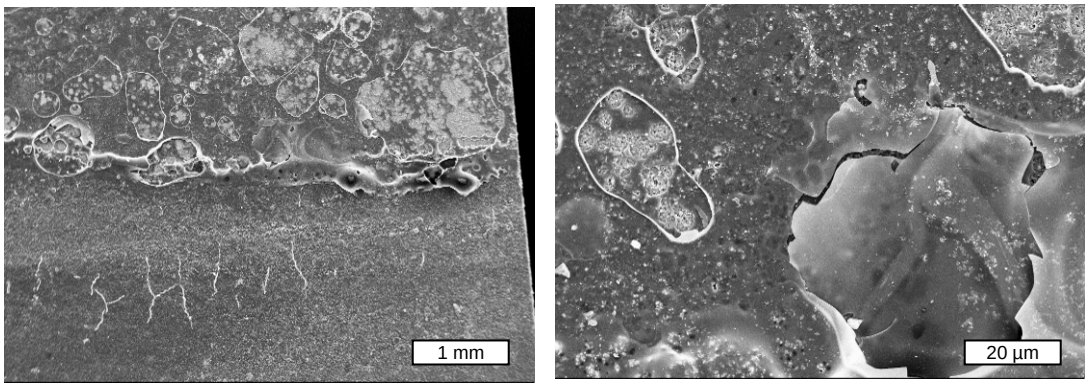

Figure 73: The uncoated area of specimen with thick preform-RBSC coating reveals a significant oxidation and deformation of the bare SiC substrate.

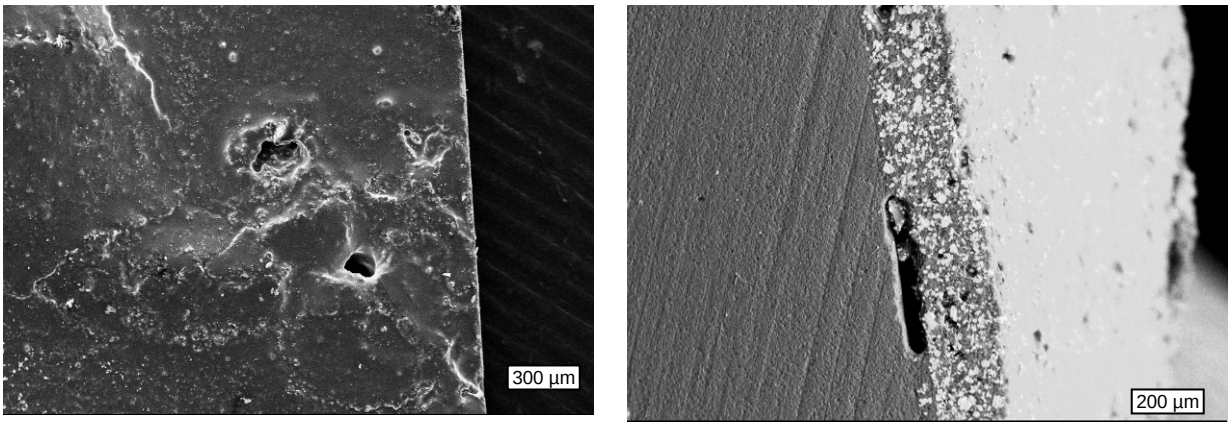

(a) (b)

Figure 74. Thick ZrB_2/SiC coatings oxidized at 1500°C in atmospheric conditions but in very lean level of oxygen (0.068% in Ar).

3.4.5.4 Arc Jet Oxidation Study

Several attempts to coat short 0.25-inch diameter UHTC and SiC pins for testing in the laboratory-scale arc-jet facility have been done. The initial experiments to coat hot-pressed ZrB_2-20v/oSiC and commercial RBSC pins were unsuccessful. In both cases the coatings separated from the pins after heat treatments during coating processing. In the first case, the reason for the delamination is believed to be a reaction between the ZrB_2 and Si at the coating-substrate interface during the siliconization step. At the interface there is no excess of carbon and the two components can react with each other to form a thin zirconium silicide interface layer that is unfavorable to adhesion. In the second case, a post-coating examination revealed depleted, porous surface layer in the SiC material. Apparently, the commercial reaction-bonded SiC contained residual Si or a silica glassy phase that was reactively consumed by the carbon in the coating system during processing. This finding re-emphasized an important point – the optimal application process and resulting performance of particular coating systems will depend on the details of the composition and processing of nominally identical substrate materials.

Subsequently, SiC pins were custom machined from the same hot-pressed SiC material used for the coated furnace test specimens. The UHTC coatings adhered to these SiC pins much better as shown in Figure 75. The problematic area of this coating is actually at the top flat surface and the circumference around the top, which were partially wiped during the dip coating as shown in Figure 75b. A better technique should be used in future studies of pins to produce a coating in this area with higher integrity and uniformity. Several hot-pressed ZrB_2-30 v/o-14v/oSiC pins were also coated by a similar technique showing adequate adhesion to the pins.

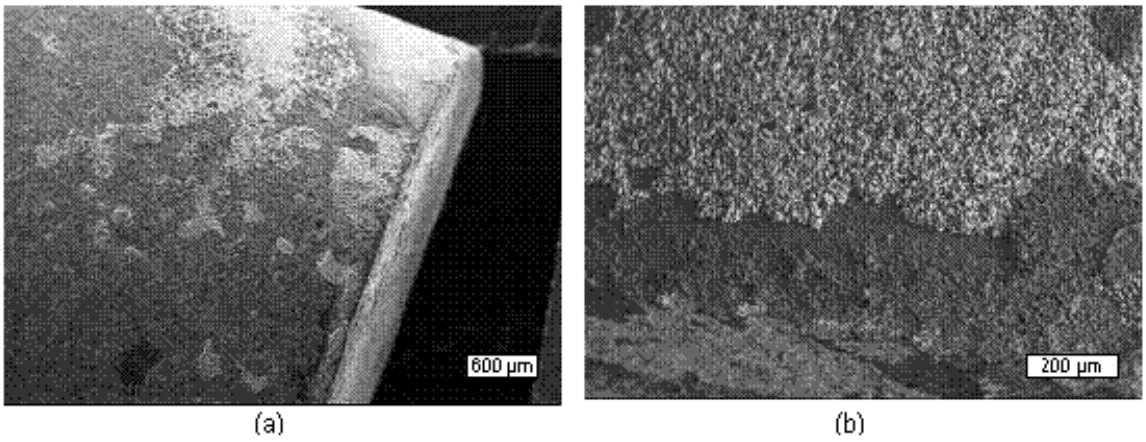

Figure 75. SiC pin dip coated with ZrB_2/SiC 30 µm layer. The coating adheres well to the sides of the pin but not very well around the top due to the dip/wipe technique that was used to deposit the preform layer.

Attempts were made to test coatings on top of these two types of pins in the arc-jet facility, under the following conditions: arc power of ~1 kW, gas flow rates of 15 slm Ar and 0.2 slm O_2, a total chamber background pressure of ~85 Pa with a sample-nozzle separation of about 4 cm. Estimated stagnation pressures were ~300 Pa. Under these conditions surface temperatures on an uncoated SiC pin were measured by two separate optical pyrometers as ~1200°C. Similar surface temperatures were measured on the coated SiC pin run for 5 minutes. A longer 10 minute exposure of a coated SiC pin reached apparent surface temperatures approaching 1450°C, but these temperature measurements are suspect because of significant metal contamination accumulating on the sample surface. After the second pin testing the apparatus had a catastrophic short circuit. Repairing the apparatus was estimated to be labor intensive with no guarantee that better operation would be achieved. No further tests were performed.

The ZrB_2/SiC coatings survived quite successfully the arc jet tests. The 5 min exposure (~1200°C) does not show a major change in the coating appearance and bonding to the substrate as shown in Figure 76. A slight depletion of material may have occurred (i.e., evaporation of sub-oxide species). The backscattered SEM analysis of the cross section of this specimen clearly shows the Zr-containing layer as a strongly bonded coating that was hardly eroded by the jet flow (Figure 76c).

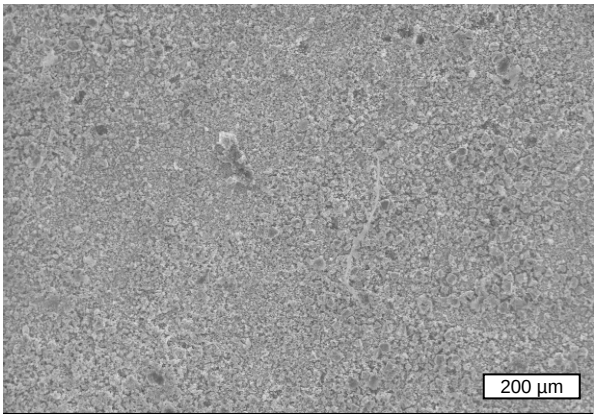

(a)

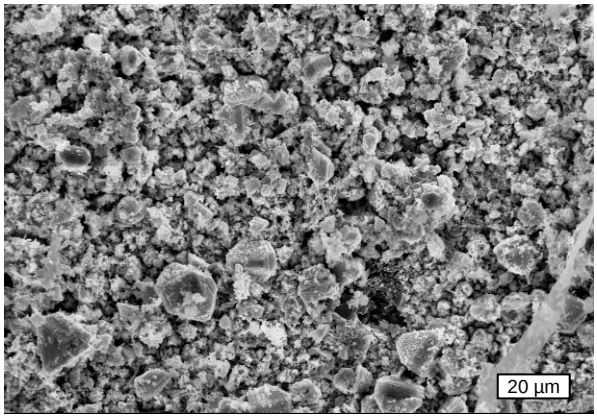

(b)

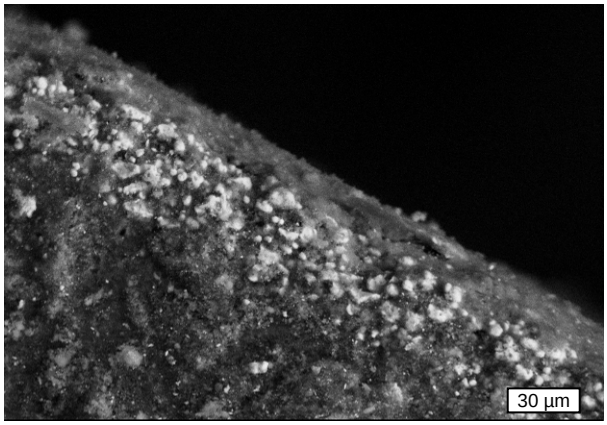

(c)

Figure 76: Coated SiC pin exposed to arc jet conditions for 5 min. The coating was hardly depleted and maintained good bonding to the substrate.

An experiment of exposing a similar coating for 10 minutes (~1450°C) reveals a significant deposition of metallic Cu-Hf needles as illustrated in Figure 77. Under the metallic debris a glassy phase is shown, but it does not reflect severe oxidation. This debris is generated by the degradation of the jet nozzle. Some areas are not covered with the metallic debris. The overall coating seems to have a very similar appearance to the pre-tested sample. Thus, the gross defects at the top and around the area close to the top of the pin may be the consequence of the coating technique and not the result of the test itself (Figure 78). However, it seems that the circumference coating was slightly eroded along the first 50 µm from the top. The erosion formed a graded layer, but the bonding to the substrate remained good.

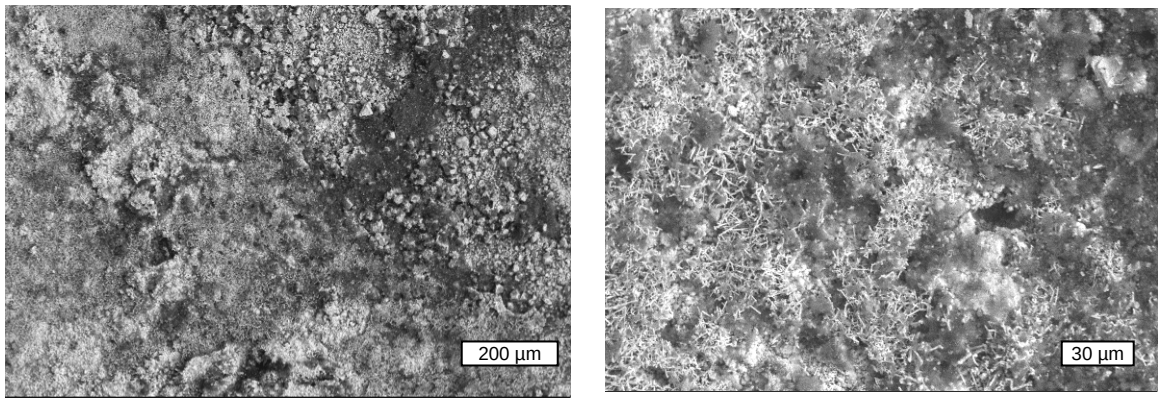

(a) (b)

Figure 77. Oxidized top coating of a SiC pin tested by the arc jet apparatus for 10 min. A Cu-Hf needles are observed at the surface. Only low level of a glassy layer is developed.

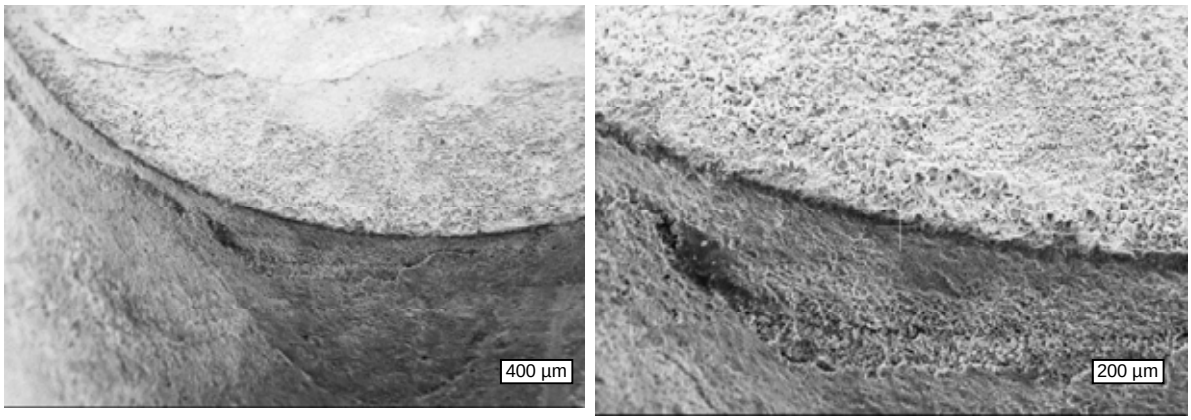

(a) (b)

Figure 78. Oxidized top coating of a SiC pin tested by the arc jet apparatus for 10 min. Some erosion may occur at the top 50 µm of the side coating.

In Figure 79 the cross section of the tested pin shows that the coating maintained its density and good bonding to the SiC substrate at about 3 mm from the top of the pin. The thin layer at the external part of the coating is the remains of the thin SiC layer formed during the carburization step of the coating processing.

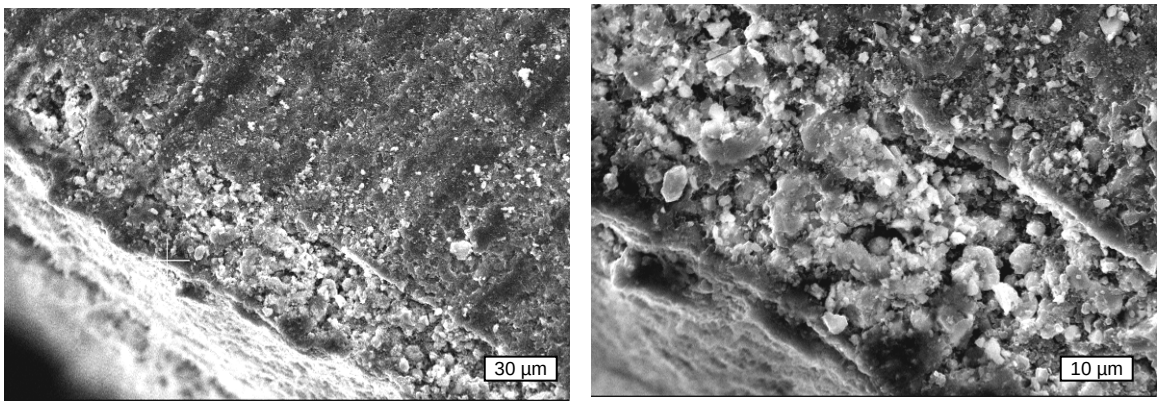

(a) (b)

Figure 79. Cross-section close to the top of a pin exposed to arc jet conditions for 10 min reveal a dense ZrB_2/SiC coating with good adhesion to the substrate.

4 CONCLUSIONS

UHTC particulate composite coatings, made of ZrB_2/SiC and ZrB_2/ZrC/SiC compositions and exceeding 100 μm in thickness, can be processed by slurry approaches combining polymeric precursors to silicon carbide and carbon. The approaches can also involve in-situ reactions at elevated temperature between the coating constituents or with additional reagents added subsequent to the initial slurry processing. One of the two main approached studied in this effort was found to be very suitable for generating dense coatings. This approach has the potential to become a generic coating approach for composite coatings containing a SiC phase (Si_3N_4 phase is also feasible). Also, the ratio of the SiC phase relative to other phases (non-silicon based materials) in the particulate composite coating can be varied to mitigate CTE mismatch and optimize performance characteristics.

The second evaluated slurry approach can be used as a practical matrix former for fiber reinforced ceramic composites. Potentially, particulate composite structures can be generated too, but the slurries will be required to be formulated as "dry" compositions and processing to obtain full densification will be a critical issue, if the width of the monolithic structure is large.

Specific conclusions related to the two evaluated approaches in this study are set below. Both approaches are considered as practical processing approaches but for different applications.

4.1 Approach 1 -- ZrB_2 Powder (or Alternative Compound) mixed with Polymeric Precursors

This approach was the main focus at the initial stage of the investigation. The polymer physical characteristics, its post pyrolysis composition and the ratio of mixing the individual polymer with the ZrB_2 powder significantly affect the final properties of the coating. The adhesion of the derived coating to the substrate is highly influenced by the initial adhesion of the polymer (resin) at the curing stage. Therefore, polymers with low surface tension such as polymethylcarbosilane, polyhydridomethylsiloxane and polynaphthalene did not provide good coatings. In contrast, allylhidridopolycarbosilane, hydroxylated-polyhydridomethylsiloxane and phenolic resins that wet substrates very well provided adequate coatings once the ratio between the polymer and the powder was individually adjusted.

The post pyrolysis compositions of some of the polymeric precursors exhibited unexpected reactivities that can not be explained intuitively by thermodynamic considerations. For example, the siloxane precursors lead to various amorphous SiOC compositions after pyrolysis. These compositions were expected to be stable to at least 1400°C in their amorphous stage and then convert gradually to SiC by in-situ carbothermal reduction reaction. Yet, the main observed feature was the significant elimination of the Si-containing phase, which occurred by an unknown mechanism that assumingly, involved the volatilization of SiO. Phenolic-derived carbon was found to be reactive with the ZrB_2 forming an additional phase of ZrC. This reaction is also unfavorable thermodynamically, and requires another "side" reactivity in order to occur spontaneously at 1500°C. These two unexplained reactivities can be very intriguing topics for further fundamental studies.

4.1.1 Slurries with Stoichiometric Precursor to SiC (SMP-10)

The most successful coatings produced by Approach 1 were obtained by formulating ZrB_2 powder with a polymeric precursor to stoichiometric SiC (SMP-10, produced by Starfire Systems). The low viscosity of the polymer, its adhesion properties, combined with its high ceramic yield and good post pyrolysis stoichiometry makes it a good commercial candidate (with the exception of its cost) for coating and matrix processing. Good bonding of coatings to the SiC substrate was accomplished including coatings that were thicker than 100 μm. However, such coatings still possess residual porosity due to the local shrinkage of the polymer during pyrolysis and further shrinkage during crystallization of the amorphous post-pyrolyzed product. Attempts to reinfiltrate these pores with additional amount of polymer resulted in severe cracking due to stresses generated by the polymer shrinkage during the pyrolysis.

A procedure to bypass the stress development during polymer reinfiltration was to use dilute polymer solutions, hence forming an additional thin film that can shrink unidirectionally perpendicular to the micropore surface. However, in this case the coating is not completely sealed even after 5 cycles of infiltration. Consequently, these coatings did not perform well under any of the tested oxidation conditions above 1400°C.

Another problem with using SMP-10 is its air sensitivity, which makes it harder for processing during the slurry mixing and coating deposition steps. The processing of these steps need to be done in inert or at least moistureless environment to avoid uncontrolled oxygen incorporation. Oxygen incorporation will result in the formation of a SiOC fraction that may behave like the SiOC materials evaluated separately in this project.

Much better oxidation resistance was obtained when the same slurries were tested in a monolithic form. In this case, the liquid state of the slurry that provides 80:20 ZrB_2:SiC without any additional solvent (relatively low viscosity) indicates that the formulation is a good candidate for fiber-reinforced composite processing. In the bulk form, the slurry can shrink in all directions and result in significantly higher density than in a restricted coating configuration. In addition, during the early stage of oxidation the material skin can be densified by the oxidation process and seal the subsurface matrix. The matrix can be also reinfiltrated with additional polymeric precursor.

Matrix material and monolithic forms of such powder/polymer combinations can be also achieved by using the lower cost polymethylcarbosilane. The disadvantages of this polymer are the need to use solvents, because it is produced in a solid form, and the excessive level of 'free" carbon obtained after pyrolysis. The later deficiency can be overcome by incorporating powders like Zr and into the slurries that will interact with the free carbon to provide additional carbide phases. Other advantages of this polymer are its potential processing via a melt stage and its stability in air during processing.

Due to the porosity and stress level the hardness of these coatings is very low, especially after heating to the 1500°C range. The average microhardness measurement is less than 1.0 GPa kg/mm^2. Because of the residual porosity, the coatings are not suitable for protection against oxidation. More conclusions regarding the oxidation tests of these coatings and bulk are provided in the oxidation section of the conclusions.

Nonetheless, such porous coatings may be considered as bond layers for TBC/EBC coatings for composites, replacing the currently practiced silicon layer. Recently, similar

coatings based on powders mixed with preceramic polymers have been studied by Cermatech and NASA Glenn Research Center as bond layers and demonstrated positive results. These coatings were made of SiC powders and polymeric precursors to SiC. One explanation to their adequate performance as bond layers is the fact that these are porous coatings.

4.2 Approach 2 -- Preform-RBSC Coating Processing

The approach is based on a three-step process. First, a preform is made out of a slurry combining powder mixed with phenolic resin. Most of the project work consisted of using ZrB_2 or ZrB_2/SiC powder for generating the preform slurries. After the pyrolysis of the phenolic resin the carbon-derived material is siliconized with molten silicon. At this stage a very efficient infiltration of the Si is attained, which results in a densification of the coating. The excess of silicon is then successfully eliminated by further reaction with an external source of carbon. At the end of the process there is no evidence for residual Si by XRD and EDS analyses. Most of carburization step investigated in this project was performed by embedding the siliconized specimens in carbon black powder and reheating the specimens to 1500°C. However, it was confirmed that even a gaseous source of carbon can efficiently react with the residual Si and eliminate its presence. The approach of eliminating excessive free silicon from RBSC structures should be of general interest for other RBSC applications and need to be further studied and developed.

This coating approach achieved the target characteristics of thick, dense, and hard coatings with composition of approximately 30 vol% SiC and 70 vol% of mixed ZrB_2/ZrC phases. Coatings with 100 µm thickness were accomplished by design. Additionally, there is strong evidence that coatings of 200 to 500 µm may be feasible. Microhardness in the range of SiC was observed for these UHTC coatings (20 to 40 GPa). A few successful attempts to make similar coatings on top of C/SiC composite specimens provided promising results. Yet, coatings covering the rough seal layer that already exists at the surface of such composites would require special attention in future development to eliminate interface stresses. The seal layer possesses "designed" cracks to manage the CTE mismatch. Conceptually, the gaps in the designed cracks are closed at elevated temperature and provide a complete seal. Coatings on top of such gaps will have to perform similarly with the same tectonic movement ability.

The 70 vol% of the ultrahigh temperature phase (mostly ZrB_2/ZrC in this study) is the maximum level that can be achieved by the direct siliconization technique. However, higher volume ratios of the UHTC phases can be obtained, if the siliconization is performed with a silicon alloy containing Zr or Hf. Such alloys can contain up to 20 mol% of the transition metal with a eutectic melting point below the melting point of the silicon itself, according to phase diagrams. This step can be then associated with the carburization of the residual metals. This approach has been tried in this project by performing a set of designed experiments with Si/Hf alloy. Unfortunately, the Hf in the alloy reacted severely with the BN crucible used for the siliconization. It would be necessary to use a crucible that will not react with either the Si or the Hf. A potential material for tooling will be the oxide or the boride of the metal to be uses (i.e., HfO_2, HfB_2, ZrO_2, or ZrB_2). In contrast, SiC, Si_3N_4 and Al_2O_3 will react with the Hf or Zr component.

Incorporation of metal powder into the base formulation of the preform coating is another potential method to achieve higher volume fraction of the transition metal compound phase in the overall UHTC composition. The metal powder can partially react with the phenyl-derived

carbon and further react with either active gases or during the carburization stage. The potential of using gaseous carbon precursors has been demonstrated in the study. A similar approach can be developed with boron-containing gases such as hydroboranes, boron chloride adducts or organoboranes (that provide both boron and carbon sources).

A lower volume fraction of the transition metal phases (higher fraction of the SiC phase) can be easily achieved by incorporating SiC powder into the preform formulation. This technique has been successfully demonstrated at the beginning of the preform-RBSC development effort, after predicting that higher SiC phase would be required to mitigate the CTE mismatch. This approach was planned for producing a graded coating composition. The necessity of a graded coating approach may become again a critical requirement for thick coatings deposited over rugged composite surfaces for enhancing the coating durability during thermal cycling conditions.

One unexpected discovery during the development of the preform approach was the formation of a significant ZrC phase. The mechanism of forming this phase is not clear since the basic reaction of ZrB_2 with C is unfavorable thermodynamically. This reactivity may become a useful aid to reduce the boron content or assist the coating densification (see discussions below). A new AFOSR project at SRI plans to further explore this and other unexpected phase transformation phenomena observed identified in the study.

One conclusion deduced from the oxidation studies is that the boron content may be too high for UHTC coating and potentially be distractive under both passive and active oxidation conditions. A few attempts to replace all or part of the ZrB_2 phase in the preform coating with carbide or oxide phases of Zr and Hf led to more porous coatings or coatings that did not bond well to the SiC substrate. The microstructural analysis revealed a remarkable reactivity of recrystallization and probably the formation of mixed metal phases of the transition metals. The recrystallization was associated with local densification (sintering like patterns). This reactivity was observed when HfO_2, HfC, and even ZrC powders were added as a secondary phase aside the ZrB_2 powder. The separate presence of these additional phases was no longer detected by XRD analysis of the final UHTC coatings. Instead, the presence of Hf was detected in the same areas where the Zr resides too. These reactivities are very intriguing and may become a means to densify both coatings and structural UHTC compositions using slurry techniques, once the rearrangement mechanism is understood. Therefore, these observed phenomena will be study as a part of the above mentioned AFOSR project.

4.3 Oxidation Study

The original plan for the oxidation studies of the developed UHTC coatings was designed to compare of the oxidation behavior of coatings under (a) atmospheric and (b) low pressure, (c) high and (d) low partial pressure of oxygen, (e) molecular and (f) partially dissociated oxygen, and (g) arc jet conditions. One major aspect was to identify conditions at which the oxidation of the UHTC coatings becomes active and to observe the severity of such active oxidation.

In spite of a sincere attempt to upgrade a lab scale arc jet apparatus, built at SRI, for performing at elevated temperatures without metal contamination originated by the jet nozzle decomposition only a few tests were performed at a relevant high temperature. Yet, the metal contamination was severe under these conditions and the arc jet circuitry failed after a few experiments. More meaningful were the oxidation results in the presence of atomic oxygen,

generated by the high power microwave discharge generator connected to a high temperature furnace. The level of the atomic oxygen in the experiments was estimated to be around 10 mol% of the overall oxygen content.

Coatings made by Approach 1, were stable only under atmospheric conditions at and below 1400°C. The residual porosity in the coatings was found to be detrimental at 1500°C or under low pressure or low partial pressure of oxygen. Under such active oxidation conditions, the coating porosity cannot be sealed by a volume expansion of the evolved oxide phases and/or by molten glass phase mobility. Instead, the porosity leads to excessive volatilization of SiO and BO_x gaseous species through the pore structure. Under passive oxidation conditions, a low melting point glass is formed causing bubbles and delamination of the coatings. Attempts to seal the coatings by infiltrating a polymeric precursor to SiC into the coating pores did not enhance the oxidation stability significantly.

Much better performance was observed with bulk materials that were fabricated from the same slurries used for the coatings investigated in Approach 1. Such bulk materials are considered as matrix candidates for UHTC fiber reinforced composites. One reason for the better performance is the higher density of the bulk material at the microscale level, which allows better conditions to seal the surface and therefore inhibits the diffusion of gases in (oxygen) and out (SiO, CO, BO_x) of the structure. The oxidation of the bulk material reveals the formation of an oxide layer at the outer 30 to 50 μm. The oxide layer scale and partial oxidation of the layer underneath (causing expansion of material into the residual pores as well as an amorphous intergranular phase, prevents further oxidation.

Coatings generated by Approach 2 performed much better under most of the tested conditions because of their higher density as well as their better adhesion to the substrate. However, attaining good oxidation resistance performance requires that coatings will be at least 100 μm thick. Such thick coatings still possess a significant ZrB_2 and SiC phases and lower ZrO_2 phase when oxidized under atmospheric conditions at 1500°C for 1h. It should be noted, that the ZrC phase disappeared, which may suggest that it was formed at the outer layer of the original ZrB_2 grains during the RBSC processing.

Oxidation under reduced oxygen level (still under overall pressure of 1 atmosphere) resulted in stable coatings but with greater level of porosity. Also, deep defects in such thick coatings result in local attack (micro level) of the substrate surface and creation of planar holes at the interface between the coatings and the substrate. Oxidation at low pressure still exhibits a very active oxidation behavior. Coatings heated at 1500°C/1h under active oxidation conditions are completely oxidized and the bonding of the oxidized coating to the substrate degraded.

One of the main conclusions from the oxidation studies is the need to develop coatings that are much leaner in their boron content. The oxidized boron under passive oxidation condition is responsible for a low melting point glass formation and under low pressure condition it is as volatile as SiO or CO at elevated temperature. Replacement of a portion of the boride phase with carbide or oxide phases in the UHTC coating compositions is expected to improve the overall coating performance.

5 RECOMMENDATIONS

Recommendations for further development of slurry based UHTC coatings and structures are divided into several categories. Some are related to immediate improvement or development of the compositions already evaluated during the performance of this project. Other recommendations are for longer-term developmental efforts. An additional set of recommendations is provided to address issues related to the fundamental understanding of UHTC coating performance and their tailoring, as well as unique phase development phenomena that may result in better processing of these materials in general and coatings in particular. Recommendations for further development of RBSC aspects are also given.

5.1 Improving Preform-RBSC Coating Process and Tooling

Regardless the final composition of the coatings developed according to Approach 2, there is a need to improve the techniques and equipment for the evolved process to accommodate the coating capability of sizable parts, especially for composites structures that need to be coated around their entire structure surface. The main issue in such scaling up is to obtain an efficient siliconization step that will provide complete infiltration into the preform without leaving a thick silicon layer at the external coating surface, or frozen chunks of silicon at the bottom of specimens processed by the posting the specimens over Si powder in a vertical BN crucible (as was processed efficiently with small specimens).

The siliconization process can be optimized by utilizing a vertical furnace equipped with a BN container larger than the specimen to be coated and filled with molten Si. The furnace will be kept open under an Ar veil. The specimen with the preform coating will be then dipped into the molten silicon using a SiC based yarn, net or a structure as the specimen holding aid. Due to the low viscosity of the molten Si, excessive build up of an external Si layer is not anticipated.

An alternative approach will be to dip the preform coating in slurry made of Si powder and a decomposable organic binder. The amount of the Si layer will be adjusted to the stoichiometric level required just for the bonding reaction, while assuring that there would be no formation of a SiC layer at the external surface of the coating. The specimens will be placed vertically in a furnace and heated to 1500°C. This approach is simpler than using a molten Si pool but it may be disadvantageous because of the vulnerability of the loosely bonded Si powder prior to its melting at 1410°C.

Another alternative approach for processing the loosely bonded Si layer is to place the specimen horizontally and coat only the one side facing up with the require amount of Si powder. The specimen will be then heated above the melting point of the Si. This process will require repeating the process for each side of the specimen, if the protective coating is desired to be on top of more than one side.

Another aspect for further development is an efficient carburization process of the residual Si. Although embedding of the siliconized specimen in carbon powder is a simple and efficient process, a better process for large scale operation will be the development of a gas phase carburization process. In this case, the carburization step will proceed immediately after the siliconization step without cooling the furnace between the siliconization and carburization steps.

The development of better carburization step may find additional applications outside the UHTC coatings, since excess of elemental Si exists in RBSC structures and its elimination is highly desired for high temperature and harsh environment applications.

5.2 Adapting Preform-RBSC Coating Process for SiC/SiC and C/SiC Composites

It is anticipated that adapting Approach 2 as coatings for CMCs will require additional optimization of formulation and processing steps. First, the formation of a seal SiC layer seems to be important, especially if reinforcing C fibers tips are exposed at the surface to be coated and can react by themselves with the molten Si. The roughness of such seal layer, as existed in the CVI processed composite specimens coated in this project may become problematic by enhancing stresses at the interface with the UHTC coating. Methods to form such smooth seal layer will be required in this case.

Also, it is not clear if the cracks already exist in the current seal layers for CTE mismatch mitigation are going to affect the thermal cycling of the UHTC coatings. It is possible that such coating will have to follow the same cracking pattern to avoid stresses during thermal cycling of the composite.

5.3 Graded and Multi layer Approaches Using the Preform-RBSC Approach

Development of UHTC coatings thicker than 100 μm is anticipated. The thicker coatings will enhance the cycling stress generation at the interface between the substrate and the coating. The assessment of a graded or a multilayer coating approaches for obtaining thicker coatings is therefore recommended to mitigate these thermally induced stresses as well as provide additional functionalities to the coating (e.g., improving thermal barrier properties).

Additional reason for developing a graded or a multilayer coating approach is to prevent excessive volatilization of substoichiometric metal oxides under active oxidation conditions. Under such conditions, it would be better to reduce the boron and potentially also the silicon contents in the outer layer of the coatings.

5.4 Optimized Compositions for Better Oxidation Resistance Coatings

One of the study's conclusions assume that the level of boron in the coating composition is too high leading to (a) glass with low melting point and viscosity under atmospheric conditions or (b) significant evaporation under low pressure conditions. Partial replacement of the boride phase with a carbide, nitride or oxide phases would improve the coating performance under atmospheric conditions.

An oxide phase may reduce the thermal stability, because of lower melting point, but improves the performance under low pressure conditions. The selected oxide should be based on a high melting point materials as well as high phase transformation temperatures. Good candidates are HfO_2, ThO_2, UO_2, Y_2O_3, La_2O_3 or stabilized ZrO_2. If HfO_2, ThO_2, and UO_2 are selected, they should be incorporated as very fine particles to prevent their rapid sedimentation in the slurries due to their high specific density. Also, the level of incorporating an oxide phase should be limited to a level that does not affect much the emissivity of the protective coating.

The composition optimization should involve the assessment of efficient infiltration of the molten Si into the preform layer, which might be affected by the wetting affinity of the molten Si to the microporous structure, derived by the particle size and shape of the powders incorporated to the slurry as well as the affinity between the surface of these particles and molten Si. The effects of particle size and the consequent pore structure in the preform layer have not been investigated in this exploratory project and must be an integral part of process optimization. Particle size will also affect intergranular stresses and overall coating behavior during oxidation. Literature that correlates the sizes of the transition metal compound and the SiC domains in UHTCs with their oxidation resistance performance under various conditions was not found.

The optimization phase should also consider the significant phase rearrangement during the coating processing due to chemical interactions between the different components in the slurry formulation or reactivities with the molten Si.

A proposed composition optimization effort should be associated with oxidation testing under the various cluster conditions that generate passive, active or a combined active-passive oxidation.

The coating compositions or alternatively a multilayer coating approach need to be associated with specific scenarios of the environmental condition profile that the specific aerospace vessel will be expose to during operation.

5.5 Further Development of UHTCs Based on ZrB_2/Polymeric Precursor to SiC

The concept of mixing a UHTC powder with a polymeric precursor to SiC was not found very successful for producing dense and consequently good oxidation resistance coatings. However, this approach is well suited for developing UHTC matrices for fiber reinforced composites. Slurry with appropriate compositions can be made with low viscosity with and without solvents. The derived matrix densification can be achieved by precursor reinfiltration. In this case, reinfiltrating the initially developed matrix with new precursors to UHTC materials should be considered, including the infiltration of oxide phases. Reinfiltration of precursors combining both precursors to UHTC and SiC phases is another appealing option.

The combination of UHTC powder and SiC polymeric precursor may be practical for forming structural UHTC (Non-CMC) under (a) hot press conditions at relatively low temperature or (b) for the formation of partially porous structures that can be then reinfitrated with a polymeric precursor for strength enhancement of sealed with an appropriate coatings. The improvement of strength and oxidation resistance of porous monolithic structures by preceramic polymer reinfiltration was observed in previous studies at SRI to obtain net shape structures based on reaction bonded silicon nitride (RBSN). Similarly, this approach was found useful for improving the oxidation resistance of such structures.

5.6 Assessing the Generic Capability of Preform-RBSC Coating Process.

The developed Preform-RBSC (or RBSN) approach can be extended to other than ZrB_2 powders. A few experiments were performed during the performance of this project, but were abandoned because of unexpected phase changes or assumed lack of wetting by the molten

silicon. It is highly advised to assess the extent to which the preform-RBSC process can be generalized. The approach has the potential to be generic for UHTC borides, carbides and nitrides as well as oxide powders. The phase transformation observed during processing with other powders as well as the partial transformation of the ZrB_2 may be beneficial for obtaining dense coatings, provided that the transformation mechanisms are well understood and controlled. Thus, assessment of the generality of this approach should be carefully performed associated with fundamental studies of the phase conversions.

6 REFERENCES

1. I. E. Campbell and E. M. Sherwood (Eds.), High-Temperature Materials and Technology, Wiley, New York (1967).
2. J. B. Berkowitz-Mattuck, "High-Temperature Oxidation III, Zirconium and Hafnium Diborides," J. Electrochem. Soc., 113, 908-914 (1966); "High-Temperature Oxidation IV, Zirconium and Hafnium Carbides," J. Electrochem. Soc., 114, 1030-32 (1967).
3. W. C. Tripp and H. C. Graham, "Thermogravimetric Study of the Oxidation of Zirconium Diboride in the Temperature Range of 800° to 1500°C," J. Electrochem. Soc., Solid State Science, 118 (7) 1195-1199 (1971).
4. R. A. Cutler, "Engineering Properties of Borides" in Engineering Materials Handbook, Vol. 4: Ceramics and Glasses. ASM International, Metals Park, Ohio (1987).
5. E. L. Courtright, H. C. Graham, A. P. Katz and R. J. Kerans, "Ultra-high Temperature Assessment Study of Ceramic Matrix Composites," Rept. No. WL-TR-91-4061, Wright-Patterson AFB, Ohio (1991).
6. C. B. Bargeron, R. C. Benson, R. W. Newman, A. N. Jette and T. E. Phillips, "Oxidation Mechanisms of Hafnium Carbide and Hafnium Diboride in the Temperature Range 1400 to 2100C," Johns Hopkins APL Tech. Dig., 14 [1] 293-5 (1993).
7. K. Upadhya, J. M. Yang and W. Hoffman, "Advanced Materials for Ultra-High-Temperature Structural Applications," Am. Ceram. Soc. Bull., 76 [12] (1997).
8. W. C. Tripp, H. H. Davis and H. C. Graham, "Effect of an SiC Addition on the Oxidation of ZrB_2," Am. Ceram. Soc. Bull., 52, 612-616 (1973).
9. M. M. Opeka, I. G. Talmy, E. J. Wuchina, J. A. Zaykoski and S. J. Causey, "Mechanical, Thermal, and Oxidation Properties of Refractory Hafnium and Zirconium Compounds," J. Eur. Ceram. Soc., 19, 2405-2414 (1999).
10. L. Kaufman, "Boride Composites–A New Generation of Nose Cap and Leading Edge Materials for Reusable Lifting Re-entry Systems," AIAA Paper No. 70-278, AIAA Advanced Space Transportation Meeting (February 1970).
11. J. D. Bull, D. J. Rasky and C. J. C. Karika, "Stability Characterization of Diboride Composites under High-Velocity Atmospheric Flight Conditions," in Proceedings of the 24th International SAMPE Technical Conference, pp.1092-1105 (1992).
12. J. Bull, M. J. White and L. Kaufman, "Ablation Resistant Zirconium and Hafnium Ceramics," US Patent 5,750,450 (May 12, 1998).
13. R. Loehman, Private Communication
14. W. G. Fahrenholz and G. Holmes, Private Communication.
15. F. Monteverde and A. Bellosi, "The Efficacy of HfN as Sintering Aid in the Manufacture of Ultra-High Temperature HfB2 Matrix Ceramics," J. Mat. Res., 19(12), 3576 (2004).
16. A. Bellosi and F. Monteverde "Ultra-Refractory Ceramics: The Use of Sintering Aids to Obtain Microstructure and Properties Improvement," in Key Eng. Mat., Eds. H. Mandal and L. Ovecoglu, 264-268, 787 (2004).

17. L. Kaufman, “Investigation of Boride Compounds for Very High Temperature Applications,” AFML Report No. RTD-TDR-63-4096, Part II (February 1965).

18. L. Kaufman, “Calculation of Multicomponent Refractory Composite Phase Diagrams,” NSWC Report No. TR 86-242 (June 1986).

19. E. Rudy and St. Windisch: US Air Force Tech Doc. Report AFML-TR-65-2, Part 1, Vol. IX (February 1966).

20. Y. D. Blum and H-J. Kleebe, Chemical Reactivities of Hafnium and its Derived Boride, Carbide and Nitride Compounds at Relatively Mild temperatures, J. Mater. Sci., 39, 6023-42 (2004).

21. Y. D. Blum, S. Young, and D. Hui, Chemical Reactivity in Search of Better Processing of HfB2/SiC UHTC, in Composites, Ceramic Transactions, 177, edited by J. P. Singh, N. P. Bansal, B. G. Nair, T. Ohji, and A. de-A. Lopez, 103-114 (2005).

22. Y. D. Blum, S. Young, D. Hui, and E. Alvarez, Hafnium Reactivity Below 1500°C in search of Better Processing of HfB_2/SiC UHTC Composites, submitted to Cocoa beach Meeting Proceedings (2006).

23. G. A. Zank, (a) U.S. Patent 5,449,646 (September 12, 1995); (b) U.S. Patent 5,527,748 (June 18, 1996).

24. P. P. Paul and S. T. Schwab, “Methods for Making High Temperature Coatings from Precursor Polymers to Refractory Metal Carbides and Metal Borides,” US Patent 6,042,883 (March 28, 2000).

25. P. P. Paul and S. T. Schwab, “Method for Making Ceramic Matrix Composites Using Precursor Polymers to Refractory Metal Carbides and Metal Borides,” US Patent 6,120,840 (September 19, 2000).

26. S. T. Schwab, C. A. Stewart, K. W. Dudeck, S. M. Kozmina, J. D. Katz, B. Bartram, E. J. Wuchina, W. J. Kroenke, and G. Courtin, “Polymeric Precursors to Refractory Metal Borides,” J. Mater. Sci., 39, 6051-6055 (2004).

27. K. Su and L. G. Sneddon, “Polymer-Precursor Routes to Metal Borides: Syntheses of TiB_2 and ZrB_2,” Chem. Mater., 3, 10-12 (1991)

28. K. Su and L. G. Sneddon “A Polymer Route to Metal Borides,” Chem. Mater., 5, 1659-1668 (1993).

29. K. Forsthoefel and L. G. Sneddon, “ Precursor Routes to Group 4 Metal Borides and Metal Boride/carbide and Metal Boride/nitride Composites,” J. Mater. Sci., 39, 6043-6049 (2004).

30. Z. Hu, M. D. Sacks, G. A. Staab, C-A Wang, and A. Jain, Ceramic Engineering and Science Proceedings, edited by H-T Lin and M. Singh, 23(4), 711-717(2002).

31. M. D. Sacks, C-A Wang, Z Yang, and A Jain, “Carbothermal Reduction Synthesis of Nanocrystalline Zirconium Carbide and Hafnium Carbide Powders Using Solution-Derived Precursors,” J. Mater. Sci., 39, 6057-6066 (2004).

32. Y. Kurokawa, H. Ota, and T. Sato, “Preparation of Carbide Fibers by Thermal Decomposition of Cellulose-Metal (Ti, Zr) Alkoxide Gel Fibers,” J. Mater. Sci. Lett., 13, 516-518 (1994).

33. Y. Kurokawa, S. Kobayashi, M. Suzuki, M. Shimazaki, and M. Takahashi, “Preparation of Refractory Carbide Fibers by Thermal Decomposition of Transition Metal (Ti, Zr, Hf, Nb, Ta) Alkoxide- Cellulose precursor Gel Fibers,” J. Mater. Res., 13, 760-765 (1998).

34. H. Preiss, E. Schierhorn, and K.-W. Brezinka, “Synthesis of Polymeric Titanium and Zirconium Precursors and Preparation of Carbide Fibers and Films,” J. Mater. Sci., 33, 4697-4706 (1998).

35. G. S. Girolami, J. A. Jensen, J. E. Gozum, and D. M. Pollina, “Tailored Organometallics as Low-Temperature CVD Precursors to Thin Films,” Mater. Res. Soc. Symp. Proc., Mater. Research Soc., 121, 429-438 (1988).

36. J. A. Jensen, J. E. Gozum, D. M. Pollina, and G. S. Girolami, “Titanium, Zirconium, and Hafnium Tetrahydroborates as Tailored CVD Precursors for Metal Diboride Thin Films,” J. Am. Chem. Soc., 110, 1643-1644 (1988).

37. G. W. Rice and R. L. Woodin, “Zirconium Borohydride as a Zirconium Boride Precursor,” J. Am. Ceram. Soc., 71, C181-C183 (1988).

38. V. V. Volkov, K. G. Myakishev, and S. I. Yugov, “Synthesis of Zirconium Tetrahydroborate by the Reaction of Zirconium Chloride with Lithium Tetrahydroborate,” J. Appl. Chem., USSR (Eng. Trans.), 48, 2184 (1975).

39. R. A. Andrievski, G. V. Kalinikov, S. E. Kravchenko, B. P. Tarasov, and S. P. Shilkin, “Synthesis of Boride Ultrafine Powders and Films,” Polym. Mater. Sci. Eng., 73, 294-5 (1995).

40. F. N. Tebbe and R. T, Baker, “Borides and Boride Precursors Deposited from Solution,” US Patent 5,364,607 (November 15, 1994).

41. S. M. Johnson, Y. Blum, C. Kanazawa, H.-J. Wu, J. R. Porter, P.E.D. Morgan, D. B. Marshall, and D. Wilson, “Processing and Properties of an Oxide/Oxide Composite,” Key Engineering Materials, Trans. Tech. Publications, Switzerland, 127-131, 231-238 (1997).

42. S. M. Johnson, Y. D. Blum, C. Kanazawa, and H-J Wu, “Low-Cost Matrix Development for an Oxide-Oxide Composite,” Metals and Materials, 4(6), 1119-1125 (1998)

43. Yigal Blum, D. B. MacQueen, D. Hui, J. Sibold, D. Galloway, and S. Wheeler, “Dense Silicon Carbide Matrix for SiC/SiC Composites for Fusion Energy Reactors,” Presented at Pacific Rim 4 Conference, (November 8, 2001).

44. D. Seyferth, N. Bryson, D. Workman, and C. A. Sobon, J. Am. Ceram. Soc., 74, 2687-2689 (1991).

45. P. Kennedy, in “Non-Oxide Technical and Engineering Ceramics,” edited by S. Hampshire (Elsevier Applied Science, London) 301 (1986).

46. N. Frage, S. Hayun, V. Tourbabin, and M. P. Dariel, “Low Temperature Synthesis of Dense B4C-SiCTiB_2 Composites,” Paper AM-S12-13-2005, in “The American Ceramic

Society 170th Annual Meeting and Explosition Abstract Book." The Am. Ceram. Soc. Publisher, 104 (April 2005).

47. T. Holmes, M. Aghajanian, P. G. Karandikar, and J. Mears, "Effect of B4C/SiC Ratio on the Physical, Mechanical and Ballistic Properties of Reaction Bonded Ceramics, Paper AM- S12-11-2005, in "The American Ceramic Society 170th Annual Meeting and Explosition Abstract Book." The Am. Ceram. Soc. Publisher, 105 (April 2005).

48. P. Popper, "The Reaction of Dense Self-Bonded Silicon Carbide," In: Special Ceramics; Heywood: London, 209 (1960).

49. E. Fitzer and R. Gadow, "Reinforced Silicon Carbide," Ceram. Bull., 65(2), 326 (1986).

50. E. Fitzer and R. Gadow, "Investigation of the Reactivity of Different Carbons with Liquid Silicon," In: Proceedings of the International Symposium on Ceramics for Engines; Technoplaza Co. Ltd., Tokyo, Japan, 561-572 (1983).

51. W. P. Minnear, "Interfacial Energies in the Si/SiC System and the Si + C Reaction," Am. Ceram. Soc. Commun., C-10-11 (January 1982).

52. P. Pampuch, E. Walasek, and J. Bialoskorski, "Reaction Mechanism in Carbon-Liquid Silicon Systems at Elevated Temperatures," Ceram. Int., 12, 99 (1986).

53. Y. M. Chiang, J. S. Haggerty, R. P. Messner, and C. Demetry, "Reaction-Based Processing Methods for Ceramic—Matrix Composites," Ceram. Bull., 68(2), 420 (1989).

54. P. Sangsuwan, J. A. Orejas, J. E. Gatica, S. N. Tewari, and M. Singh, "Reaction-Bonded Silicon Carbide by Reactive Infiltration," Ind. Eng. Chem. Res., 40, 5191-98 (2001).

55. Y. D. Blum, D. B. MacQueen, and H.-J. Kleebe, "High Carbon Content SiOC Nanocomposites", Manuscript in preparation, to be submitted to *J. Chem Mater*. (2004).

56. Rosner, D.E., and Allendorf, H.D., "Comparative Studies of the Attack of Pyrolytic and Isotropic Graphite by Atomic and Molecular Oxygen at High temperatures", *AIAA Journal*, Vol. 6, 1968, pp. 650-654.

57. Allendorf, H.D., and Rosner, D.E., "Primary Products in the Attack of Graphite by Atomic Oxygen and Diatomic Oxygen above 1100 K", *Carbon*, Vol. 7, 1969, pp. 515-518.

58. Rosner, D.E., and Allendorf, H.D., "High Temperature Kinetics of the Oxidation and Nitridation of Pyrolytic Silicon Carbide in Dissociated Gases", *Journal of Physical Chemistry*, Vol. 74, 1970, pp. 1829-1839.

59. Balat, M.J.H., "Determination of the Active-to-Passive Transition in the Oxidation of Silicon Carbide in Standard and Microwave-Excited Air", *Journal of the European Ceramic Society*, Vol. 16, 1996, pp. 55-62.

60. Stewart, D.A., Rakich, J.V., and Lanfranco, M.J., "Catalytic Surface Effects Experiment on the Space Shuttle", AIAA Paper 81-1143, 1981.

61. Stewart, D.A., Rakich, J.V., and Lanfranco, M.J., "Catalytic Surface Effects on Space Shuttle Thermal Protection System during Earth Entry of Flights STS-2 through STS-5", NASA CP-2283, March 1983.

62. Stewart, D.A., Rakich, J.V., and Chen, Y.-K., "Flight Experiment Demonstrating the Effect of Surface Catalysis on the Heating Distribution Over the Space Shuttle Heat Shield", NASA CP-3248, 1995.

63. J. Marschall, A. Chamberlain, D. Crunkleton, and B. Rogers, “Catalytic Atom Recombination on ZrB_2/SiC and HfB_2/SiC Ultra-High Temperature Ceramic Composites,” *Journal of Spacecraft and Rockets*, in-press, 2004.

64. Marschall, J., and Chen, Y.-K., "Modeling Surface Oxidation in Transient Aerothermal Heating Environments", AIAA Paper 2004-0485, January, 2004.

65. Vincenti, W.G., and C. H. Kruger, J., *Introduction to Physical Gas Dynamics*, Krieger Publishing Company, Malabar, 1967.

66. Fletcher, D.G., and Bamford, D.J., "Arcjet Flow Characterization using Laser-Induced Fluorescence of Atomic Species", AIAA Paper 98-2458, .

67. Pope, R.B., "Measurements of Enthalpy in Low-Density Arc-Heated Flows", *AIAA Journal*, Vol. 6, 1968, pp. 103-110.

68. Bull, J.D., Rasky, D.J., and Karika, J.C., "Characterization of Selected Diboride Composites", Name of Conference, Cocoa Beach, Florida, NASA Conference

69. Bull, J.D., Rasky, D.J., Tran, H.K., and Balter-Peterson, A., "Material Response of Diboride Matrix Composites to Low Pressure Simulated Hypersonic Flows", Name of Conference, Cocoa Beach, Florida, NASA Conference Publication 3235, Part 2, 1993, pp. 653-673.

70. Metcalfe, A.G., Elsner, N.B., Allen, D.T., Wuchina, E., Opeka, M., and Opila, E., "Oxidation of Hafnium Diboride", *Electrochemical Society Proceedings*, Vol. **99-38** (1999) 489-501.

71. Y. D. Blum and G. A. McDermott, "Dehydrocoupling Treatment and Hydrosilylation of Silicon-Containing Polymers, and Compounds and Articles Produced Thereby", US Patent 5,750,643 (May 12, 1998)

72. S.M. Johnson, Y. D. Blum, C. Kanazawa, and H-J Wu, "Low-Cost Matrix Development for an Oxide-Oxide Composite, Metals and Materials", Vol 4, No.6, pp1119-1125, (1998).

73. E. J. Opila, M. C. Halbig, "Oxidation of ZrB_2-SiC,” Ceramic Engineering & Science Proceedings, 22 (3), 221-228 (2001).

74. A. Rezaie, W. G. Fahrenholtz and G. E. Hilmas, "Oxidation of ZrB2-30vol%SiC at 1500°C", Presented at Cocoa Beach meeting (January 2006)

7 LIST OF SYMBOLS, ABBREVIATIONS, AND ACRONYMS

UHTC	Ultra high temperature ceramics
AFRL	Air Force Research Laboratory
ZrB_2	Zirconium Carbide
ZrC	Zirconium Carbide
SiC	Silicon carbide
HfB_2	Hafnium diboride
HfO_2	Hafnium oxide
ZrO_2	Zirconium oxide
Hf C	Hafnium carbide
RBSC	Reaction bonded silicon carbide
SMP-10	Polymer precursor to SiC (commercial)
SiOC	Silicon oxycarbide
µm	micrometer
$ZrSi_2$	Zirconium silicide
CVI	Chemical vapor infiltration
SEM	Scanning electron microscopy
EDS	Energy dispersive spectroscopy
XRD	X-ray powder diffraction
HfN	Hafnium nitride
B_2O_3	Boron oxide
BO_x	Boron suboxide
SiO_2	Silicon oxide
SiO	Silicon monoxide
BN	Boron nitride
CO	Carbon monoxide
MB_2	Metal diboride
MC	Metal carbide
ACerS	American Ceramic Society
MO_2	Metal oxide
NSWC	Naval Surface Weapon Center
P_{O2}	Partial pressure of oxygen
AFOSR	Air Force Office of Scientific Research
MJ	Mega joules
CTE	Coefficient of thermal expansion
PHMS	Polyhydridomethylsilane
PHMS-OH	Hydroxylated Polyhydridomethylsilane
HRJ-14209	Commercial phenolic resin
SP-6877	Commercial phenolic resin
PN	Polynaphthalene
PMCS	Polymethylcarbosilane
ppm	Parts per million
ZrBC	Zirconium borocarbide
ZrOB	Zirconium oxyboride
CMC	Ceramic matrix composite
$MoSi_2$	Molybdenum silicide
Si_3N_4	Silicon nitride